BUREAU OF MINERAL RESOURCES, GEOLOGY AND GEOPHYSICS

RECORD

BMR RECORD 1987/6

CALIBRATION OF THE 54 MM DIAMETER BMR WELL-LOGGING DENSITY TOOL

P.N Chopra and C.J. de Bruyn

CALIBRATION OF THE 54 MM DIAMETER BMR WELL-LOGGING DENSITY TOOL

P.N Chopra and C.J. de Bruyn

BMR RECORD 1987/6

TABLE OF CONTENTS

ABSTRACT

The 54 mm diameter down-hole density tool in the BMR's well-logging system has been calibrated by logging three carefully selected boreholes and one of the calibration pits constructed by the South Australian Department of Mines and Energy (SADME). The boreholes which were chosen in order to allow calibration over a wide range of densities, penetrated low porosity sediments, acid volcanics, basic intrusives, low density coal measure sediments and high density massive sulphide sequences. Calibration has been achieved by comparing the density well-logs with laboratory measurements of the rock densities. In the case of the selected boreholes, laboratory density measurements have been made on core from the holes using two different methods; conventional Archimedes Principle measurements and a gamma ray spectroscopy technique. In the case of the calibration pit, the densities determined by SADME have been used. Separate calibrations of the short-spaced and long-spaced detectors in the density tool have been made by fitting the results to the theoretically-based relation:

$$I = A.\rho.e^{B.\rho}$$

where:

I = the intensity of the backscattered gamma ray beam (in counts per 200 milliseconds)

A and B = adjustable constants

ρ = the rock density in g cm^{-3}

A non-linear least squares regression of the backscattered gamma ray intensities against the laboratory determined densities was carried out with a FORTRAN program written for the purpose. For the density range 1.44 to 4.5 g cm^{-3}, the following calibration equations were obtained:

$I = 472.87.\rho.e^{-0.951.\rho}$ for the short-spaced detector, and

$I = 3965.1.\rho.e^{-2.439.\rho}$ for the long-spaced detector.

The estimates of in-situ densities obtained from the well-logs using these calibration equations have been found to be accurate to within 0.05 g cm^{-3} for smooth-walled, water-filled boreholes for rock densities between 1.44 and 4.5 g cm^{-3}.

INTRODUCTION

It is common practice in the mineral well-logging industry to furnish density logs to clients in units of counts per second (cps), usually with one or more reference marks provided to permit a nominal "eye-ball" estimation of absolute densities. These reference marks generally derive from "secondary calibrations" performed on site prior to the actual logging. Typically such calibrations are made using one or more "standard" blocks of known density and employing a constant geometry between the standard/s and the density tool. Unfortunately however, the physical environment of the density tool during such calibrations is often very different from that existing in a borehole, particularly when operating the tool below the water table. As a result the relevance of these "secondary calibrations" is often questionable and hence, the usefulness of the reference marks derived from them and included with the cps well-logs is also often debatable.

Notwithstanding the potential for errors in the calibration marks themselves, further errors are introduced to "eye-ball" density estimates by the very non-linear nature of the relationship between recorded gamma ray intensity and rock density.

The overall conclusion from the foregoing discussion must be that there is a bona fide need for a primary calibration procedure in which the environment of the density tool is as close as possible to that encountered in routine logging. Such a calibration must then be combined with a density log presentation format in which the log data are plotted in $g\ cm^{-3}$ if meaningful in-situ rock density estimates are to be obtained.

GENERAL THEORY

The principle by which the density well-logging tool operates is a form of gamma ray spectroscopy. The tool emits gamma rays into the rocks around a borehole and detects the intensity of gamma rays backscattered by interactions between this gamma radiation and the atoms making up the rock. There are three principal processes by which

the interaction between a gamma ray photon and an atom can take place: Compton scattering, photo-electric absorption, and pair production (Figure 1).

1) Compton Scattering. This process results from the collision of an incident gamma ray photon with an outer shell electron of an atom. This collision causes the ejection of the electron from the atom and the scattering away of the incident photon with a lower energy. Compton scattering generally occurs at gamma ray energies between 0.5 and 2 Mev.

2) Photo-electric Absorption. In this process the collision between a gamma ray photon and an electron results in the loss of all the photon's energy to the latter which is then emitted as a photo-electron. In this instance, the photon is completely absorbed. This process occurs at relatively low incident gamma ray energies (i.e. <0.5 Mev) and/or when the atomic mass of the interacting element is high.

3) Pair Production. For incident photon energies above approximately 1 Mev, the gamma ray photons can react with the nuclei of atoms by the process of pair production. In this interaction, when the incident photon reaches the nucleus of the atom it "materialises" into an electron and a positron. The positron rapidly annihilates with the simultaneous production of two 0.5 Mev photons, the so-called secondary low energy radiation.

Most density tools are designed in such a way that Compton scattering will be the primary interaction process between the emitted gamma rays and the rocks around the borehole. This is so because the attenuation of the gamma ray beam due to Compton scattering is, for a given energy, dependent only on the number of electrons in the irradiated medium which is itself a reflection of the mean atomic number ($\bar{A}$) of the medium. Measurement of the gamma ray absorption due to pair production on the other hand would be influenced by the simultaneously produced secondary low energy radiation, while photoelectric absorption is dependent both on the electron density and the mean atomic weight ($\bar{Z}$).

In order to eliminate variations in the extent of Compton scattering arising from differences in initial photon energy levels, a mono-energetic gamma source is used. The energy level is chosen so that the energy of the gamma photons is too low to give rise to pair production yet high enough to prevent any significant photoelectric absorption taking place before the gamma rays reach the detector. Such an energy level is said to be within the so-called Compton scattering window (see Figure 2). For most elements encountered in geophysical logging the probability of photoelectric absorption becomes significant only after gamma ray energies fall below about 300 keV (Hallenburg, 1984; p. 250) while, as mentioned earlier, the threshold for pair production is approximately 1 Mev. The gamma source used in the BMR density tool is ^{137}Cs which has a gamma energy of 0.662 Mev which is well within the Compton scattering window.

TRANSMITTED AND BACKSCATTERED GEOMETRIES

There are two experimental geometries which can be used to measure the attenuation of gamma rays caused by their interactions with matter: a geometry based on transmission of gamma rays, and one based on their backscattering (see Figures 3a and 3b).

In the transmitted geometry, the material is placed between a collimated source and a detector and the beam is attenuated by Compton scattering as it passes through the material. The difference in intensity of the emitted and transmitted beams is a measure of the bulk density of the material. This procedure for measuring rock densities is both fast and simple and it is a technique which has been used here to advantage to determine rock densities in the laboratory.

In well-logging density tools, the distance between adjacent holes is normally too large to make use of a transmitted radiation geometry. Borehole density tools must therefore rely on backscattered radiation from the source to the detector through the surrounding rocks with

shielding in the tool to prevent direct transmission of radiation. In such a backscattered geometry, the intensity observed by the detector depends on two closely related properties of the material irradiated: the backscattering power and the attenuation coefficient. The former property determines the number of photons that are scattered back toward the detector while the latter one governs the number of photons that are absorbed.

The relationship between rock density and detected gamma intensity is quite different for the two types of geometry. In the case of transmitted radiation, a logarithmic relation between the observed gamma intensity and density exists, so that when the density is zero the observed intensity will equal that emitted while when the density is infinite, the observed intensity will be zero. In the case of the backscattered geometry however, the observed intensity will be zero for both extremes of density. Between these extremes, a domain of increasing intensity with density and a domain of decreasing intensity with density can be recognised (Figure 4). The transition between the increasing and the decreasing domains depends on the source to detector spacing and lies, for the tool described in this record, for the short-spaced detector at about 1.0 g cm^{-3} and for the long-spaced detector at about 0.5 g cm^{-3}. With progressively increasing densities in the increasing domain, the backscattering power is progressively more important than the attenuation, while the opposite is true for densities in the decreasing domain.

GAMMA RAY ATTENUATION DUE TO COMPTON SCATTERING

1) Transmitted Geometry

For the transmitted geometry, the attenuation of a gamma ray beam in an irradiated substance arising from Compton scattering can be expressed by the spectroscopic relation:

$$I = I_o e^{-u_c d} \qquad (1)$$

in which I is the intensity of the transmitted beam, I_o the intensity of he incident beam, d the thickness of the layer of irradiated material and u_c the Compton linear attenuation coefficient. The latter coefficient is a material constant which is proportional to the number of electrons per unit volume (i.e. the electron density) and the energy of the incident photons. Hence for a mono-energetic source, u_c is proportional only to the electron density (N_e).

Now the electron density of an element is given by:

$$N_e = \rho.N.Z/A \qquad (2)$$

where ρ is the density, N is Avogadro's number, Z the atomic number and A the atomic weight. Thus for a given incident photon energy, u_c is proportional to $\rho.Z/A$. Since the ratio of the atomic number to the atomic weight of most elements found in common geological settings is found to be approximately constant (see Table 1) u_c can be taken as being approximately proportional to the density of the material,

i.e. $$u_c \simeq \text{constant}.\ \rho \qquad (3)$$

In practice the errors introduced by this approximation are found to be small for all but the heavier elements in which the photoelectric effect becomes important and for environments in which large amounts of hydrogen occur.

TABLE 1

The Ratio of Atomic Number to Atomic Weight for Common Rock Forming Elements

Atomic Number	Element	Z/A
1	Hydrogen	0.9921
6	Carbon	0.4995
8	Oxygen	0.5000
11	Sodium	0.4785
13	Aluminium	0.4818
14	Silicon	0.4985
16	Sulphur	0.4991
17	Chlorine	0.4865
20	Calcium	0.4990
26	Iron	0.4656
29	Copper	0.4564
30	Zinc	0.4589

2) Backscattered Geometry

The path of a single gamma ray photon in the backscattered geometry is illustrated in Figure 5. The photon, with an initial energy E_1 travels a distance r_1 to an electron at point P and is scattered backwards with a decreased energy E_2 over a distance r_2 to the detector. As discussed by Mathew (1976), the number of photons that reach point P is proportional to:

$$(1/r_1^2)e^{-u_1.\rho.r_1} \qquad (4)$$

where u_1 is the Compton linear attenuation coefficient for photons with energy E_1. Photons scattered from point P in the direction of the detector suffer further attenuation such that the intensity of the gamma rays reaching the detector will be given by the proportional relation (Mathew, 1976):

$$I \propto (\rho/r_1^2)e^{-[\rho.(u_1 r_1 + u_2 r_2)]} \qquad (5)$$

where u_2 is the Compton linear attenuation coefficient for gamma rays with energy E_2.

Since the path length travelled by gamma ray photons reaching the detector is a function of the source to detector spacing in the tool, and this spacing is constant in the BMR tool, the intensity of the detected gamma rays is again a function of the electron density of the material irradiated.

For ease of presentation in the modelling of the backscattered intensity and rock density data to be presented below, equation (4) can be rewritten as:

$$I = A.\rho.e^{-B.\rho} \qquad (6)$$

where A and B are constants.

FACTORS AFFECTING WELL-LOG DENSITY MEASUREMENTS

The intensity of the gamma ray beam measured by the detectors in a well-log density tool can be influenced by factors other than just the density of the rock type penetrated by the borehole. These factors can be broadly grouped into two categories: physical effects and instrument effects.

1) Physical effects

The sodium iodide crystal detectors in the density tool sense not only the gamma rays emitted from the ^{137}Cs source but also gamma radiation originating from the decay of isotopes of potassium, uranium and thorium in the rocks surrounding the borehole. In practice density tools such as the one used here are designed to minimise the effects of such natural radiation. This is achieved through the use of detector assemblies which are relatively insensitive to natural gamma ray emissions and by using a ^{137}Cs source which has a high output (generally >100 milli-Curies). The latter results in a decrease in the level of importance of variations in natural gamma background emissions to the overall recorded gamma intensity. Notwithstanding these steps however, it is nevertheless true that reliable density estimates are unlikely to be obtained when the rocks surrounding a borehole are particularly rich in radioactive nuclides, as for example with a uranium ore deposit.

Reliable estimates of the density of the rocks surrounding a borehole are also jeopardised by the presence of appreciable amounts of mudcake on the borehole wall. Such mud, particularly if it is barytes rich, can impose its own signature upon the recorded gamma ray intensities to the extent that the resulting density estimates are substantially in error. These errors can be circumvented by applying corrections to the density estimates either by directly measuring the thickness and density of the mudcake or by using a "Spine and Ribs plot" (Wahl et al, 1964). Such corrections have not been applied in the present work because mudcake was not detected in any of the holes logged.

Errors are also introduced into estimates of in-situ rock

densities by borehole rugosity which can result in the interposing of water or air-filled pockets between the density tool and the borehole wall against which it is pressed. In such a situation the gamma ray signals reaching the detectors will again reflect, at least in part, the absence of rock in the vicinity of the probe. While in theory a correction similar to the mudcake one discussed above could be applied to the density estimates, in practise this is not a realistic option with the existing density tool. This is so because borehole diameter is presently measured with only a single arm caliper mounted on the opposite side of the density tool to the gamma ray detectors. Hence borehole asperities are only imperfectly resolved. For the purposes of the present calibrations therefore, no data have been used from portions of the boreholes where the walls are rough or the hole diameter is uneven, as indicated by the caliper log.

A systematic difference in tool response is observed between density logging in water and in air-filled boreholes arising from the differing backscattering power and attenuation of water and air. Since most of the logging likely to be carried out with the present density tool is likely to involve water-filled holes, the present calibration measurements have all been made at depths below the standing water level in the respective boreholes. Similarly, since the presence of PVC or other casing also influences the density estimates, the present measurements have been made in uncased holes.

2) Instrument Effects

Due to the random nature of the gamma photon emissions and the multiplicity of ray paths between the source and the detector, there is always a finite chance that the arrival of one photon at the detector may occur so close to the preceding one that it cannot be separated by the detection circuitry. The length of time during which a succeeding photon arrival cannot be detected is termed the system deadtime. This deadtime introduces errors to the measurement of gamma intensities and imposes limits on the maximum count rates that can be reliably determined. The deadtime for the present density tool has not been determined in the present work and hence constitutes an unknown error in the density estimates obtained from the logs.

Since the calibration of the density tool response is in terms of the intensity of the gamma rays reaching the detectors, it follows that any reduction in the strength of the ^{137}Cs source due to radioactive decay will compromise the calibration. Fortunately the ^{137}Cs used in the tool has a half life of 30.23$\pm$ 0.16 years (Weast, 1981) which means that the calibrations reported here should be reasonably applicable for at least 1-2 years. That the source strength is only decaying slowly with time is born out by plots of the secondary calibrations performed regularly with the density tool. These calibrations involve the recording of the intensity of gamma emissions backscattered by two standards of known density - a block of perspex and a block of an aluminium alloy. The results of these calibrations are plotted in Figure 6 for the years 1983 to 1986.

EQUIPMENT AND METHODS

FIELDWORK

The well-logging system used by the BMR was designed and built by GEOEX (Haigh and Henderson, 1979). It is equiped with 9 logging tools (density, neutron, self-potential, single point resistance, sonic, lithological gamma, caliper, deviation, and induced polarisation), a Comprobe winch with 1450 metres of multiconductor cable, and an operating system built around a Hewlett Packard 9835A desktop computer and 6940 multiprogrammer. Log data are stored digitally on 1/2 inch magnetic tape during logging and can be plotted either immediately following logging or at a later date as required. The whole system is housed in a purpose built truck (Figure 7).

The density probe which is the subject of the present paper simultaneously measures the density of the rocks around the boreholes with two separate detectors. The short-spaced detector is situated 15 cm from the ^{137}Cs source at the bottom of the probe, and the long-spaced detector is situated 48 cm from the source. A single arm caliper device which is also housed in the tool is used to determine the diameter and rugosity of the boreholes logged. This caliper,

together with a bowspring assembly, also serves to press the side of the tool carrying the collimated ^{137}Cs source against the opposite borehole wall. The principal components of the density tool are illustrated in Figure 8.

The logging results presented here have been obtained at a uniform logging speed of 3 metres per minute. This logging speed is only half that normally employed with the system. The slower logging speed was used in an attempt to reduce the statistical errors introduced by the variability of output of the ^{137}Cs source. The effects of this noise have been further reduced by applying a moving average filter to the recorded data. Details of this filtering are given on each log.

Three boreholes have been logged for this work in addition to one of the calibration pits constructed by the South Australian Department of Mines and Energy (SADME). The boreholes were selected in order to provide as wide a range of rock densities as possible for the calibration exercise. In each case the boreholes were of HQ size (i.e. nominal diameter of 9.68 cm) and were uncased. Specific details for each of these boreholes are as follows:

1) Borehole W. This borehole is situated within the mining lease of the Woodlawn Mines Company near Tarago in south eastern New South Wales and approximately 70 km north east of Canberra. The hole was drilled vertically several years earlier by the Company to a total depth of in excess of 700 metres but for the present work logging was carried out only to a depth of 342.2 metres. The quality of the borehole wall was found to be good with the exception of three minor washouts which occurred along lithologic boundaries at 56, 84 and 111 metres. The water table was encountered at a depth of 36 metres.

The rock types intersected by the borehole include sericitic shales, tuffaceous shales, siliceous shales, dolerites, quartzitic tuffs and massive sulphides (principally pyrite, chalcopyrite and sphalerite).

2) Borehole BMR155. This borehole was drilled by the BMR as part of its stratigraphic drilling programme in the Canberra region between May 1976 and May 1979 (Henderson 1978, 1983). The hole was drilled vertically to a total depth of 240.4 metres using HQ equipment on land

adjoining the Barton Highway approximately 25 kilometres north west of Canberra. Due to partial collapse of the bottom of the hole during the intervening 7 years however, the hole could only be logged for the present work to a depth of 204.0 metres. The quality of the borehole wall was found to be generally good though some washouts were encountered between 39 and 43 metres, between 108 and 111 metres and between 166 and 169 metres.

The rock types intersected by this borehole comprise a meta-sedimentary sequence of limestones, siltstones, mudstones, calci-lutites and marbles with a few volcanic intercalations of dacite and ashstone.

3) Borehole Newcastle 2. This borehole was purpose drilled for the present work. The hole is situated on the BHP Company's Stockton Borehole Colliery Lease near the town of Barnsley in the Hunter Valley of New South Wales. This vertical borehole was drilled with HQ equipment to a depth of 31 metres and was sited in order to intersect representative low density coal measure rocks. The rock types recovered included coal of the Great Northern seam of the Newcastle Coal Measures, fine grained porous sandstone, coarse grained porous sandstone and conglomerate. The quality of the borehole wall in the arenites and rudites was generally good but some washing out of the coal occurred during the drilling. A standing water level of 4.2 metres was maintained during the logging.

4) SADME Calibration Pit AM-4. This calibration pit was constructed at Glenside in South Australia by SADME. The pit which is 8.54 metres deep, has been constructed with 4 materials of differing density, viz.: a topmost 1.4 metre thick layer of foam with a density of 1.86 g cm^{-3} above 2.76 metres of "API mix" which has a density of 2.19 g cm^{-3} which in turn overlies a further 1.84 metres of foam with a density of 2.00 g cm^{-3}. The bottom 1.98 metres is composed of barytes with variable densities of up to 3.2 g cm^{-3}.

LABORATORY WORK

Rock samples were selected from the core inventory of the 3 boreholes for laboratory measurements of density and porosity. The selection of core was based on rock type, layer thickness, core quality, the stability of density probe response over the depth interval represented by the core, and borehole wall quality. The aim was to obtain rock samples which covered a wide range of densities and which were at the same time representative of units thick enough to be resolvable by the density probe.

Two types of density measurements were made on the core samples selected. Firstly, core from boreholes W and BMR155 amounting to a total length of approximately 11 metres was taken to the CSIRO Division of Mineral Physics in Port Melbourne for measurements of dry bulk density using a CORAN apparatus. This machine was designed and built by the CSIRO for the rapid determination of the densities of freshly retrieved oil shale cores (Mathew et al, 1984). The principle by which CORAN operates is gamma ray attenuation due to Compton scattering in a transmitted geometry. Rock core is placed between a ^{137}Cs source and a detector and the resulting intensity of the transmitted gamma ray beam determined. This intensity is then related to the density of the core through equation (1). When the intensity of the gamma ray source is constant, as it can be assumed to be when a long half-life radioactive nuclide is used, (1) can be rewritten as:

$$\rho = A/d - (B.\ln I)/d + C \qquad (7)$$

where A, B and C are constants that can be determined by a calibration. Such a calibration was performed prior to using the CORAN apparatus by recording the gamma ray intensities transmitted by 8 calibration samples with densities in the range 1.62 to 2.82 g cm^{-3}. The density of each of these regular cylindrical samples was calculated from measurements of their weights, as determined by a sensitive electronic balance, and estimates of their dimensions made using a vernier caliper. The values used for the gamma ray intensities

transmitted by each sample consisted of the mean of three separate counts over 10 seconds as registered by the detector. The calibration data were then analysed with a linear regression program to obtain best estimates of the constants A,B and C. The results of this regression analysis are given in Appendix A.

Approximately 550 measurements of the dry bulk densities of the core samples were then made with the CORAN apparatus. These measurements were generally made every 2 cm along the pieces of core in order to assess the extent and scale of any variations in the density in these specimens.

A second series of density measurements was then made on core from the W and BMR155 boreholes together with a number of measurements on core from the Newcastle 2 hole. For all these measurements discs ~3.5 cm long were cut from the 6.35 cm diameter core. The discs were then cored along their axis to produce 2.5 cm diameter cylinders suitable for the measurements. The final stage in sample preparation was to dry the samples at 105^{o}C for 24 hours to drive off water held in interconnected pores and adsorbed to the sample surfaces. These sample preparation procedures produced 43 samples of 7 different rock types from borehole W, 38 samples of 9 different rock types from borehole BMR155 and 29 samples of 4 lithologies from borehole Newcastle 2 (see Appendices B and E for details).

The samples were measured in the BMR Core and Cuttings Laboratory in Fyshwick, ACT for dry weight, bulk volume and porosity. Dry weight was measured with a sensitive electronic balance, bulk volume was determined by the Archimedes principle using mercury as the immersion medium, and porosity was estimated with a heliometer. The latter device measures the volume of helium that invades a sample under the action of a small positive pressure.

Dry bulk densities were calculated from the dry weight and bulk volume measurements. Wet bulk densities were then calculated on the assumption that the measured porosity would have been saturated with fresh water when the samples were originally in-situ since all the samples came from below the water tables in the respective boreholes.

PROCESSING AND NUMERICAL MODELLING OF THE RESULTS

As discussed above, 2 types of laboratory rock density measurements have been made on the core from the BMR155 and W boreholes. For the purposes of the numerical modelling of the density tool response for these boreholes however only one set of data, the CORAN data, have been used. These data are preferred because they are continuous over depth intervals of up to 50 cm which makes them more readily comparable to the well-logging data and because they allow an assessment of the extent of fine scale density variations in the core. Each individual CORAN density measurement is however made through a relatively small volume of rock core since the cross-sectional area of the gamma ray beam used is only $\sim$1 cm^2 and the diameter of the core is only $\sim$6.3 cm. This contrasts with the well-logging tool which for the short spaced detector produces rock density estimates averaged over 15 cm, and for the long spaced detector, averaged over 48 cm. In order to make the CORAN results more comparable to the density tool's response it has therefore been necessary for the purposes of the calibrations to average the former. A moving filter length of 15 has been used for this averaging.

The CORAN data, which correspond to dry bulk density estimates, have not been corrected for the effect of water filling the available pore space in-situ because in all cases for the BMR155 and W samples measured, the porosities have been <2% (see below). In the case of the core from the Newcastle 2 borehole however, substantial porosities have been recorded in the samples and as a result CORAN was not used for the density measurements. With regard to these samples, the Fyshwick laboratory data for wet bulk densities have been used for the numerical modelling.

FORTRAN computer program &CALMD was written to perform non-linear regression analyses of the laboratory and field data to an equation of the form of (6). In these regressions the field data were regressed against the laboratory results (i.e. the former data were assumed to be of a lower quality than the latter). The results obtained with program &CALMD were then plotted with the aid of a FORTRAN plot

library written for use on the BMR's Hewlett Packard 1000 computers by P.L. McFadden.

RESULTS

GEOPHYSICAL WELL-LOGS

The results of the well-logging of the 3 boreholes and the logging of the SADME calibration pit are presented in Appendix C. These plots give details of all the logs run in the hole, i.e.: long-spaced density, short-spaced density, caliper, natural gamma, neutron, self-potential and resistance. The density log results are given in their unprocessed state, i.e. in counts per second.

Also included in the logs presented in Appendix C are lithologic logs made on the core recovered from the drilling operations. These lithologic records allow an assessment of the sensitivity of all the logs to be made, though for the present paper only the density results will be considered.

The influence of variations in borehole diameter and smoothness is apparent in all three logs obtained from the boreholes. Wherever there is a marked enlargement of hole diameter, as indicated by the caliper log, a pronounced increase in the intensity of gamma rays returned to the two detectors results. This is so because for all three boreholes, the densities of the rocks surrounding the hole are sufficiently high to put the tool response in the domain of increasing intensity with decreasing density (see Figure 4).

Inspection of the density logs for the BMR155 borehole suggest that the densities of the different rock types penetrated by this borehole are all fairly similar. This conclusion is also supported by the results of the laboratory studies on the core from this borehole (see below). In contrast, the W and Newcastle 2 boreholes show wide ranges of rock density, with the logs of the former showing good resolution of the massive sulphide layers and the logs of the latter providing clear indications of the presence of the coal.

LABORATORY RESULTS

The results of the dry bulk density measurements made on the core from the BMR155 and W boreholes with the CORAN density analyser are tabulated in Appendix D. Similarly, the results of the laboratory determinations of dry bulk densities, wet bulk densities and porosities made on the core from all three boreholes are listed in Appendix E. As is discussed below, the density estimates obtained with the two methods are in excellent agreement.

A compilation of the field and laboratory results used in the calibration of the density tool is presented in Table 2. Data are listed for each of the boreholes and for the AMDEL Calibration pit in terms of rock type (or material in the case of the Calibration pit), density and count rate recorded with the density probe for the particular horizon in each hole. In the case of the BMR155 and W boreholes, the tabulated rock densities are calculated moving averages of the CORAN data made using a filter length of 15 (see above). For the Newcastle 2 borehole the stated densities are wet bulk densities as evaluated in the Fyshwick laboratory, while the calibration pit densities have been provided by SADME. In each case the count rates recorded by the density probe are given as mean values (in counts per 200 milli-seconds) bracketed by estimates of the maximum and minimum count rates recorded at each horizon.

TABLE 2

List of Data Used for the Calibration of the Density Tool

BOREHOLE	ROCK OR MATERIAL TYPE	DENSITY ($g\ cm^{-3}$)	COUNT RATE ($counts\ 200ms^{-1}$)					
			SHORT-SPACED DETECTOR			LONG-SPACED DETECTOR		
			mean	max	min	mean	max	min
AMDEL								
PIT	FOAM	1.86	148	154	142			
AM4	FOAM	2.00	142	148	136	60	64	56
	API MIX	2.19	130	134	125	43	46	39
NEWCA-	COAL	1.41	175	176	174	180	183	177
-STLE	CONGLOMERATE	2.37	117	122	112	27	31	23
2								
BMR155	SANDSTONE	2.66	100	104	96	15	16	14
	MUDSTONE	2.71	98	102	94	14	15	13
	LIMESTONE	2.72	96	100	92	14	15	13
W	SILICIFIED SHALE	2.70	97	100	94	14	15	12
	SERICITIC SHALE	2.73	96	99	94	13	16	10
	SHALE	2.75	95	97	93	12	14	11
	SHALE	2.77	93	95	90	12	15	10
	DOLERITE	2.92	87	89	84	10	11	8
	MASSIVE SULPHIDE	3.00				7	8	5
	MASSIVE SULPHIDE	3.80	52	57	46			
	MASSIVE SULPHIDE	4.00	45	50	40	1	2	0
	MASSIVE SULPHIDE	4.10	43	48	38			
	MASSIVE SULPHIDE	4.20	40	50	30			
	MASSIVE SULPHIDE	4.30	38	43	33			
	MASSIVE SULPHIDE	4.40	35	45	25			
	MASSIVE SULPHIDE	4.50	32	33	30	1	1	0

NUMERICAL MODELLING

The data of Table 2 were used to constrain best estimates of the adjustable constants A and B in equation (6) using a non-linear regression routine. The results for the short-spaced and long-spaced detectors are plotted separately in Figures 9 and 10 and are summarised in Table 3. The short-spaced detector data have been analysed twice. In Figure 9a, all the relevant data in Table 2 have been used to constrain the fit, while in Figure 9b, the massive sulphide data have not been used. These two separate fits have been made in order to gauge the contribution to tool response arising from the expected increase in the amount of photoelectric absorption and the greater divergence of the Z/A ratio as density increases. The long-spaced detector results have not been treated in this way because of the paucity of data at densities above 3 g cm^{-3}.

Table 3

Results of Non-Linear Regressions to Calibration Data

Detector	Results of the Regression			Data Used in the Regression	Text Figure Number
	A	B	S^2		
Short-spaced	445.14	-0.923	58.21	all data	9a
Short-spaced	472.87	-0.951	15.20	data <3 g cm^{-3}	9b
Long-spaced	3965.1	-2.439	13.34	data <3 g cm^{-3}	10

DISCUSSION

The results of the regressions given in Table 3 are notable in that in all cases, the sums of the squares of the residuals of the data about the fits are small. For example, the value of S^2 of 15.20 in Figure 9b implies a variance about the fit of only ± 1.1 counts squared per second squared and a standard deviation of only ± 1.0 counts per second. The corresponding values for the fit in Figure 10 are ± 0.89 and ± 0.94 respectively. In other words, the quality of the fits is in each case very good. This in turn means that density estimates made using these calibrations are likely to be accurate.

A number of remarks can be made about the two plots of the short-spaced detector data. Firstly, though the >3 g cm^{-3} massive sulphide data are not manifestly discordant to the fit in Figure 9b, they all lie above this fit which is constrained only by the lower density data. Since the chances of this distribution resulting purely from random variations is 1 in 256 for the 8 data points, this clearly is a very unlikely explanation. This distribution is however readily explained by recalling that the Z/A ratio at higher densities begins to diverge from the constant value of 0.5 assumed in the analyses. In such a situation, equation (6) can be re-written as:

$$I = A' . \rho . e^{-B' . (Z/A) . \rho} \qquad (8)$$

where A′ and B′ are different constants and the other parameters have their usual meaning

Clearly a reduction in the Z/A ratio will be reflected in equation (8) by an increase in the exponential term and hence in the intensity. Thus for higher densities, the recorded gamma ray intensities can be expected to be distributed systematically above a fit constrained by lower density data where Z/A $\simeq 0.5$. This deviation from the fit will be non-linear with increasing density both because of the exponential term in (8) and the non-linearity of the change in Z/A with increasing

Z. The position is further complicated by the intrusion of photoelectric absorption effects with increasing density. The result of these effects is to lower the intensity recorded for a given density because now photons are attenuated both by Compton scattering and Photoelectric absorption.

Since the >3 g cm^{-3} data in Figure 9b all lie above the plotted fit, it follows that the influence of decreasing Z/A must overshadow the reduction in intensity expected due to photoelectric absorption for the particular rock and mineral types logged in hole W. It is to be expected however that the magnitude and sign of such departures from the fit will differ with other high density mineral assemblages and rock textures encountered in other boreholes.

The results of the regressions have been used to replot the density log results from the boreholes logged during this work. These logs, which are plotted in g cm^{-3}, are presented in Appendix F together with the results of the caliper logs from each hole and plots of the density data in its original form. In order to allow the accuracy of these computed densities to be assessed, parts of these replotted log data have been abstracted and plotted in juxtaposition with the laboratory determined rock densities. These composite plots are presented in Figures 11, 12 and 13 for boreholes BMR155, W and Newcastle 2 respectively. Where both CORAN and Archimedes principle density measurements have been made, both are plotted. These laboratory data are unsmoothed and hence record much finer scale density variations than can be detected by the down-hole density tool. As can be clearly seen in the figures, there is excellent agreement between the two laboratory data sets and in the majority of cases between them and the processed well-logging data.

A number of observations can be made from the data presented in Figures 11, 12 and 13 which bear on the applicability of the calibrations to the interpretation of density logs made with the present down-hole tool. Firstly, in almost all instances, the well-log density estimates fall within 0.05 g cm^{-3} of the laboratory density determinations. Significant differences between the field and laboratory estimates occur only at levels in the holes where washouts

were produced during drilling (see for example Figures 11a and 11h). Fortunately, in all cases these discrepancies can be readily predicted from the accompanying caliper logs and hence incorrect density estimates can be avoided. A higher accuracy in the density estimates than the present results could not be expected given the inevitable fluctuations in gamma ray emission from the source. These fluctuations generally result in average variations in recorded gamma intensities at the detectors of $\pm$2-3 counts per 200 ms which corresponds to an uncertainty in density of ~0.05 g cm^{-3}.

A second observation that can be made from the figures concerns the scale of density variations that can be resolved with the down-hole tool. Reference to Figures 12k and 12n serves to highlight the inability of the down-hole tool to resolve in detail density variations on a 2cm scale. This is hardly surprising given the source to detector spacings of 15 and 48 cm respectively for the short and long-spaced detectors. The averaged density estimates produced from both the density well-logs do however appear to be quite sound.

Thirdly, Figure 12j illustrates the limitations on reliable density and bed thickness estimates resulting from thin interbedding of rock units. In this case, a layer of <10 cm thickness consisting of 30-40% pyrite which is interbedded between silicified shale units, is imprecisely located by the density log and its density is underestimated over its margins. The implication from this example is that reliable density estimates can only be anticipated from the density tool for bed thicknesses of the order of the source to detector spacing.

The density estimate at the centre of the massive sulphide interbed in Figure 12j is somewhat higher than that measured on the core in the laboratory. This may imply slightly greater concentrations of pyrite or other massive sulphides in the rocks around the hole than are found in the core.

While the re-plotted density logs are substantially in agreement with the laboratory data, reference to the logs in Appendix F clearly shows that the reference density marks for the perspex and magnesium alloy standard blocks used in the secondary calibrations are

discordant. For both the long-spaced and the short-spaced detectors, the secondary calibration density estimates plot at too low a density, with the 1.19 g cm^{-3} in each case being seriously in error. In other words, "eye-ball" density estimates made from these calibration marks would be prone to large errors. It is clear from these comparisons that the common practice of presenting density logs in counts per second with secondary calibration marks in g cm^{-3} is most unsatisfactory.

CONCLUSIONS

This study has produced an effective numerical model of the response of the BMR's down-hole density probe over a wide range of rock densities. The inputs to this model have been the recorded density probe responses in 4 holes and a set of independently determined rock density measurements relevant to the lithologies intersected by these holes.

Non-linear regressions of the backscattered gamma ray intensities recorded by the density tool at a number of levels in the 4 holes have been carried out against the laboratory density measurements. The resulting calibration equations for the density tool are as follows.

$$I = 471.83.\rho.e^{-0.950.\rho}$$ for the short-spaced detector, and

$$I = 4046.7.\rho.e^{-2.461.\rho}$$ for the long-spaced detector.

The estimates of average in-situ rock density obtained from the well-logs using these calibration equations have been found to be accurate to within 0.05 g cm^{-3} for smooth walled, water-filled boreholes penetrating rocks of densities between 1.44 and 4.5 g cm^{-3}.

BIBLIOGRAPHY

Haigh, J.E and R.J. Henderson, Computerised processing and presentation of borehole data. Bull. Aust. Soc. Explor. Geophys., 10, 228-231, 1979.

Hallenburg, J.K., Geophysical Logging for Mineral and Engineering Applications, Pennwell Books, Tulsa, Oklahoma, 1984.

Henderson, G.A.M., Stratigraphic holes drilled in the Canberra area, 1971 to 1976. Bureau of Mineral Resources, Geology and Geophysics, Record 1978/28, 1978.

Henderson, G.A.M., Stratigraphic holes drilled in the Canberra area, 1979 to 1981. Bureau of Mineral Resources, Geology and Geophysics, Record 1983/7, 1983.

Mathew, P.J., Gamma-gamma methods for density and composition measurement in boreholes. In: McCracken, K.G.,(ed.), Geophysical Techniques in Borehole Applications, Australian Mineral Foundation, 1976.

Mathew, P.J., T. B. Fogg and J.G. Miles, Nuclear techniques in the oil shale industry: an oil shale borehole core density analyser. CSIRO Division of Mineral Physics, Mineral Physics Communication, MPC006, 1984.

Wahl J.S., J. Tittman and C.W. Johnstone, The dual spacing formation density log, J. Pet. Tech., 1964.

Weast R.C. (ed.), CRC Handbook of Chemistry and Physics, Chemical Rubber Publishing Company, Boca Raton, 1981.

APPENDIX A

Data used in a linear regression program to determine the constants A, B and C in the formula: $q = A/d - B\ln I/d + C$.
This is the relationship between density and count rate (I) as it is used for the CORAN density analyser.

STANDARD SAMPLE	MEAN y-COUNTS	DIAMETER (cm)	lny/d	1/d	RHO ($g\ cm^{-3}$)
GR9	267251	7.050	1.7725	0.1418	1.665
GR12	300417	5.990	2.1057	0.1669	1.625
B5	232255	6.090	2.0288	0.1642	2.257
GR14	269143	6.308	1.9821	0.1585	1.837
M1	214804	5.496	2.2339	0.1820	2.692
B6	233433	5.182	2.3853	0.1930	2.618
A13	228187	5.040	2.4480	0.1984	2.819
W1	170071	6.960	1.7305	0.1437	2.684

Final result of the linear regression

COEFFICIENTS

Variable	Mean	Coefficient	Standard error
lny/d	2.086	-15.2409	0.4173
1/d	0.1686	201.615	5.180
constant		0.0799751	

RESIDUAL ANALYSIS

q ($g\ cm^{-3}$) observed	q ($g\ cm^{-3}$) predicted	q ($g\ cm^{-3}$) residual
1.66500	1.65461	0.01039
1.62500	1.63691	-0.01191
2.25700	2.26456	-0.00756
1.83700	1.82711	0.00989
2.69200	2.72742	-0.03542
2.61800	2.63773	-0.01973
2.81900	2.77084	0.04816
2.68400	2.67780	0.00620

APPENDIX B

Rock type and depth interval of selected core from borehole W and depth of one inch diameter samples.

ROCK TYPE	DEPTH INTERVAL (m)	DEPTH OF ONE INCH SAMPLE (m)
DOLERITE	88.50 - 88.80	
	89.40 - 89.70	
SERICITIC SHALE	133.95 - 134.00	
	134.10 - 134.25	
	134.40 - 134.50	
	134.60 - 134.80	
	135.20 - 135.60	135.31
		135.35
		135.39
	137.20 - 137.65	
DOLERITE	145.40 - 145.60	145.43
		145.47
		145.51
		145.55
		145.59
	145.65 - 145.85	145.69
		145.73
		145.77
		145.81
	145.90 - 146.10	
	148.35 - 148.40	
	148.45 - 148.58	
	148.60 - 148.70	
	152.20 - 152.35	
	152.45 - 152.60	
TUFFACEOUS SHALE	162.20 - 162.40	162.29
		162.33
		162.37
	163.40 - 163.60	
	165.15 - 165.35	165.21
		165.25
		165.29
MASSIVE SULPHIDE	170.35 - 170.65	170.52
		170.55
	191.45 - 191.60	
	192.80 - 193.00	192.85
		192.89
	194.65 - 194.75	194.68
	201.00 - 201.38	201.05
		201.09
		201.17
		201.21
		201.31
		201.35
	201.40 - 201.80	

APPENDIX B (Continued)

Rock type and depth interval of selected core from borehole W and depth of one inch samples.

ROCK TYPE	DEPTH INTERVAL (m)	DEPTH OF ONE INCH SAMPLE (m)
SHALE	232.00 - 232.35	
	232.40 - 232.60	232.49
		232.57
	232.60 - 232.80	
	234.25 - 234.65	
	238.30 - 239.20	238.89
		238.93
SILICIFIED SHALE	256.75 - 257.15	256.95
		256.99
		257.02
	257.25 - 257.45	
	257.90 - 258.35	258.05
		258.09
		258.13
QUARZITIC TUFF	297.05 - 297.45	
	299.80 - 299.90	299.83
	299.90 - 300.10	299.99
		300.03
		300.05

APPENDIX B (Continued)

Rock type and depth interval of selected core from borehole BMR155 and depth of one inch diameter samples.

ROCK TYPE	DEPTH INTERVAL (m)	DEPTH OF ONE INCH SAMPLE (m)
DACITE	38.65 - 38.85	
	38.85 - 39.00	38.89
		38.93
		38.97
	39.30 - 39.55	39.38
		39.42
		39.46
LIMESTONE	44.15 - 44.30	
	45.00 - 45.10	
MUD/ SILTSTONE	75.00 - 75.10	75.06
	75.12 - 75.18	
CALCI-LUTITE	84.55 - 84.65	
	84.70 - 84.80	
	85.60 - 85.85	85.70
		85.78
		85.82
	86.15 - 86.30	

ROCK TYPE	DEPTH INTERVAL (m)	DEPTH OF ONE INCH SAMPLE (m)
MARBLE	101.80 - 101.95	101.86
		101.90
	103.20 - 103.35	103.26
		103.30
	103.35 - 103.50	103.40
		103.44
SANDSTONE	139.00 - 139.20	139.04
		139.09
		139.12
	140.70 - 140.90	
	140.90 - 141.05	141.00
LIMESTONE	157.65 - 158.00	157.86
		157.91
		157.94
	159.10 - 159.40	159.18
		159.22
		159.26
CALCAREOUS SANDSTONE	164.95 - 165.08	165.00
	165.08 - 165.20	
	166.30 - 166.50	166.40
		166.44
MUD/ LIMESTONE	183.00 - 183.15	183.04
		183.08
	183.65 - 183.80	183.70
		183.74
	184.80 - 185.00	184.90
		184.94
MUDSTONE	202.10 - 202.45	202.30
		202.33
		202.38
	203.60 - 203.70	

APPENDIX C

LEGEND

Borehole BMR155:


SNDST Sandstone

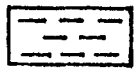
SLST Siltstone

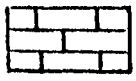
LMST Limestone

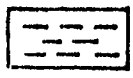
MDST Mudstone


DAC Dacite


ASH Ashstone

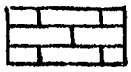
MARB Marble


CASST Calcareous sandstone

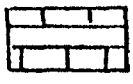
CA-LU Calci-lutite

BMR THEORETICAL GEOPHYSICS AND SPECIAL PROJECTS

COMPUTERISED BOREHOLE LOGGING

ROCK PROPERTIES
BARTON HWY

BOREHOLE NO. BMR 155

DEPTH LOGGED 206.82 M.

DATE LOGGED 12.11.85

DATE PROCESSED 5.3.1986

LOGGING SPEED

DENSITY PROBE

NEUTRON PROBE

DATUM ABOVE GROUND LEVEL

OPERATOR: JAMP LMLA

DATA LOG. FILE 74586 B.

DATA PLOT. FILE 74586 B1

WATER LEVEL

PLOTTING SCALE 1:250

CALIPER

SELF POTENTIAL mV

NATURAL GAMMA cps

SHORT SPACED DENSITY cps

RESISTANCE Ohm.m

NEUTRON cps

LONG SPACED DENSITY cps

DEPTH (M.)

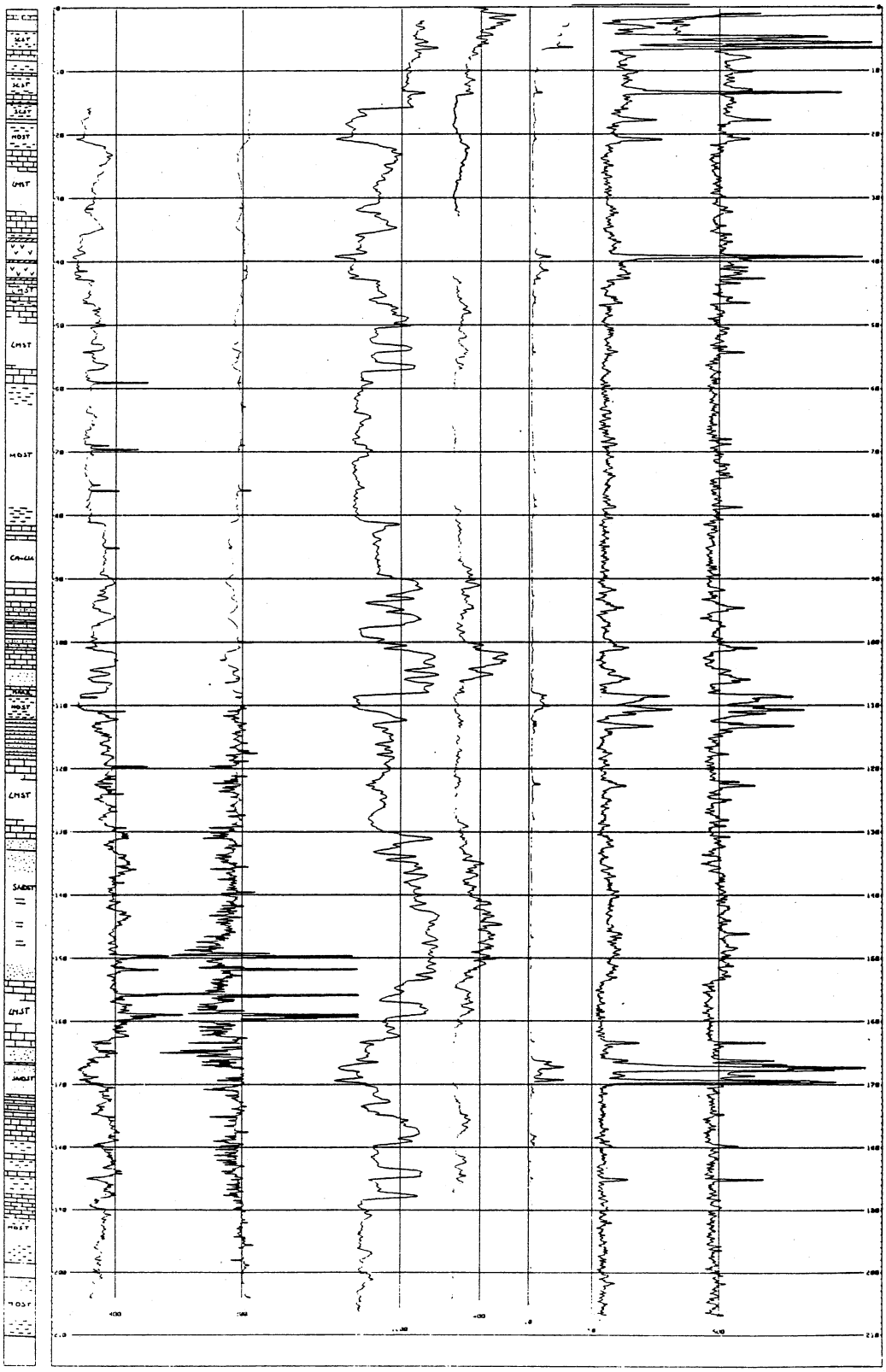

LEGEND

Borehole W:

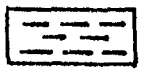
SHALE Shale

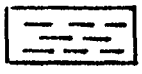
SRSH Sericitic shale

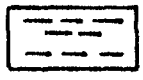
SLSH Silicified shale

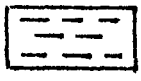
TFSH Tuffaceous shale


DLRT Dolerite


MVSD Massive sulphide

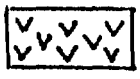
QETF Quartzitic tuff

BMR THEORETICAL GEOPHYSICS AND SPECIAL PROJECTS

COMPUTERISED BOREHOLE LOGGING

ROCK PROPERTIES
WOODLAWN

LOGGING SPEEDS:
DENSITY PROBE .5 M/MIN
NEUTRON PROBE .5 M/MIN
DATUM ABOVE GROUND LEVEL 0.00 M.
OPERATOR : GREP CREW
DATA LOG VER: 76106.01
DATA PLOT VER:76106.01
WATER LEVEL: 2.45 M.

PLOTTING SCALE: 1/250

BOREHOLE NO.W

DEPTH LOGGED 342.20 M.
DATE LOGGED 28 11 85
DATE PROCESSED 05 12 85

SELF POTENTIAL mV
66 132 198 264 330

NATURAL GAMMA cps
0 250 500
CAL AMP1 200

LONG SPACED DENSITY cps
0 50 100 150

SHORT SPACED DENSITY cps
0 100 200 300 400 500 600
20 30

RESISTANCE Ohms
0 66 132 198 264

NEUTRON cps
400 800 1200 1600
CAL 0 63

CALIPER cm
10 12.5 15
CAL CM 10

DEPTH (M.)

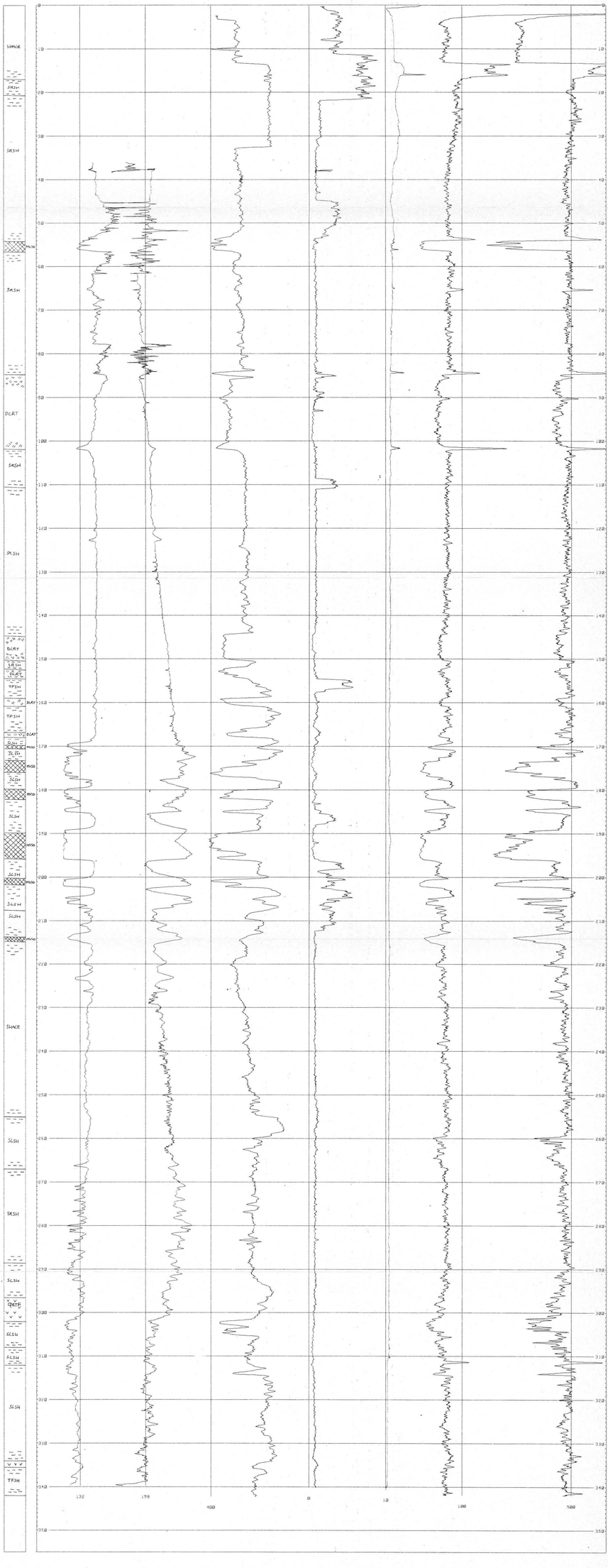

LEGEND

Newcastle 2

Shale

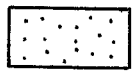

Finegrained sandstone

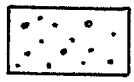

Coarse-grained sandstone

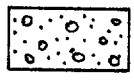

Sandy conglomerate

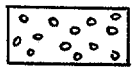

Conglomerate

Laminated siltstone/ sandstone

Coal

BMR ROCK PROPERTIES RESEARCH

COMPUTERISED BOREHOLE LOGGING

BMR SCIENTIFIC
AMDEL PITS

LOGGING SPEEDS
DENSITY PROBE 3 M/MIN
NEUTRON PROBE 3 M/MIN
DATUM ABOVE GROUND LEVEL .74 M.
OPERATOR: P. CHOPRA
DATA LOG VER: 7821Z.01
DATA PLOT VER 7860Z.31
WATER LEVEL: 4.71 M.

PLOTTING SCALE 1:10

BOREHOLE NO. AM 4

DEPTH LOGGED 8.19 M.
DATE LOGGED 23 03 85
DATE PROCESSED 28 10 86

RESISTANCE Ohms
Full Scale = 1
80 100 120 140 160

NEUTRON cps
Full Scale = 1
100 200 300 400
CAL #J

LONG DENSITY cps
Full Scale = 1
0 200 400 600
1:.74

CAL GM/CC 1:1.8

SELF POTENTIAL mV
Full Scale = 1
-20 0 20 40 60

SHORT DENSITY cps
Full Scale = 1
0 200 400 600 800
CAL GM/CC 11.2M9

DEPTH (M.)

Foam

API Mix

Foam

Barytes

0 0.5 1 1.5 2 2.5 3 3.5 4 4.5 5 5.5 6 6.5 7 7.5

120 20 300 200 400

COMPLOT

BMR ROCK PROPERTIES RESEARCH

COMPUTERISED BOREHOLE LOGGING

CALIBRATIONS
NEWCASTLE

LINEAR DENSITY EQUATION IS Counts= A*Dens*EXP(B*Dens)

LOGGING SPEEDS:
DENSITY PROBE 3 M/MIN
NEUTRON PROBE 3 M/MIN
DATUM ABOVE GROUND LEVEL 1.61 M.
OPERATOR : FRANK & ALEX
DATA LOG VER: 78506.01
DATA PLOT VER: 78607.31
WATER LEVEL: 84 M.

PLOTTING SCALE: 1:50

BOREHOLE NO. RKP 1
DEPTH LOGGED 28.76 M.
DATE LOGGED 03 13 86
DATE PROCESSED 28 10 86

SELF POTENTIAL mV
80 100 120 140 160

CALIPER cm.
10 15
CAL CM 10

LONG SPACED DENSITY g/cc
1.2 1.6 2 2.4 2.8
CAL GM/CC 1.19 1.74

SHORT SPACED DENSITY g/cc
1.2 1.6 2 2.4 2.8
CAL GM/CC 1.19 1.74

RESISTANCE Ohms
1400 1500 1600 1700 1800 1900

NEUTRON cps
0 400 800 1200
CAL #1 23

DEPTH (M.)

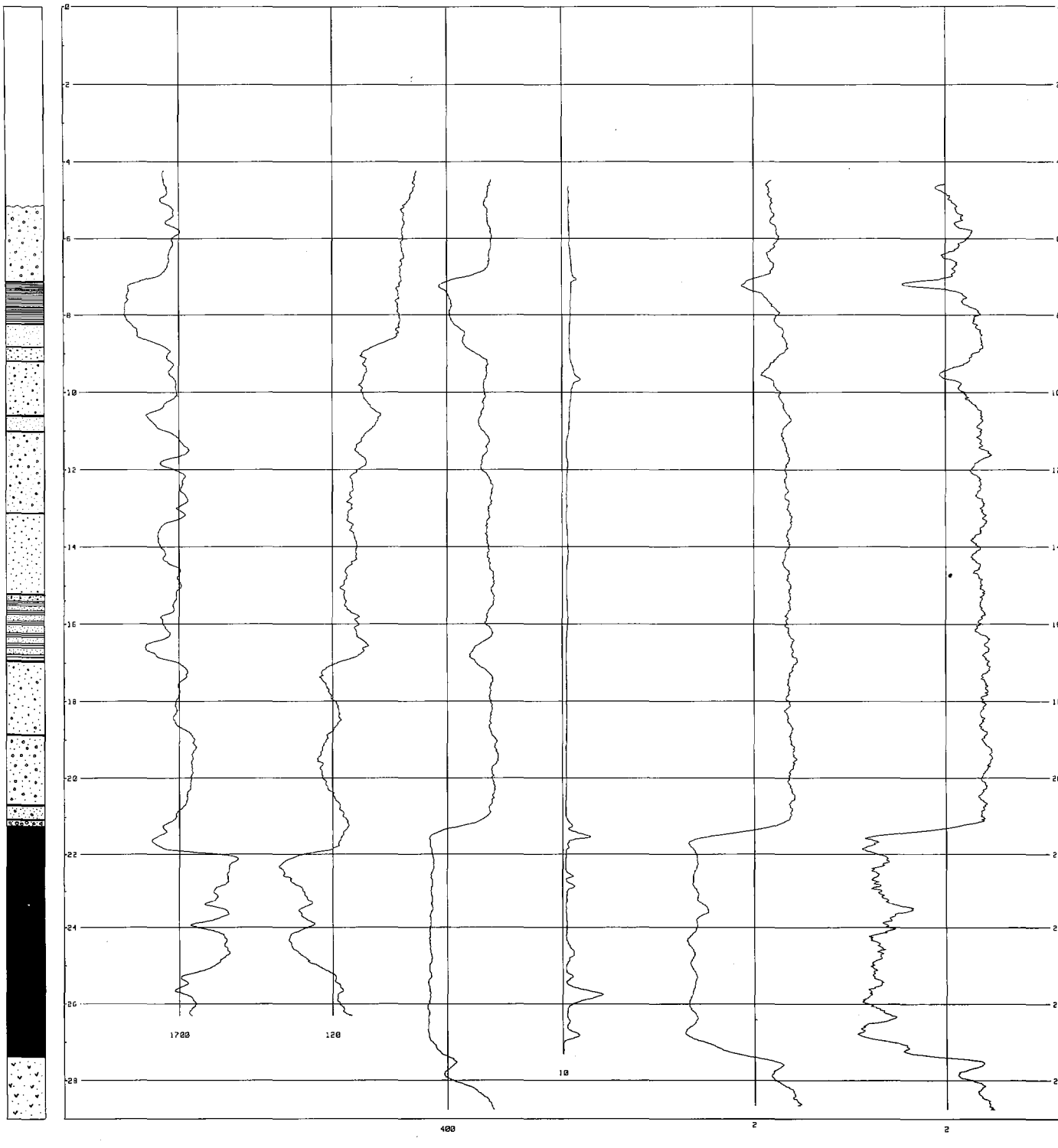

COMPLOT

APPENDIX D

Dry bulk densities measured with the CORAN density analyser.
Densities measured on core pieces from borehole W.
Listed as depth(m), density(g cm^{-3}).

DOLERITE

88.53 2.90	88.55 2.91	88.57 2.91	88.59 2.91	88.61 2.92
88.63 2.95	88.65 2.94	88.67 2.93	88.69 2.93	88.71 2.92
88.73 2.90	88.75 2.90	88.77 2.89	88.79 2.88	89.45 2.92
89.47 2.91	89.49 2.92	89.51 2.93	89.53 2.91	89.55 2.91
89.57 2.88	89.59 2.90	89.61 2.88	89.63 2.87	89.65 2.84

SERICITIC SHALE

133.97 2.77	133.99 2.77	134.11 2.74	134.13 2.74	134.15 2.74
134.17 2.75	134.19 2.78	134.21 2.75	134.23 2.75	134.41 2.73
134.43 2.74	134.45 2.73	134.47 2.73	134.49 2.75	134.63 2.80
134.65 2.79	134.67 2.79	134.69 2.78	134.71 2.79	134.73 2.80
134.75 2.78	135.25 2.75	135.27 2.74	135.31 2.74	135.35 2.75
135.39 2.74	135.43 2.75	135.47 2.74	135.51 2.74	135.55 2.73
137.21 2.75	137.23 2.75	137.25 2.75	137.29 2.75	137.33 2.73
137.37 2.73	137.41 2.73	137.45 2.74	137.49 2.72	137.53 2.72
137.57 2.72	137.61 2.74			

DOLERITE

145.45 2.82	145.47 2.81	145.49 2.81	145.51 2.81	145.53 2.81
145.55 2.82	145.57 2.81	145.59 2.81	145.69 2.83	145.71 2.83
145.73 2.83	145.75 2.84	145.77 2.84	145.79 2.84	145.81 2.83
145.91 2.84	145.93 2.83	145.95 2.82	145.97 2.83	145.99 2.83
146.01 2.82	146.03 2.83	146.05 2.84	146.07 2.85	148.38 2.83
148.39 2.82	148.40 2.82	148.47 2.83	148.49 2.87	148.51 2.85
148.53 2.84	148.55 2.85	148.57 2.86	148.63 2.86	148.65 2.88
148.67 2.88	148.69 2.87	152.21 2.82	152.23 2.82	152.25 2.80
152.27 2.81	152.29 2.80	152.31 2.79	152.33 2.80	152.47 2.82
152.49 2.80	152.51 2.79	152.53 2.79	152.55 2.79	152.57 2.79
152.59 2.79				

TUFFACEOUS SHALE

162.23 2.68	162.25 2.68	162.27 2.68	162.29 2.67	162.31 2.68
162.33 2.69	162.35 2.69	162.37 2.68	162.39 2.68	163.41 2.75
163.43 2.73	163.45 2.75	163.47 2.70	163.49 2.72	163.51 2.78
163.53 2.78	163.55 2.88	163.57 2.81	163.59 2.73	165.17 2.69
165.19 2.70	165.21 2.70	165.23 2.70	165.25 2.70	165.27 2.70
165.29 2.69	165.31 2.71			

MASSIVE SULPHIDE

170.37 3.00	170.39 2.87	170.41 2.90	170.43 2.95	170.45 3.02
170.47 2.90	170.49 3.01	170.51 2.94	170.53 3.06	170.55 3.02
170.57 3.02	170.59 3.05	170.61 2.99	170.63 3.06	191.49 3.14
191.51 3.26	191.53 3.71	191.55 3.61	191.57 3.64	192.83 3.54
192.85 3.60	192.87 3.79	192.89 3.92	192.91 4.06	192.93 4.27
194.66 4.52	194.68 4.52	194.70 4.54	194.72 4.52	194.74 4.51
201.01 3.80	201.03 3.66	201.05 3.60	201.07 3.77	201.09 3.75
201.11 3.73	201.13 3.86	201.15 3.96	201.17 4.08	201.19 4.14
201.21 4.31	201.23 4.48	201.25 4.45	201.27 4.48	201.29 4.51
201.31 4.55	201.33 4.57	201.35 4.54	201.41 4.52	201.43 4.52
201.45 4.53	201.47 4.53	201.49 4.51	201.51 4.55	201.53 4.53
201.55 4.55	201.57 4.55	201.59 4.48	201.61 4.43	201.63 4.50
201.65 4.52	201.67 4.49	201.69 4.54	201.71 4.44	201.73 4.43
201.75 4.47	201.77 4.47			

SHALE

232.01 2.63	232.03 2.64	232.05 2.65	232.07 2.64	232.09 2.77
232.21 2.76	232.29 2.73	232.31 2.75	232.41 2.70	232.43 2.69
232.45 2.67	232.47 2.68	232.49 2.67	232.51 2.65	232.53 2.66
232.55 2.66	232.57 2.65	232.59 2.64	232.65 2.78	232.67 2.76
232.69 2.78	232.71 2.77	232.73 2.76	232.75 2.76	232.77 2.75
232.79 2.77	234.27 2.76	234.29 2.77	234.33 2.77	234.37 2.79
234.41 2.76	234.45 2.77	234.49 2.78	234.53 2.78	234.57 2.78
234.61 2.76	238.31 2.73	238.35 2.75	238.39 2.77	238.43 2.83
238.47 2.81	238.51 2.87	238.55 2.76	238.59 2.76	238.63 2.75
238.67 2.77	238.71 2.73	238.75 2.74	238.79 2.75	238.83 2.74
238.87 2.74	238.91 2.74	238.95 2.74	238.99 2.75	239.03 2.75
239.07 2.76	239.11 2.75	239.15 2.76		

SILICIFIED SHALE

256.77 2.67	256.81 2.62	256.85 2.65	256.89 2.67	256.93 2.61
256.97 2.61	257.01 2.61	257.05 2.61	257.09 2.61	257.13 2.63
257.28 2.70	257.32 2.73	257.36 2.70	257.40 2.70	257.91 2.69
257.95 2.69	257.99 2.68	258.03 2.71	258.07 2.71	258.11 2.70
258.15 2.71	258.19 2.70	258.23 2.70	258.27 2.70	258.31 2.72

QUARTZITIC TUFF

297.09 2.69	297.13 2.68	297.17 2.69	297.21 2.78	297.25 2.78
297.29 2.80	297.33 2.79	297.37 2.79	297.41 2.80	299.81 2.79
299.83 2.79	299.85 2.77	299.94 2.79	299.97 2.81	300.01 2.80
300.05 2.80	300.09 2.80			

APPENDIX D (Continued)

Dry bulk densities measured with the CORAN density analyser.
Densities measured on core pieces from borehole BMR155.
Listed as depth(m), density(g cm^{-3}).

DACITE

38.68 2.61	38.71 2.62	38.73 2.63	38.75 2.60	38.77 2.59
38.79 2.61	38.81 2.60	38.87 2.63	38.89 2.63	38.91 2.64
38.93 2.65	38.95 2.64	38.97 2.66	38.99 2.64	39.34 2.62
39.36 2.64	39.38 2.60	39.40 2.61	39.42 2.62	39.44 2.63
39.46 2.61	39.48 2.61	39.50 2.59		

LIMESTONE

44.18 2.65	44.20 2.67	44.22 2.67	44.24 2.66	44.27 2.66
44.18 2.65	44.20 2.67	44.22 2.67	44.24 2.66	44.27 2.66
45.00 2.63	45.02 2.62	45.04 2.60	45.06 2.67	45.08 2.65

MUD/SILTSTONE

75.02 2.68	75.04 2.69	75.06 2.68	75.08 2.69	75.14 2.66
75.16 2.66				

CALCI-LUTITE

84.58 2.71	84.60 2.71	84.62 2.69	84.64 2.70	84.70 2.70
84.72 2.68	84.74 2.70	84.76 2.69	84.78 2.68	85.64 2.71
85.66 2.71	85.68 2.71	85.70 2.71	85.72 2.70	85.74 2.70
85.76 2.71	85.78 2.70	85.80 2.70	85.82 2.70	86.15 2.71
86.17 2.71	86.19 2.70	86.21 2.71	86.23 2.69	86.25 2.71

MARBLE

101.84 2.69	101.86 2.69	101.88 2.69	101.90 2.71	101.92 2.70
101.94 2.71	103.22 2.69	103.24 2.68	103.26 2.69	103.28 2.66
103.30 2.67	103.39 2.66	103.40 2.65	103.42 2.66	103.44 2.66
103.46 2.66	103.48 2.67			

SANDSTONE

139.04 2.64	139.07 2.64	139.10 2.66	139.13 2.65	139.15 2.67
139.18 2.65	140.72 2.65	140.76 2.65	140.80 2.67	140.83 2.65
140.87 2.66	140.94 2.65	140.97 2.65	141.00 2.65	141.01 2.65

LIMESTONE

157.68 2.71	157.71 2.72	157.77 2.73	157.80 2.72	157.84 2.72
157.88 2.73	157.91 2.71	157.94 2.72	157.97 2.72	158.00 2.71
159.12 2.66	159.14 2.67	159.16 2.67	159.18 2.68	159.20 2.68
159.22 2.69	159.24 2.68	159.26 2.69	159.28 2.69	159.30 2.70
159.33 2.70	159.35 2.69	159.37 2.70		

CALCAREOUS SANDSTONE

164.98 2.70	165.00 2.71	165.02 2.71	165.04 2.71	165.06 2.70
165.09 2.71	165.11 2.72	165.13 2.70	165.15 2.73	165.17 2.71
166.34 2.72	166.36 2.72	166.38 2.71	166.40 2.70	166.42 2.68
166.44 2.69	166.46 2.69	166.48 2.70		

MUD/LIMESTONE

183.02 2.71	183.04 2.72	183.06 2.72	183.08 2.72	183.10 2.72
183.12 2.73	183.14 2.72	183.66 2.67	183.68 2.67	183.70 2.64
183.72 2.66	183.74 2.63	183.76 2.65	184.84 2.69	184.86 2.67
184.88 2.70	184.90 2.71	184.92 2.69	184.94 2.68	184.96 2.69

MUDSTONE

202.14 2.70	202.17 2.70	202.20 2.70	202.23 2.71	202.26 2.70
202.30 2.71	202.30 2.72	202.37 2.73	202.41 2.73	203.61 2.72
203.63 2.72	203.65 2.72	203.67 2.72		

APPENDIX E

Results from the laboratory measurements in Fyshwick.
Laboratory tests carried out on samples from borehole W.
Listed are: depth, grain density, dry bulk density, porosity and wet bulk density (i.e. fresh water saturated density).

ROCK TYPE	DEPTH (m)	APPARENT GRAIN DENSITY ($g\ cm^{-3}$)	DRY BULK DENSITY ($g\ cm^{-3}$)	POROSITY (%)	WET BULK DENSITY ($g\ cm^{-3}$)
SERICITIC SHALE	135.31	2.78	2.78	0.00	2.78
	135.35	2.79	2.79	0.26	2.79
	135.39	2.78	2.78	0.06	2.78
DOLERITE	145.43	2.86	2.85	0.50	2.85
	145.47	2.85	2.85	0.31	2.84
	145.51	2.84	2.84	0.18	2.84
	145.55	2.86	2.82	1.28	2.84
	145.59	2.85	2.84	0.22	2.85
	145.69	2.85	2.84	0.45	2.84
	145.73	2.85	2.82	1.05	2.82
	145.77	2.85	2.84	0.31	2.84
	145.81	2.84	2.84	0.25	2.84
TUFFACEOUS SHALE	162.29	2.70	2.69	0.43	2.69
	162.33	2.71	2.70	0.55	2.70
	162.37	2.70	2.70	0.00	2.70
	165.21	2.73	2.72	0.24	2.73
	165.25	2.72	2.71	0.42	2.71
	165.29	2.72	2.72	0.13	2.72
MASSIVE SULPHIDE	170.52	2.91	2.91	0.18	2.91
	170.55	2.97	2.94	1.28	2.95
	192.85	3.51	3.51	0.13	3.51
	192.89	3.83	3.82	0.45	3.82
	194.68	4.65	4.63	0.36	4.64
	194.68	4.65	4.63	0.36	4.64
	201.05	3.68	3.66	0.35	3.67
	201.09	3.78	3.77	0.30	3.77
	201.17	4.12	4.11	0.31	4.11
	201.21	4.33	4.30	0.51	4.31
	201.31	4.60	4.58	0.61	4.58
	201.35	4.58	4.55	0.56	4.56

APPENDIX E (Continued)

Results from the laboratory measurements in Fyshwick.
Laboratory tests carried out on samples from borehole W.
Listed are: depth, grain density, dry bulk density, porosity and wet bulk density (i.e. fresh water saturated density)

ROCK TYPE	DEPTH (m)	APPARENT GRAIN DENSITY ($g\ cm^{-3}$)	DRY BULK DENSITY ($g\ cm^{-3}$)	POROSITY (%)	WET BULK DENSITY ($g\ cm^{-3}$)
SHALE	232.49	2.77	2.76	0.18	2.76
	232.57	2.78	2.75	1.20	2.76
	232.89	2.76	2.73	0.93	2.74
	232.93	2.76	2.75	0.25	2.76
SILICIFIED SHALE	256.95	2.71	2.67	1.18	2.69
	256.99	2.70	2.68	0.63	2.69
	257.02	2.70	2.69	0.43	2.69
	258.05	2.71	2.70	0.06	2.70
	258.09	2.70	2.70	0.13	2.70
	258.13	2.71	2.70	0.39	2.70
QUARTZITIC TUFF	299.83	2.80	2.78	0.93	2.78
	299.99	2.81	2.80	0.20	2.81
	300.03	2.84	2.83	0.32	2.83
	300.05	2.80	2.78	2.80	2.79

APPENDIX E (Continued)

Results from the laboratory measurements in Fyshwick.
Laboratory measurements carried out on samples from borehole BMR155.
Listed are: depth, grain density, dry bulk density, porosity and wet bulk density (i.e. fresh water saturated density).

ROCK TYPE	DEPTH (m)	APPARENT GRAIN DENSITY ($g\ cm^{-3}$)	DRY BULK DENSITY ($g\ cm^{-3}$)	POROSITY (%)	WET BULK DENSITY ($g\ cm^{-3}$)
DACITE	38.89	2.82	2.64	6.20	2.71
	38.93	2.79	2.67	4.06	2.72
	38.97	2.80	2.69	4.09	2.73
	39.38	2.80	2.67	4.59	2.72
	39.42	2.79	2.67	4.47	2.71
	39.46	2.83	2.69	4.97	2.74
MUD/ SILTSTONE	75.06	2.76	2.71	1.92	2.73
CALCI-LUTITE	85.70	2.73	2.70	1.40	2.71
	85.78	2.72	2.69	1.32	2.70
	85.82	2.90	2.70	6.44	2.78
MARBLE	101.86	2.73	2.72	0.55	2.72
	101.90	2.73	2.72	0.37	2.72
	103.26	2.74	2.71	1.05	2.72
	103.30	2.75	2.71	1.51	2.72
	103.40	2.73	2.71	0.90	2.71
	103.44	2.74	2.72	0.91	2.72
SANDSTONE	139.03	2.69	2.66	1.35	2.67
	139.09	2.69	2.66	0.85	2.68
	139.12	2.70	2.66	1.52	2.67
	141.00	2.70	2.63	2.64	2.66
LIMESTONE	157.86	2.72	2.72	0.12	2.72
	157.91	2.72	2.72	0.06	2.72
	157.94	2.72	2.72	0.00	2.72
	159.18	2.73	2.72	0.23	2.73
	159.22	2.73	2.72	0.33	2.73
	159.26	2.72	2.69	1.24	2.72
CALCAREOUS SANDSTONE	165.00	2.78	2.68	3.68	2.72
	166.40	2.78	2.69	3.54	2.72
	166.44	2.77	2.65	4.06	2.70

APPENDIX E (Continued)

Results from the laboratory measurements in Fyshwick.
Laboratory measurements carried out on samples from borehole BMR155.
Listed are: depth, grain density, dry bulk density, porosity and wet bulk density (i.e. fresh water saturated density).

ROCK TYPE	DEPTH (m)	APPARENT GRAIN DENSITY ($g\ cm^{-3}$)	DRY BULK DENSITY ($g\ cm^{-3}$)	POROSITY (%)	WET BULK DENSITY ($g\ cm^{-3}$)
MUD/ LIMESTONE	183.04	2.74	2.74	0.13	2.74
	183.08	2.73	2.71	0.98	2.71
	183.70	2.72	2.72	0.13	2.72
	183.74	2.72	2.72	0.13	2.72
	184.90	2.72	2.68	1.56	2.69
	184.94	2.73	2.72	0.25	2.73
MUDSTONE	202.30	2.74	2.72	0.56	2.73
	202.34	2.73	2.72	0.31	2.73
	202.38	2.75	2.72	0.98	2.73

APPENDIX E (Continued)

Results from the laboratory measurements in Fyshwick. Laboratory measurements carried out on samples from borehole Newcastle 2. Listed are: depth, grain density, dry bulk density, porosity and wet bulk density (i.e. fresh water saturated density).

ROCK TYPE	DEPTH (m)	APPARENT GRAIN DENSITY ($g\ cm^{-3}$)	DRY BULK DENSITY ($g\ cm^{-3}$)	POROSITY (%)	WET BULK DENSITY ($g\ cm^{-3}$)
FINE SANDSTONE	8.28	2.64	2.30	13.04	2.43
	8.32	2.60	2.28	12.56	2.40
	8.35	2.61	2.33	11.00	2.44
	8.42	2.63	2.32	11.89	2.44
	8.45	2.66	2.31	13.14	2.44
	8.60	2.62	2.32	11.64	2.43
COARSE SANDSTONE	8.90	2.63	2.20	16.34	2.36
	8.95	2.63	2.20	16.18	2.36
	9.00	2.64	2.21	16.06	2.37
	9.05	2.64	2.25	14.59	2.40
CONGLOM/ ERATE	17.25	2.62	2.24	14.98	2.39
	17.30	2.44	2.22	9.09	2.31
	17.33	2.62	2.26	13.90	2.39
	17.39	2.62	2.25	14.18	2.39
	17.45	2.63	2.19	16.80	2.36
	17.55	2.62	2.22	15.36	2.37
	17.59	2.64	2.22	16.07	2.38
	17.63	2.64	2.23	15.60	2.39
	17.67	2.64	2.22	15.87	2.38
COAL	22.08	1.45	1.40	3.93	1.44
	22.12	1.50	1.32	11.54	1.44
	24.89	1.48	1.26	14.99	1.41
	25.60	1.46	1.36	7.25	1.43
	25.65	1.51	1.40	7.56	1.48
	25.90	1.45	1.35	6.91	1.42
	26.30	1.34	1.28	5.07	1.33
	26.40	1.45	1.34	7.36	1.42
	26.50	1.38	1.32	4.65	1.36
	27.00	1.42	1.29	9.18	1.38

APPENDIX F

LEGEND

Borehole BMR155:


SNDST Sandstone

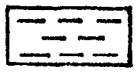
SLST Siltstone

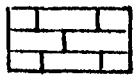
LMST Limestone

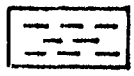
MDST Mudstone


DAC Dacite


ASH Ashstone

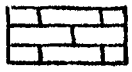
MARB Marble


CASST Calcareous sandstone

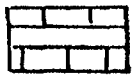
CA-LU Calci-lutite

BMR THEORETICAL GEOPHYSICS AND SPECIAL PROJECTS

COMPUTERISED BOREHOLE LOGGING

ROCK PROPERTIES

BARTON HWY

BOREHOLE NO. BMR 155

DEPTH LOGGED 206.32 M.

DATE LOGGED 12.11.85

DATE PROCESSED 5.3.1986

LONG DENSITY COUNTS/SEC

LONG SPACED DENSITY G/CC

SHORT DENSITY COUNTS/SEC

SHORT SPACED DENSITY G/CC

CALIPER CM

DEPTH (M.)

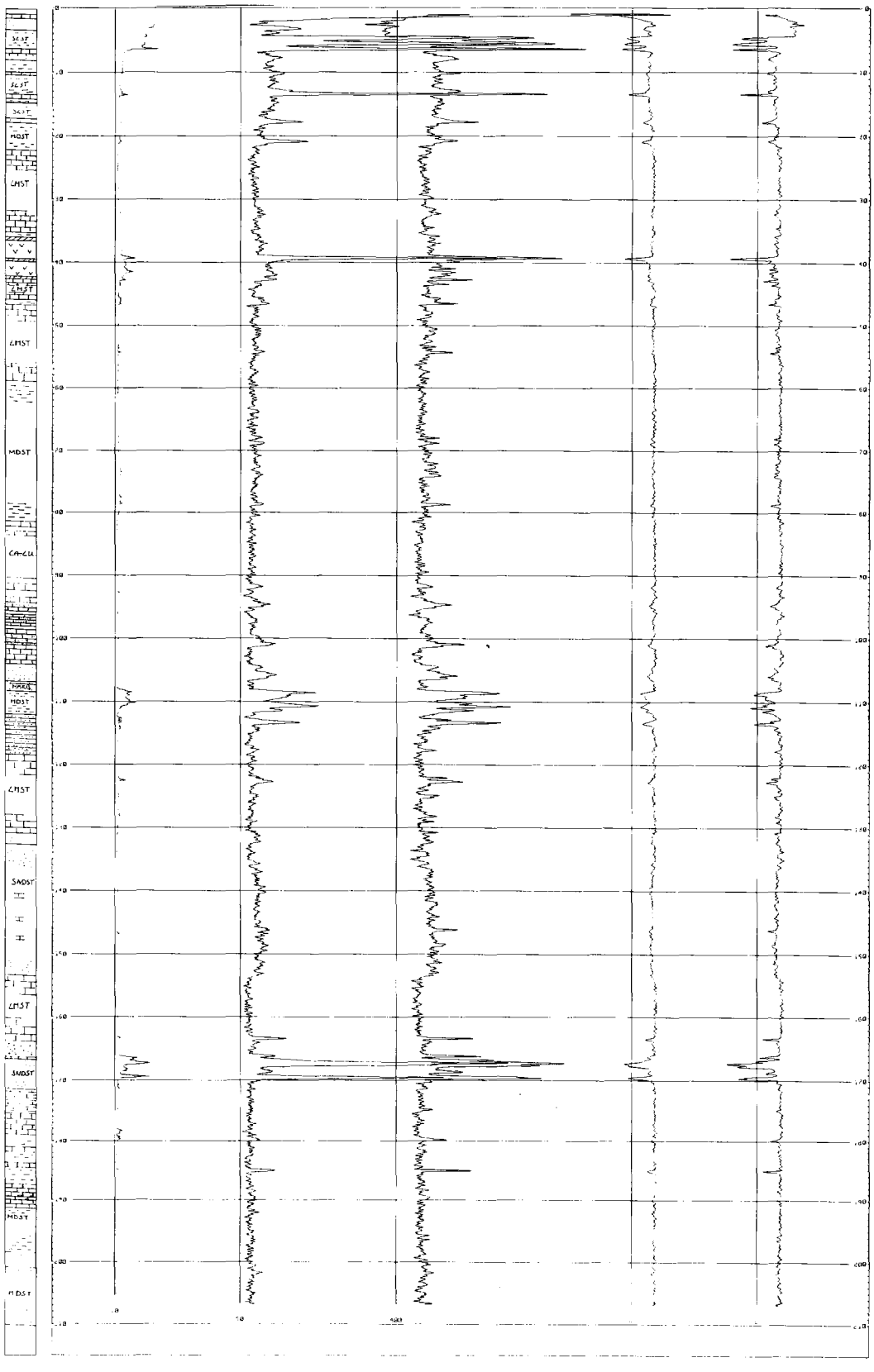

APPENDIX F (Continued)

LEGEND

Borehole W:

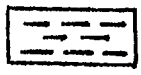
SHALE Shale

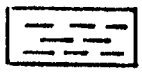
SRSH Sericitic shale

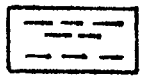
SLSH Silicified shale

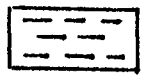
TFSH Tuffaceous shale

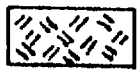
DLRT Dolerite


MVSD Massive sulphide

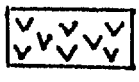
QETF Quartzitic tuff

BMR THEORETICAL GEOPHYSICS AND SPECIAL PROJECTS

COMPUTERISED BOREHOLE LOGGING

ROCK PROPERTIES
WOODLAWN

LOGGING SPEEDS:
DENSITY PROBE 5 M/MIN
DATUM ABOVE GROUND LEVEL 0.00 M.
OPERATOR GASP CREW
DATA LOG VER 7.50.01
DATA PLOT VER 7.50.01
WATER LEVEL 36.00 M.

PLOTTING SCALE: 1:250

BOREHOLE NO.W

DEPTH LOGGED 341.96 M.
DATE LOGGED 28.11.85
DATE PROCESSED 3.2.1986

LONG SPACED DENSITY cps
0 50 100

LONG SPACED DENSITY G/CC
CAL GM/CC 1.25 1.74

CALIPER cm.
CAL CM 10 20 30

SHORT SPACED DENSITY cps
0 100 200 300 400

SHORT SPACED DENSITY G/CC
CAL GM/CC 1.19 1.74

DEPTH (M.)

SHALE
SRSH
SKSH
MVOB
SMSH
QUART
JKSH
SKSH
TFSH
MVOB
SCSH
SRSH
SCSH
CHLTE
SCSH
SCSH
TFSH

APPENDIX F (Continued)

LEGEND

Newcastle 2

Shale

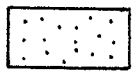

Finegrained sandstone

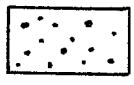

Coarse-grained sandstone

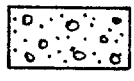

Sandy conglomerate

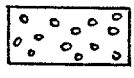

Conglomerate

Laminated siltstone/ sandstone

Coal

BMR ROCK PROPERTIES RESEARCH

COMPUTERISED BOREHOLE LOGGING

CALIBRATIONS
NEWCASTLE

LINEAR DENSITY EQUATION IS Counts= A*Dens*EXP(B*Dens)

LOGGING SPEEDS:
DENSITY PROBE 3 M/MIN

PLOTTING SCALE: 1:50

DATUM ABOVE GROUND LEVEL 1.61 M.
OPERATOR: : PRANE & ALEX
DATA LOG VER: 78506.01
DATA PLOT VER: 78607.31
WATER LEVEL: 4.20 M.

BOREHOLE NO. RKP 1

DEPTH LOGGED 28.75 M.
DATE LOGGED 03 13 86
DATE PROCESSED 24 10 86

LONG SPACED DENSITY g/cc
CAL GM/CC 1.19 | 1.24

SHORT SPACED DENSITY g/cc
CAL GM/CC 1.19 | 1.24

CALIPER cm.
CAL CM 10 | 20 | 30

DEPTH (M.)

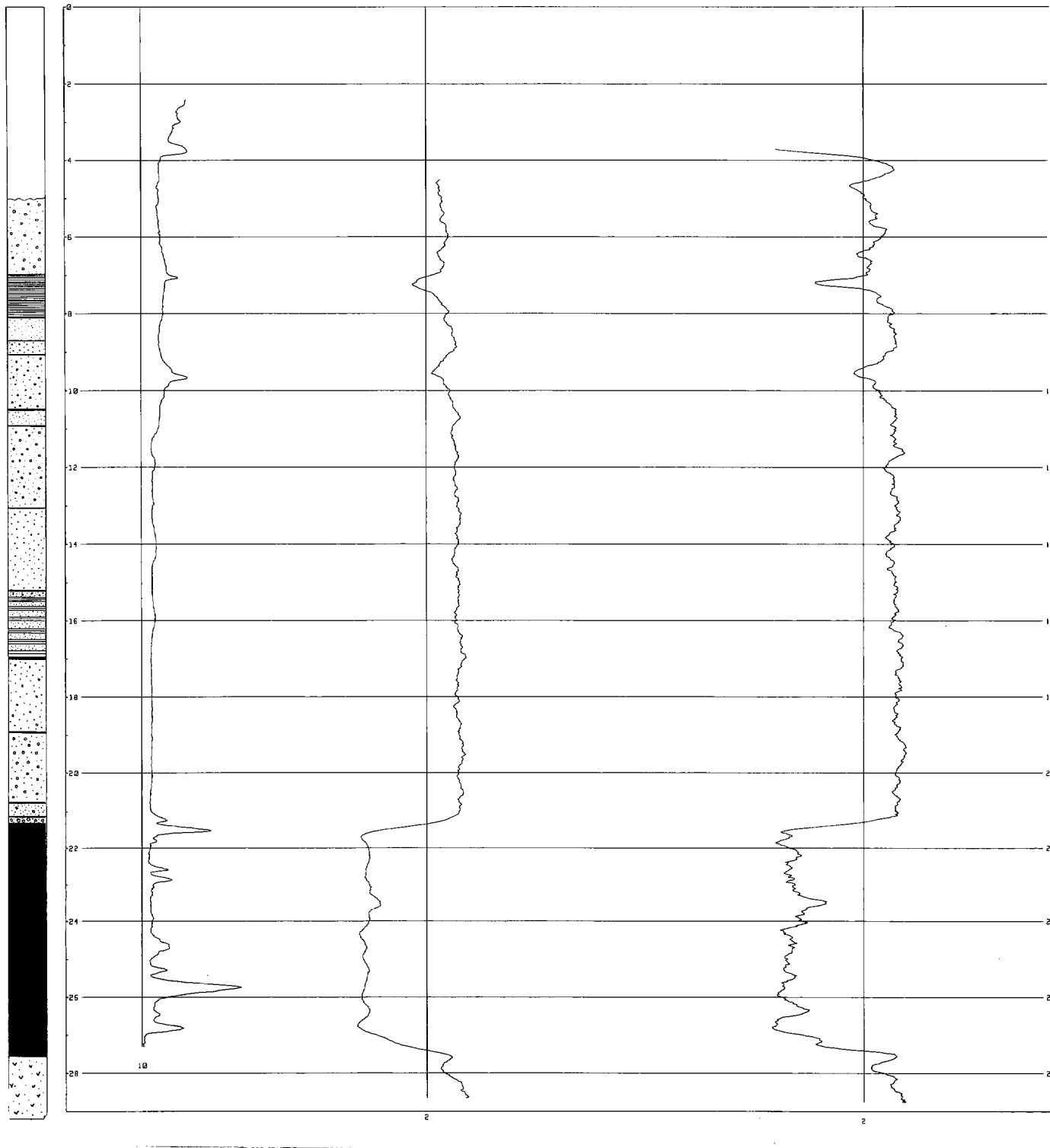

BMR THEORETICAL GEOPHYSICS AND SPECIAL PROJECTS

COMPUTERISED BOREHOLE LOGGING

BMR SCIENTIFIC
AMDEL PITS

LOGGING SPEEDS:
DENSITY PROBE 3 M/MIN
DATUM ABOVE GROUND LEVEL .24 M.
OPERATOR: P. CHOPRA
DATA _DG VER: 78212.01
DATA_P_DI VER:78607.31
DRY HOLE

PLOTTING SCALE: 1:20

BOREHOLE NO. AM 4 3M/S

DEPTH LOGGED 8.12 M.
DATE LOGGED 23 03 85
DATE PROCESSED 27 10 86

LINEAR DENSITY EQUATION IS Counts= A*Dens+EXP(B*Dens)

LONG DENSITY g/cc

CAL GM/CC 1.19 | 1.74

SHORT DENSITY g/cc

CAL GM/CC 1.19 | 1.74

DEPTH (M.)

Foam

API Mix

Foam

Barytes

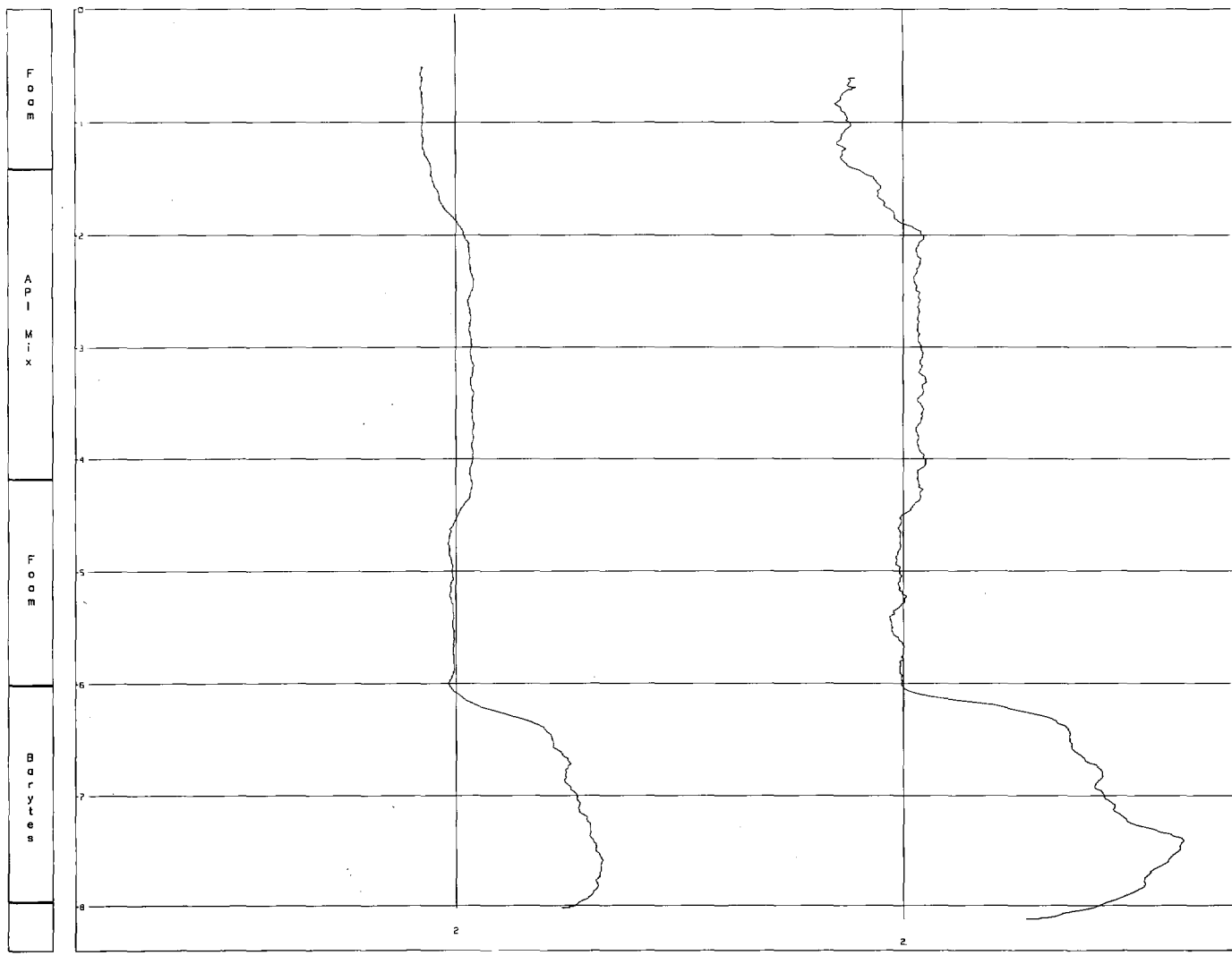

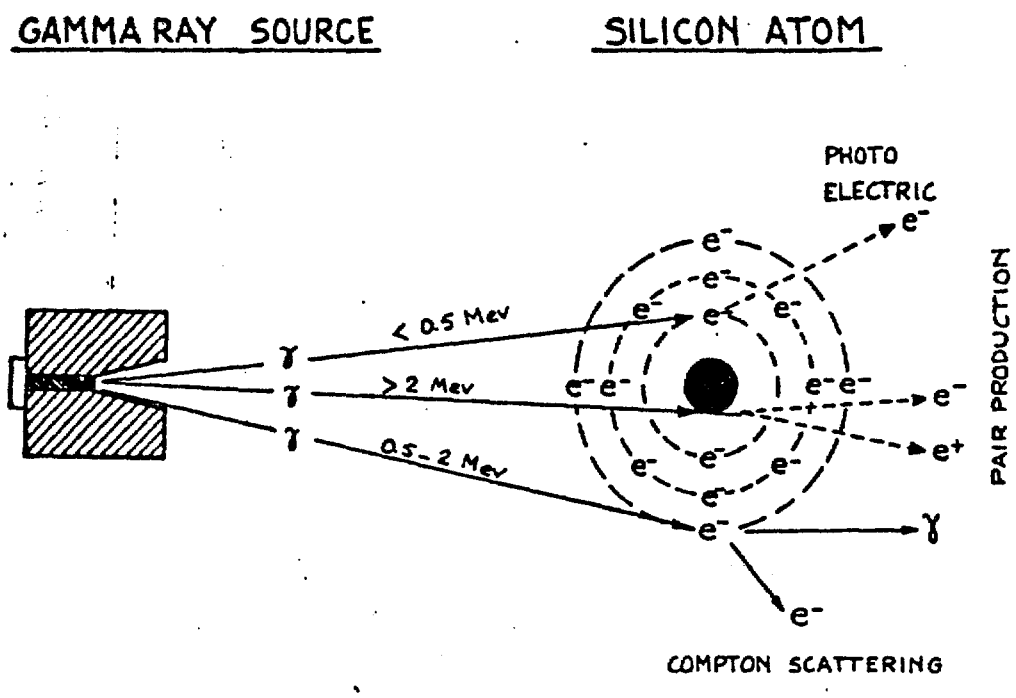

Figure 1 3 types of nuclear interaction between gamma ray photons and a silicon atom.

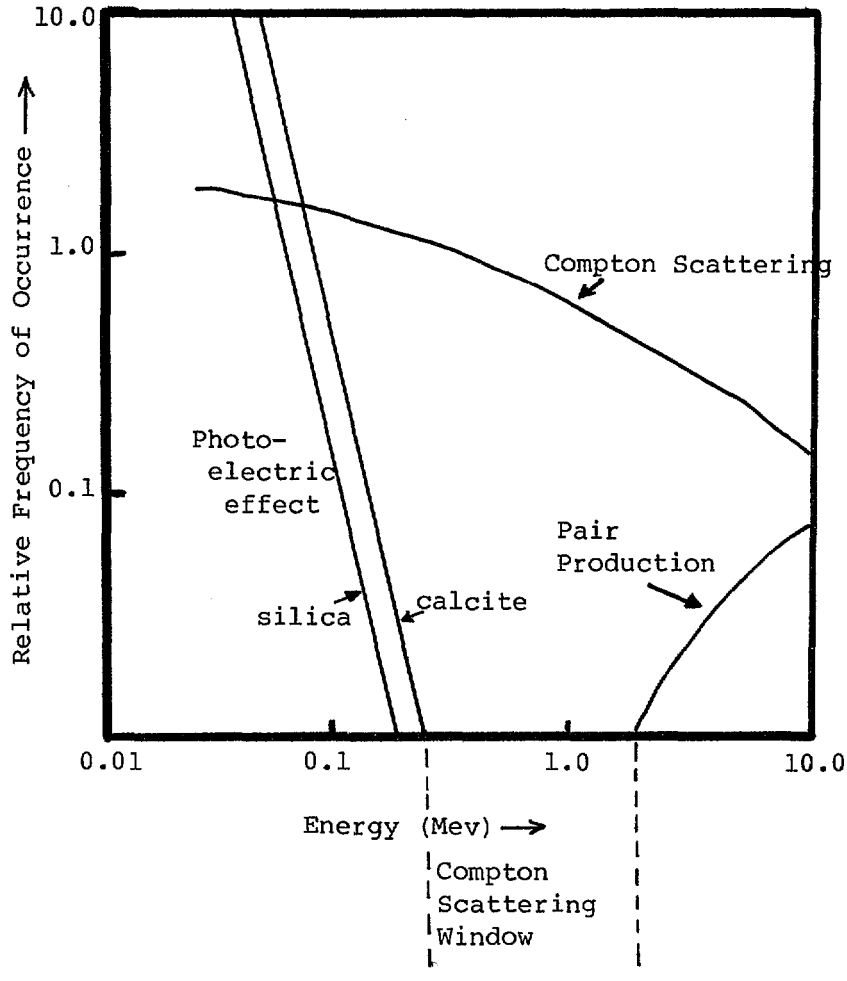

Figure 2 Relationship between mass attenuation coefficient and gamma ray energy, showing the energy window for Compton Scattering. (after Hallenburg, 1984)

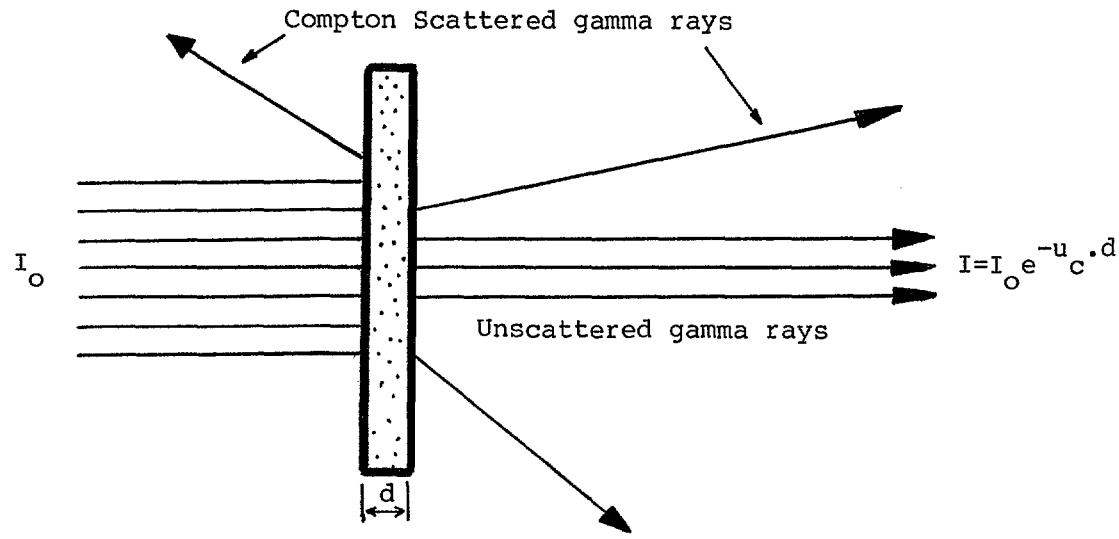

Figure 3a Transmitted geometry

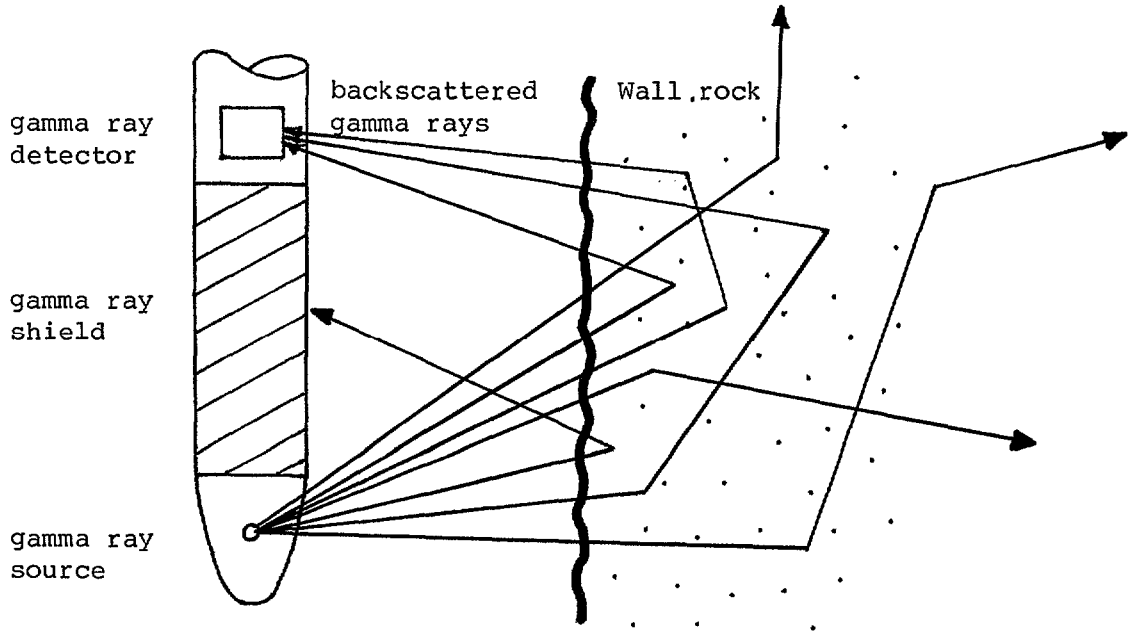

Figure 3b Backscattered geometry

(after Mathew, 1976)

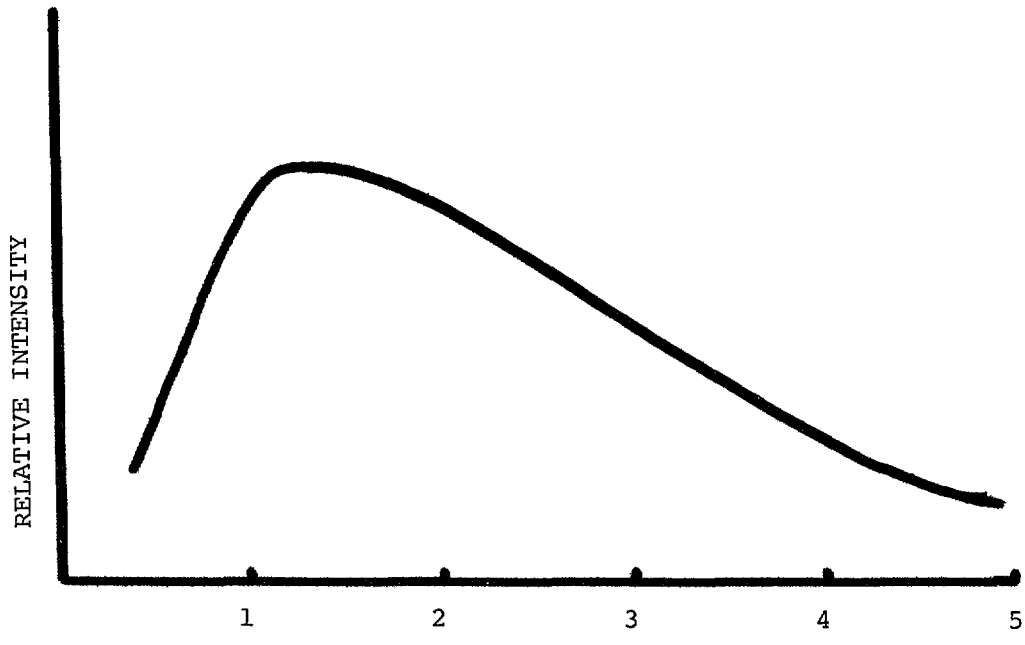

Figure 4 Relationship between medium density and backscattered gamma ray intensity

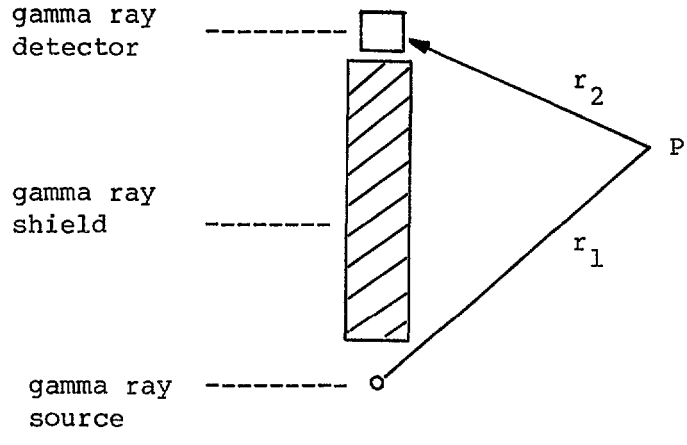

Figure 5 A two dimensional representation of the single backscattering model (after Mathew, 1976)

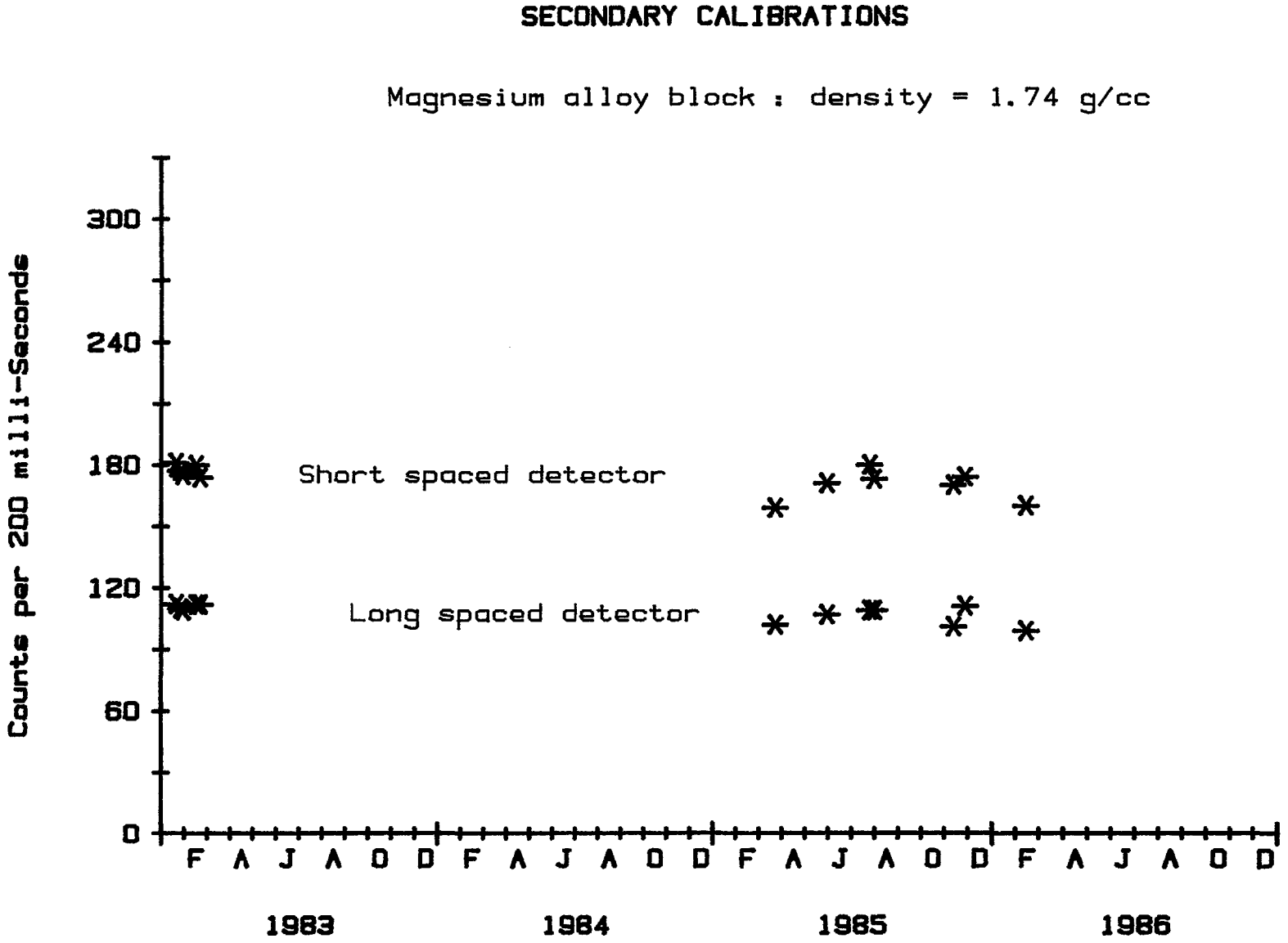

Figure 6

Secondary calibrations performed with the 54 mm diameter density tool on a magnesium-aluminium alloy block housed in the well-logging truck.

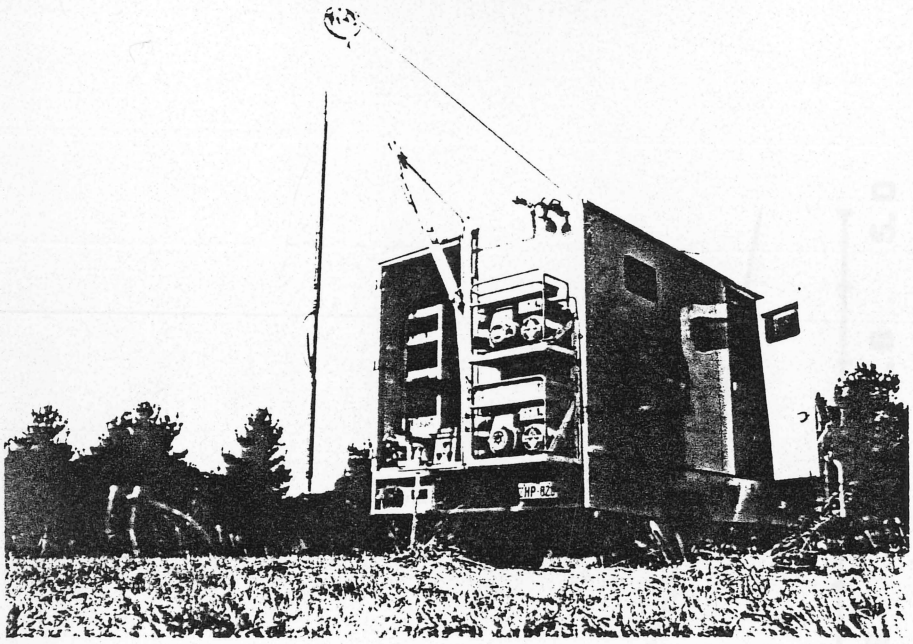

Figure 7 The BMR Well-logging truck

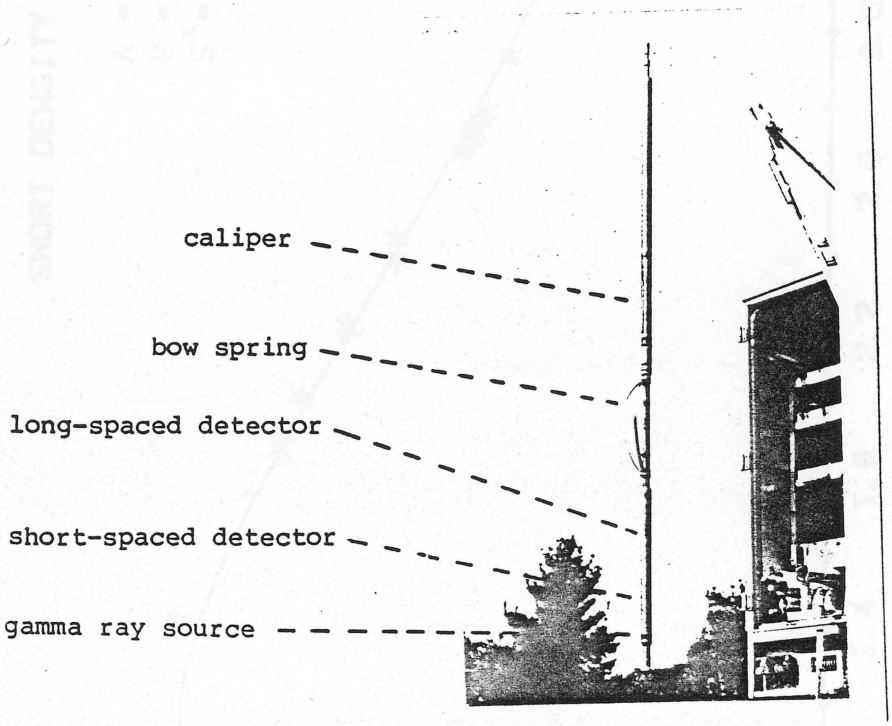

Figure 8 The 54mm diametre density tool

Figure 9a Fit to all the short-spaced detector data

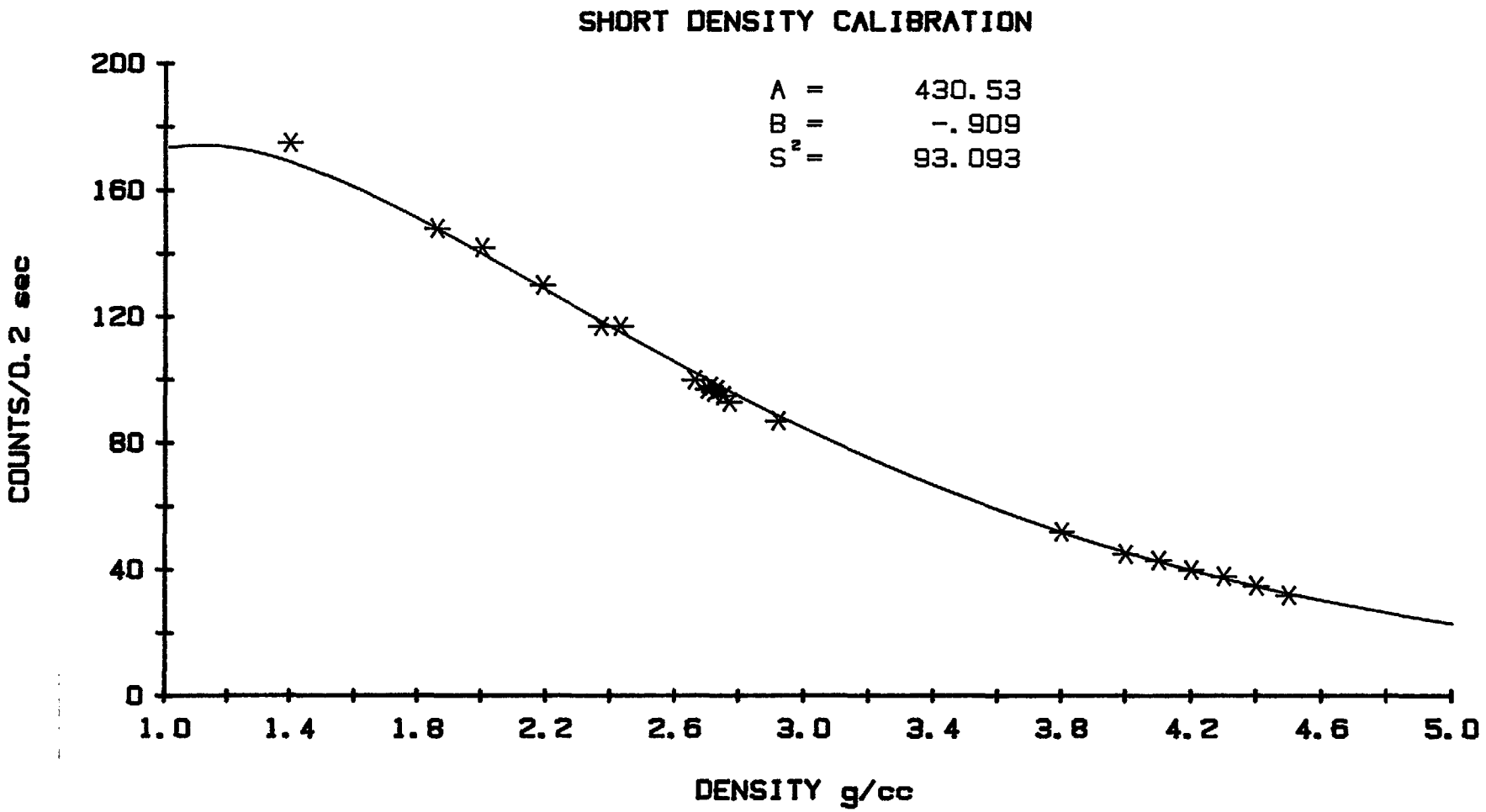

Figure 9b Fit to the short-spaced detector data for rock densities less than 3.0 grams per cubic centimetre.

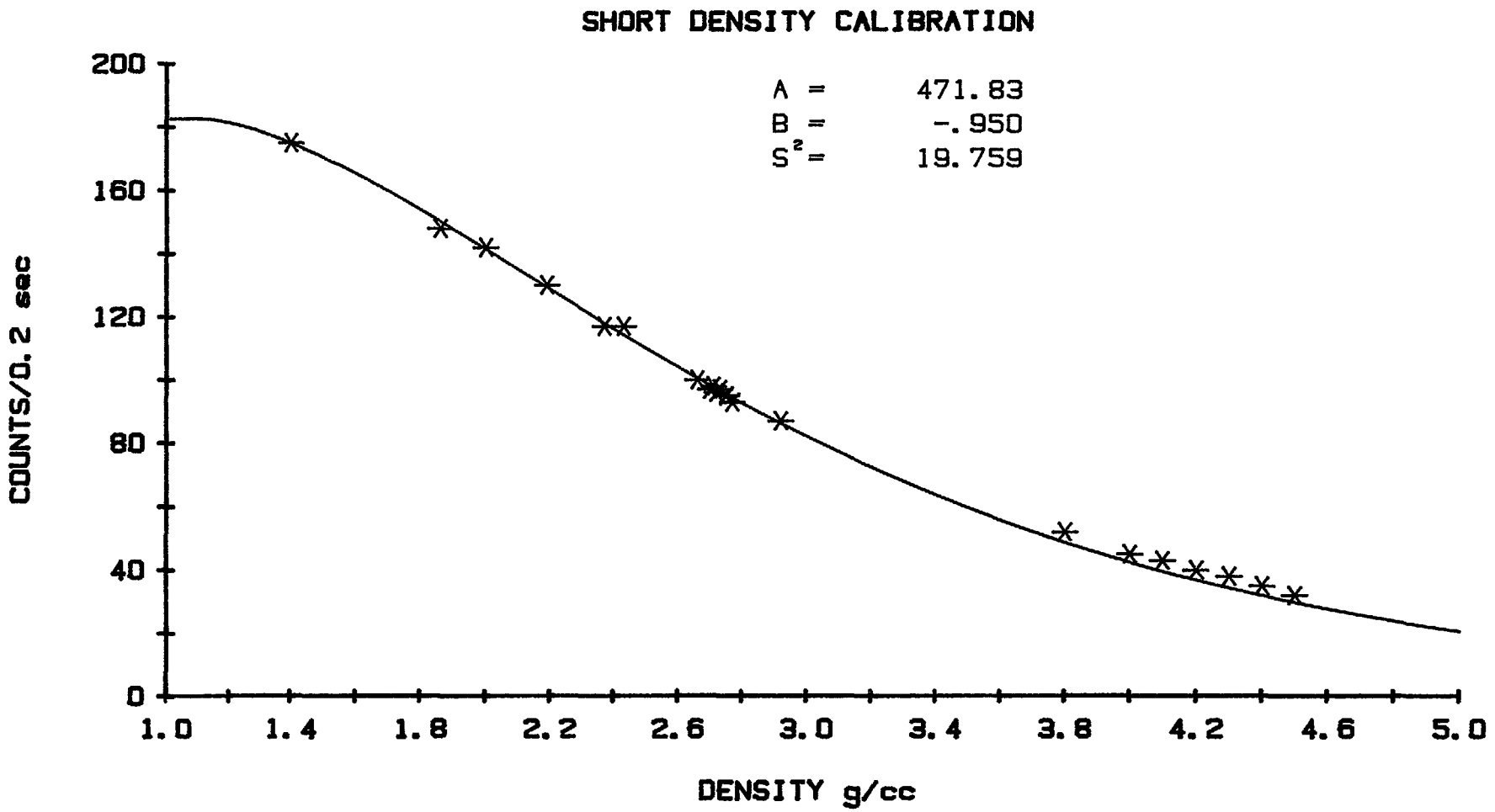

Figure 10 Fit to all the long-spaced detector data

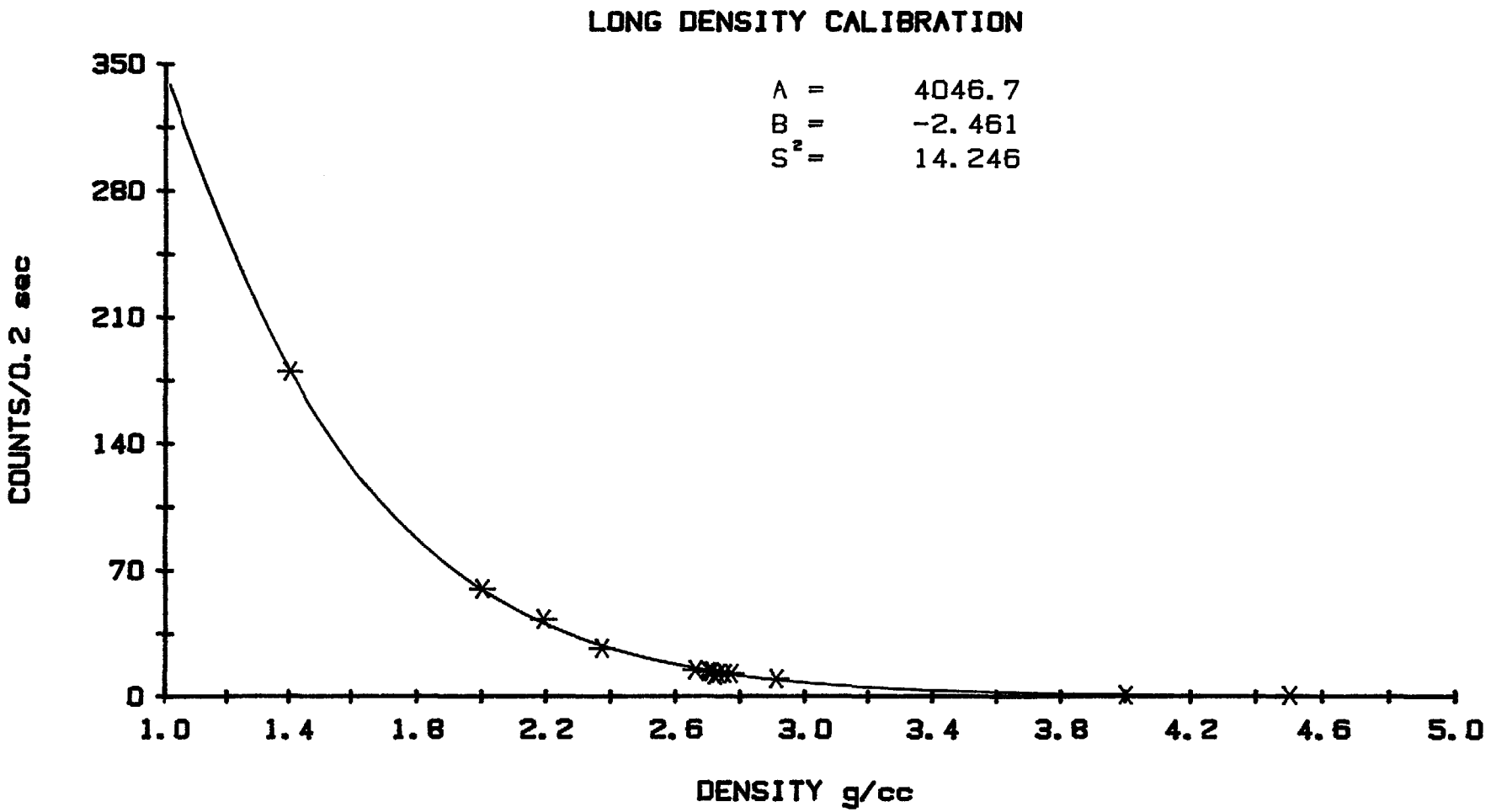

Figures 11a - 11j

Comparisons of the two sets of laboratory rock density data made on core samples from borehole BMR155 with the density estimates computed from the well-logging tool's short spaced density detector.

Symbols:

solid boxes - Archimedes principle density estimates
open boxes - CORAN density estimates
line - short spaced detector density estimates

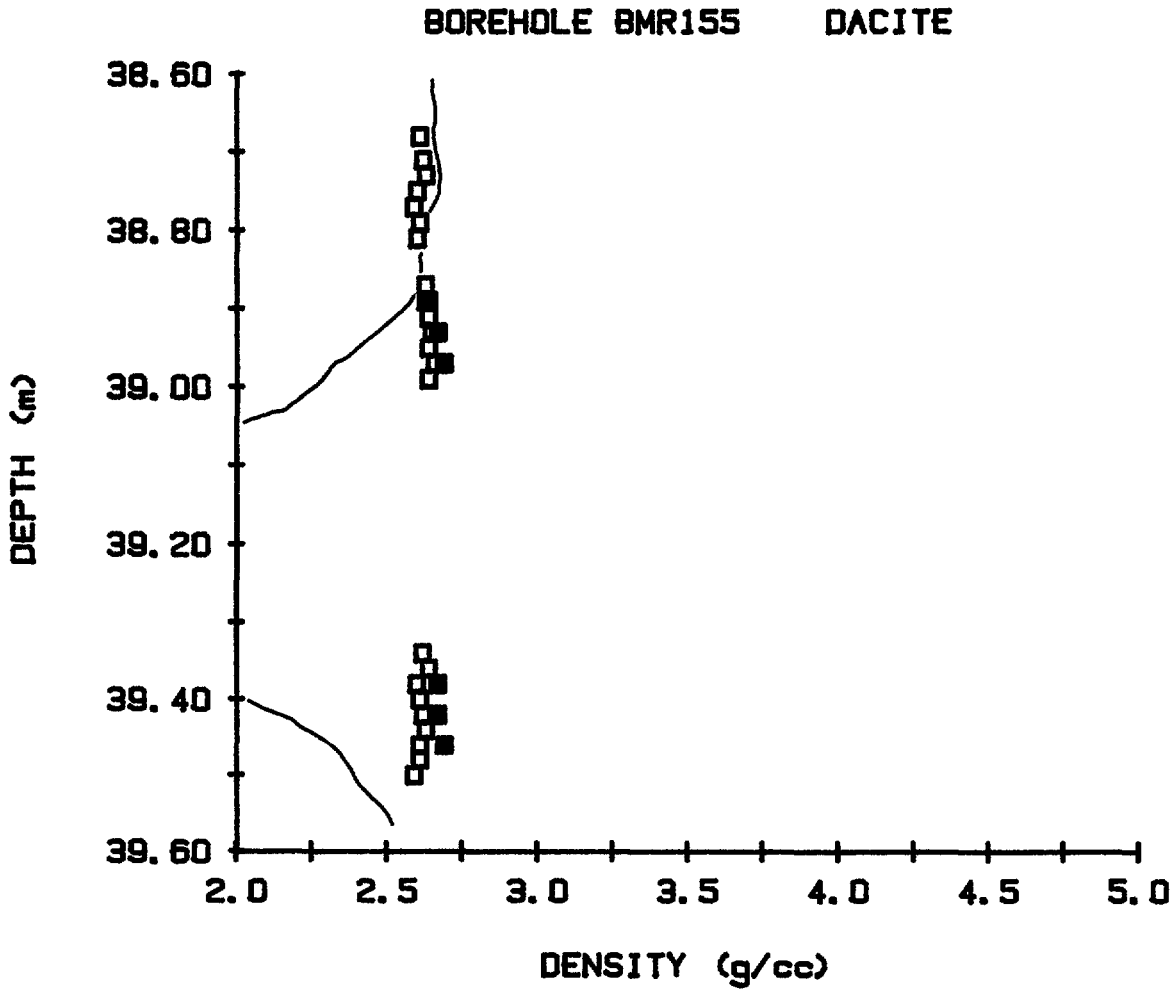

Figure 11a: The departure of the log density estimates from the laboratory estimates in the depth interval between 39.0 a 39.5 metres is due to the presence of a washout in the borehole wall (see text and Appendices C and F).

Figure 11b

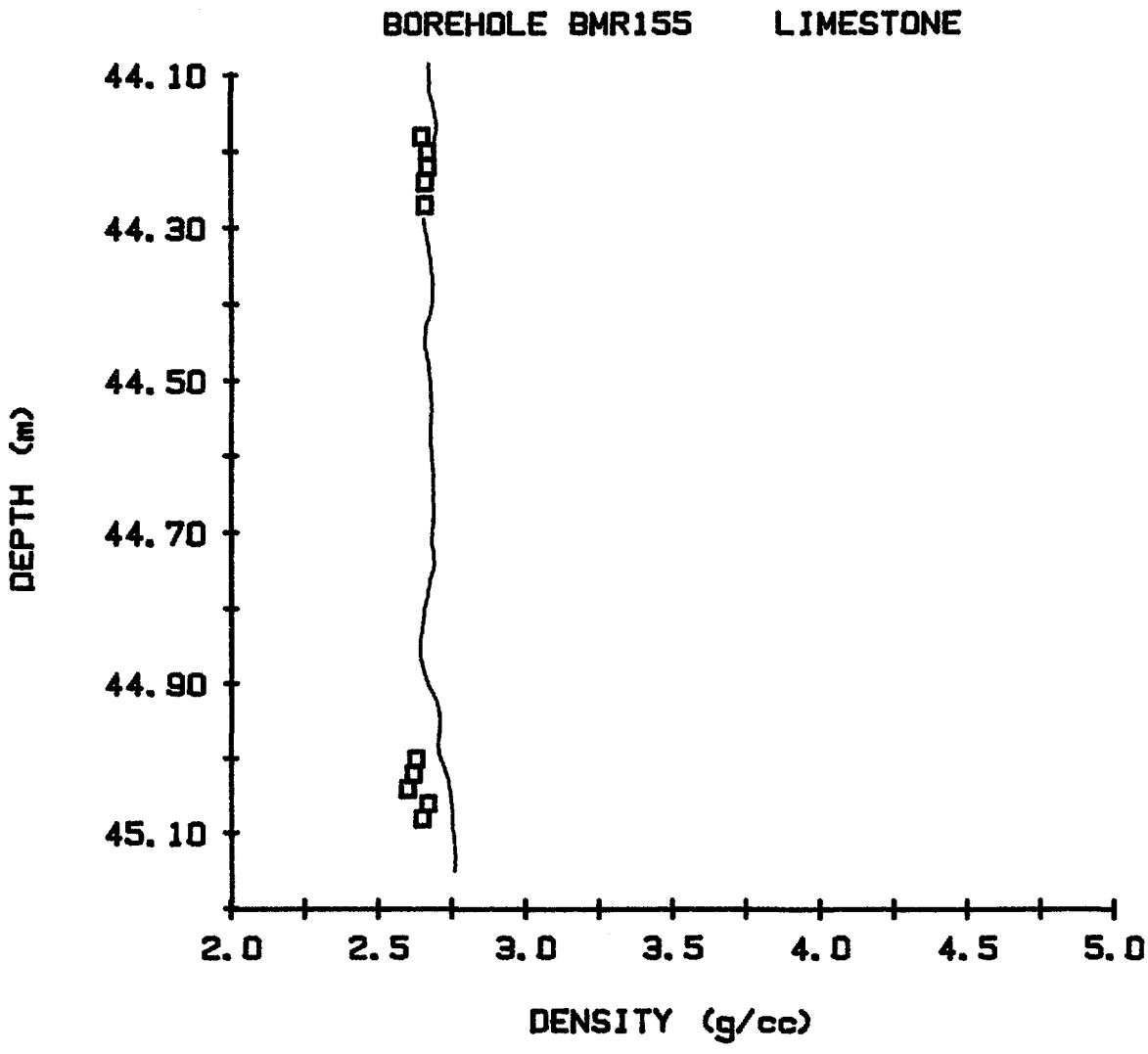

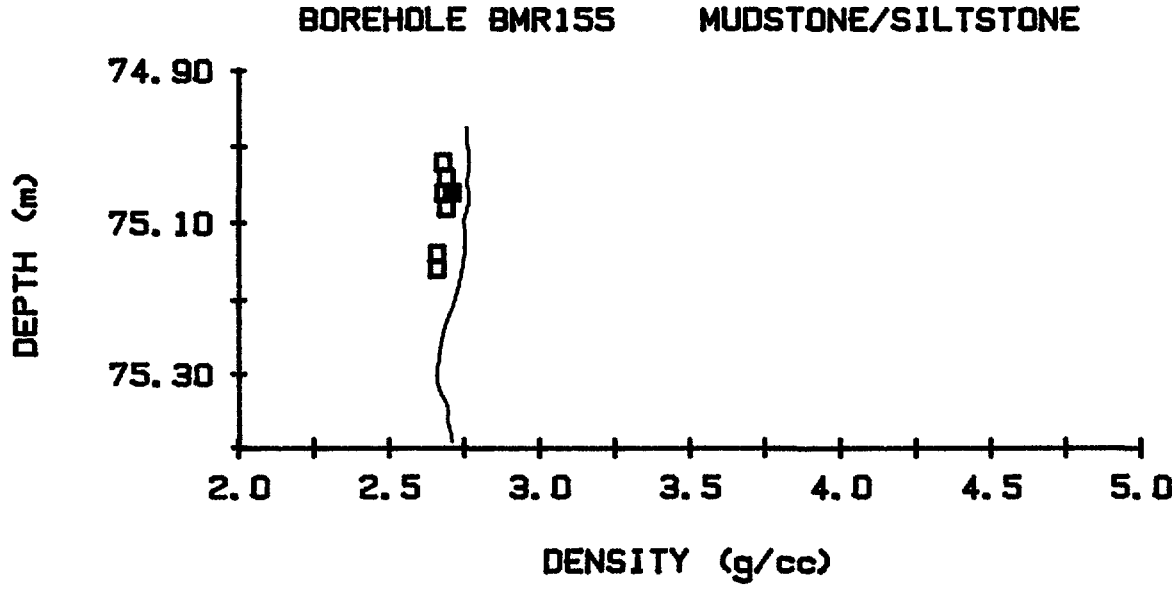

Figure 11c

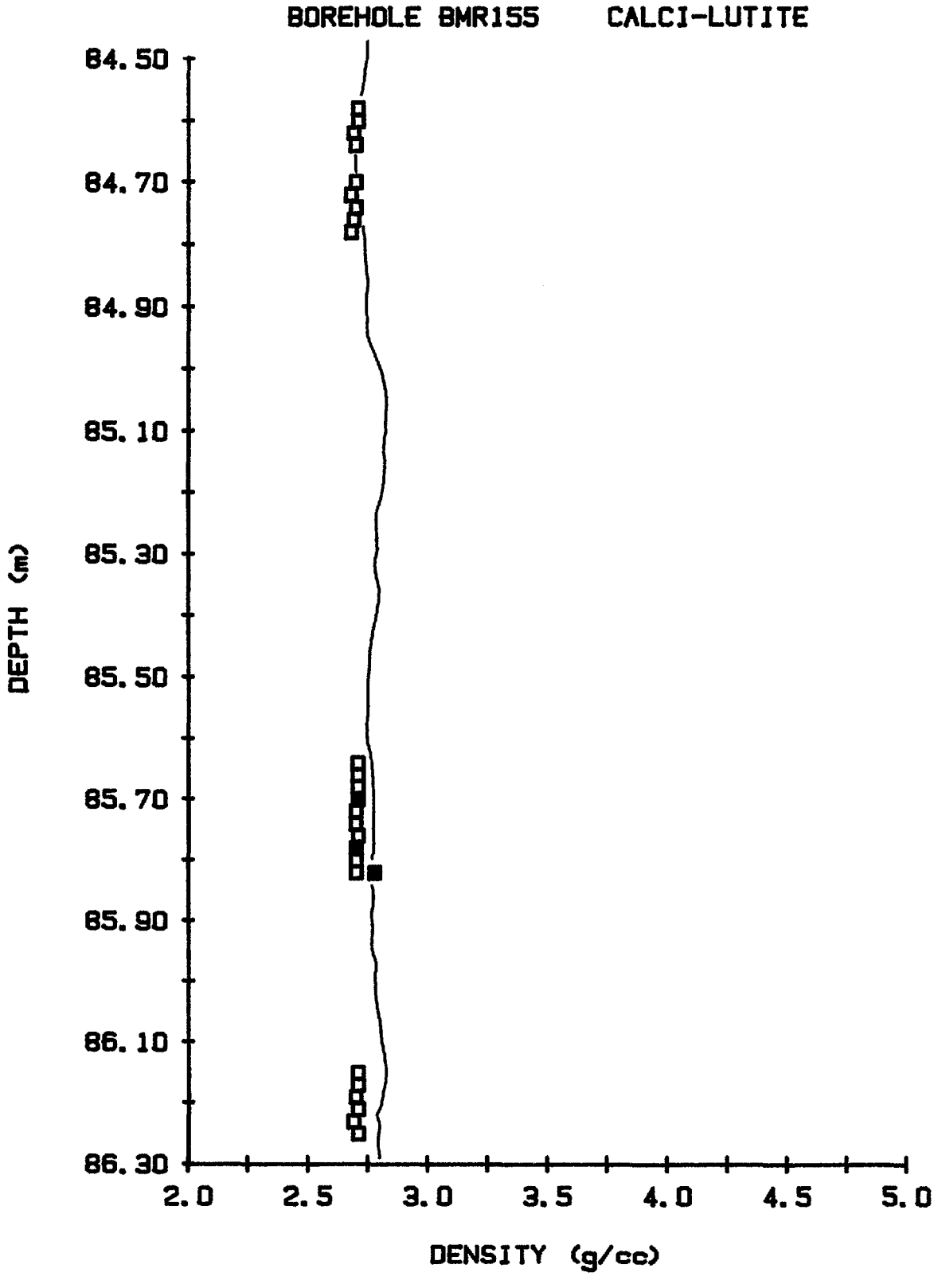
BOREHOLE BMR155 CALCI-LUTITE
84.50
84.70
84.90
85.10
85.30
85.50
85.70
85.90
86.10
86.30
DEPTH (m)
2.0
2.5
3.0
3.5
4.0
4.5
5.0
DENSITY (g/cc)

Figure 11d

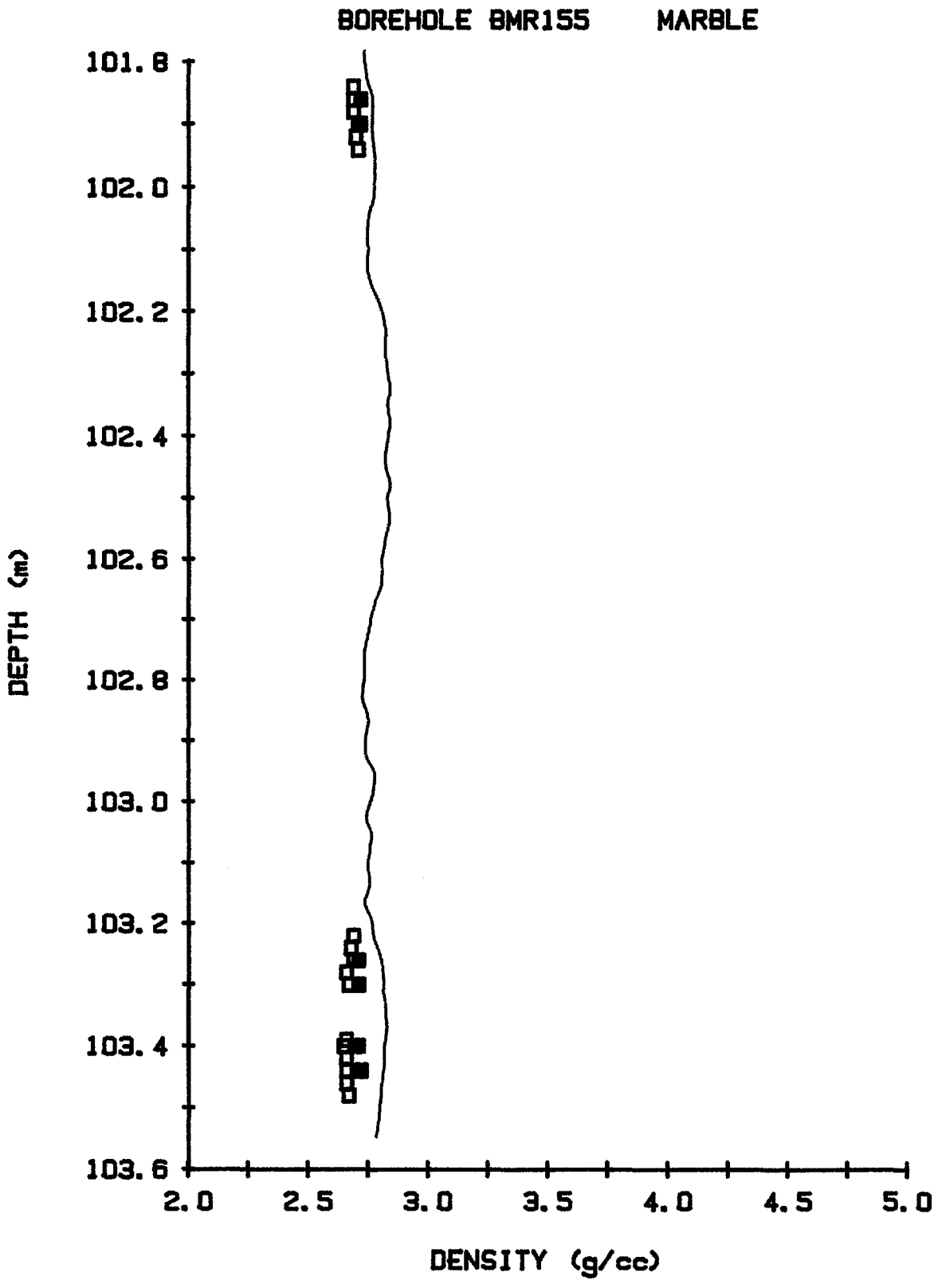
BOREHOLE BMR155 MARBLE
101.8
102.0
102.2
102.4
102.6
102.8
103.0
103.2
103.4
103.6
DEPTH (m)
2.0
2.5
3.0
3.5
4.0
4.5
5.0
DENSITY (g/cc)

Figure 11e

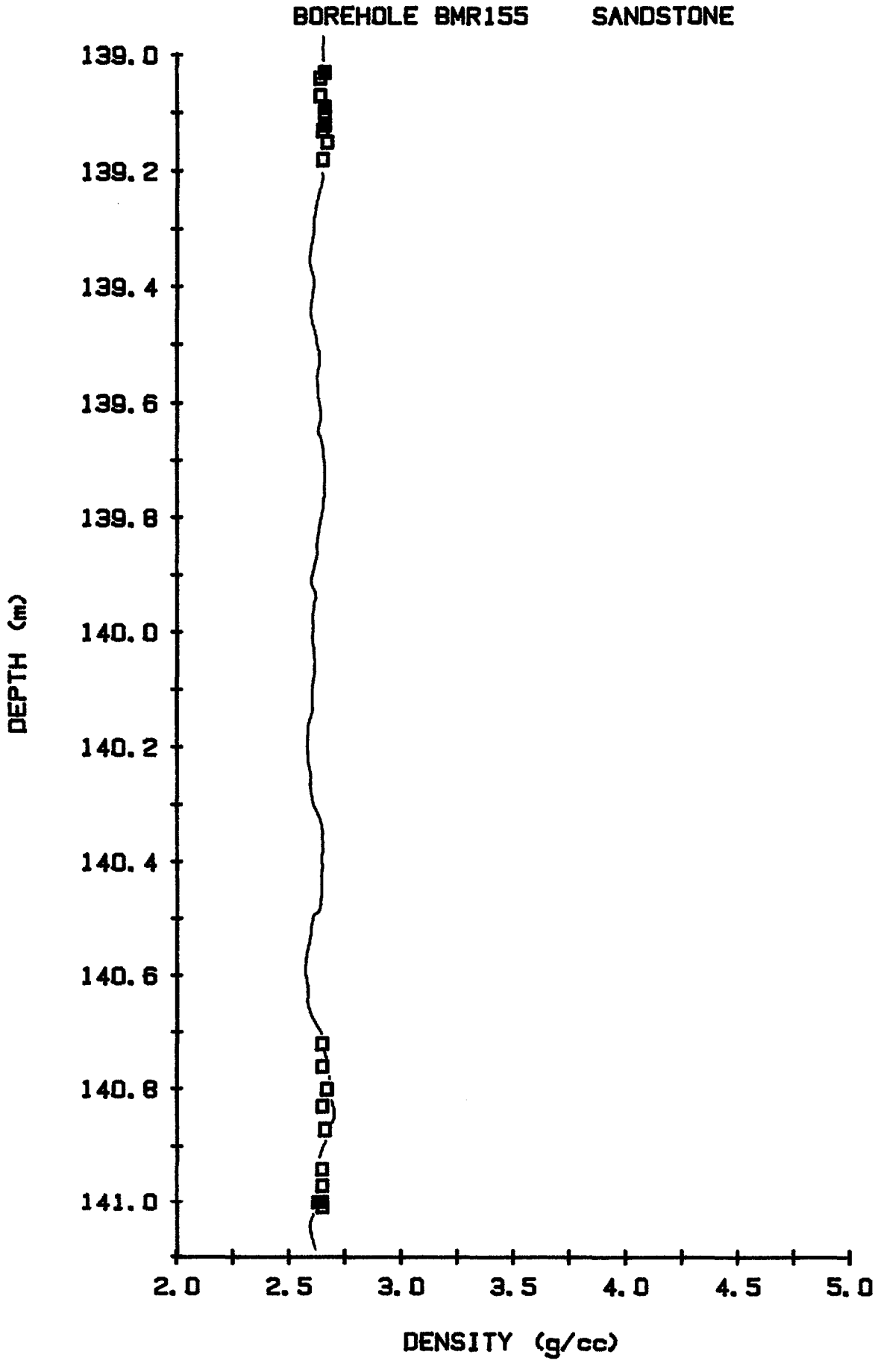
BOREHOLE BMR155 SANDSTONE
139.0
139.2
139.4
139.6
139.8
140.0
140.2
140.4
140.6
140.8
141.0
DEPTH (m)
2.0
2.5
3.0
3.5
4.0
4.5
5.0
DENSITY (g/cc)

Figure 11f

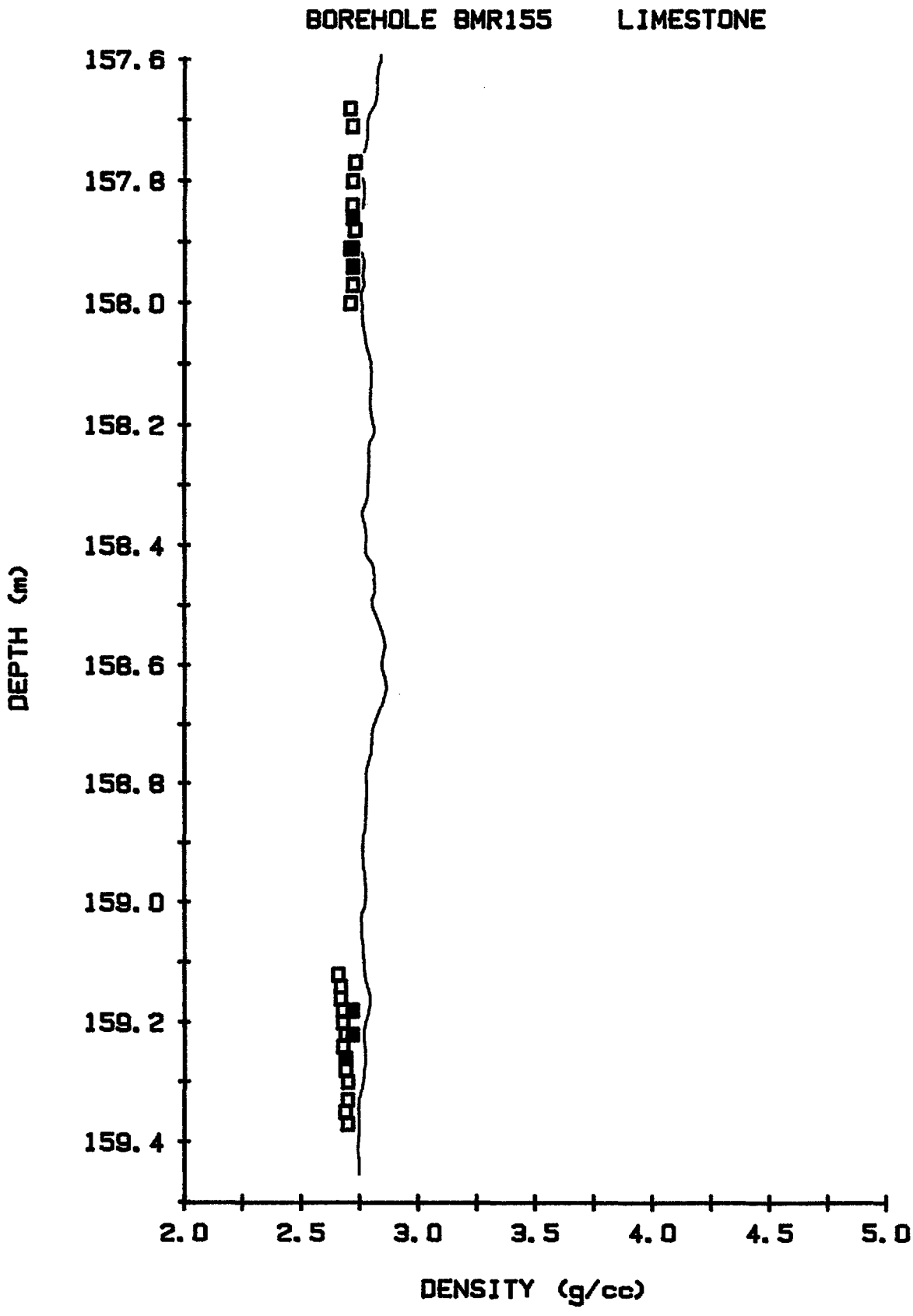
BOREHOLE BMR155 LIMESTONE
157.6
157.8
158.0
158.2
158.4
158.6
158.8
159.0
159.2
159.4
DEPTH (m)
2.0
2.5
3.0
3.5
4.0
4.5
5.0
DENSITY (g/cc)

Figure 11g

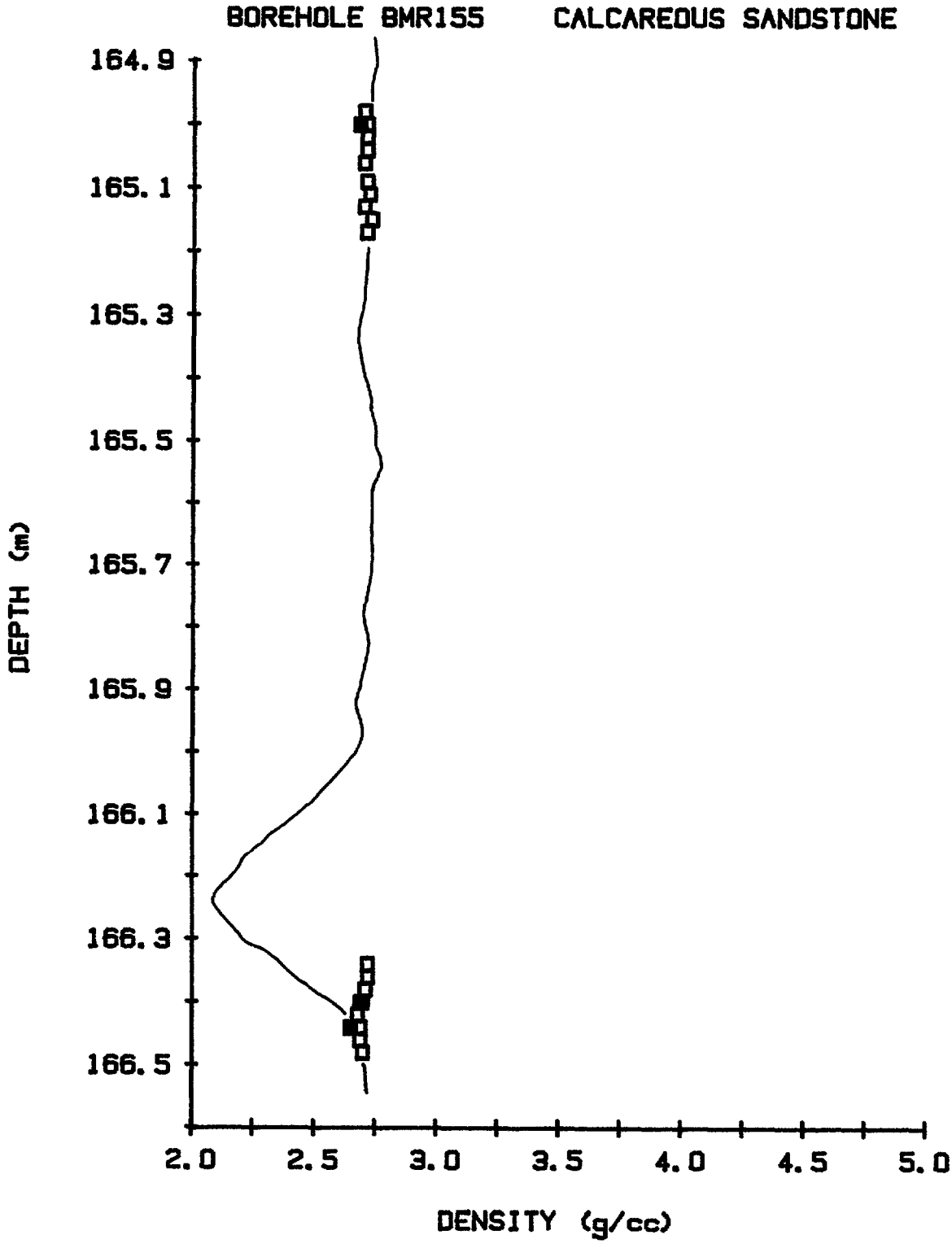

Figure 11h The departure of the log density estimates from the laboratory estimates in the depth interval between 166.3 and 166.5 metres is due to the presence of a washout in the borehole wall centred near 166.2 metres depth (see text and Appendices C and F).

Figure 11i

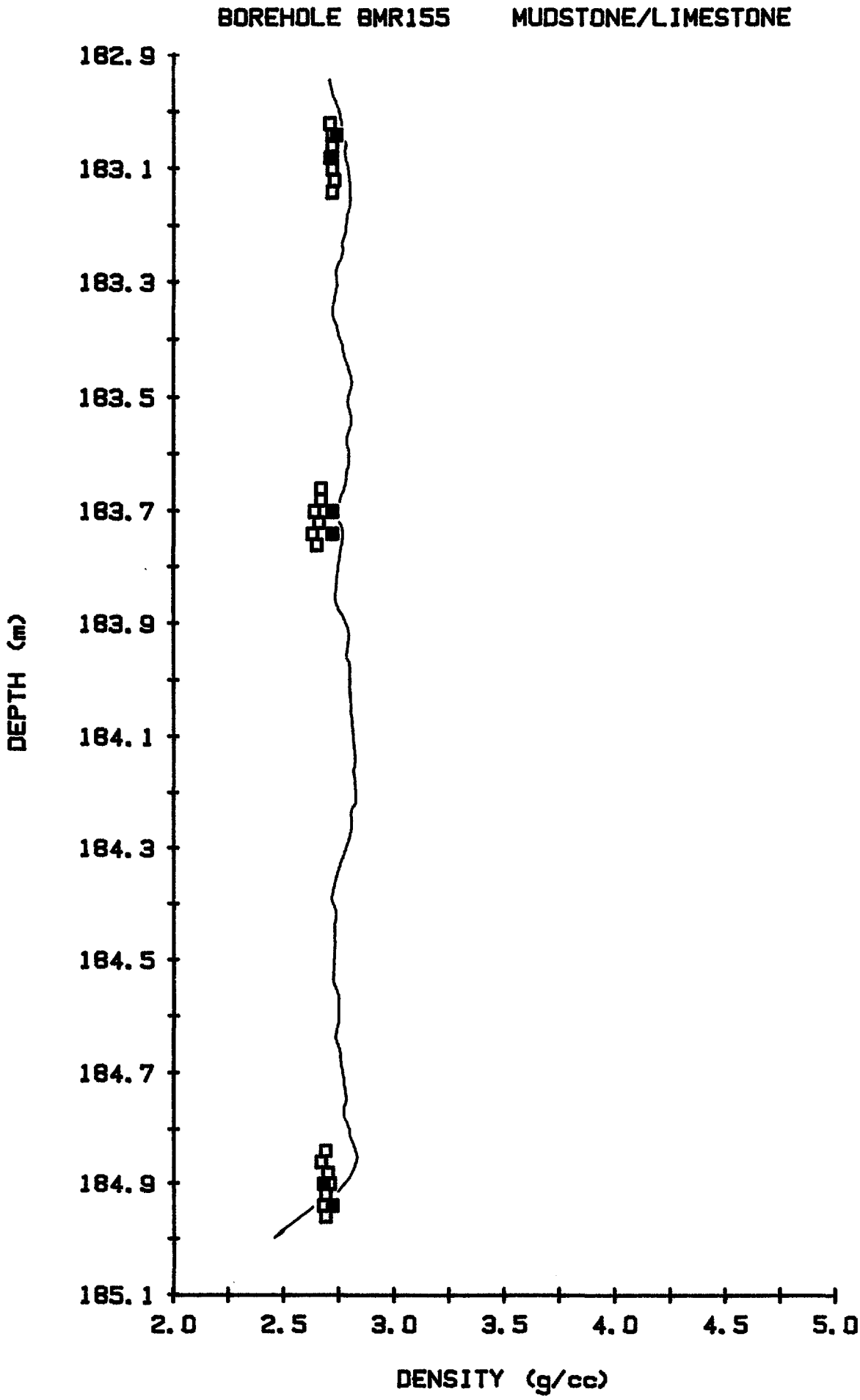
BOREHOLE BMR155 MUDSTONE/LIMESTONE
182.9
183.1
183.3
183.5
183.7
183.9
184.1
184.3
184.5
184.7
184.9
185.1
DEPTH (m)
2.0
2.5
3.0
3.5
4.0
4.5
5.0
DENSITY (g/cc)

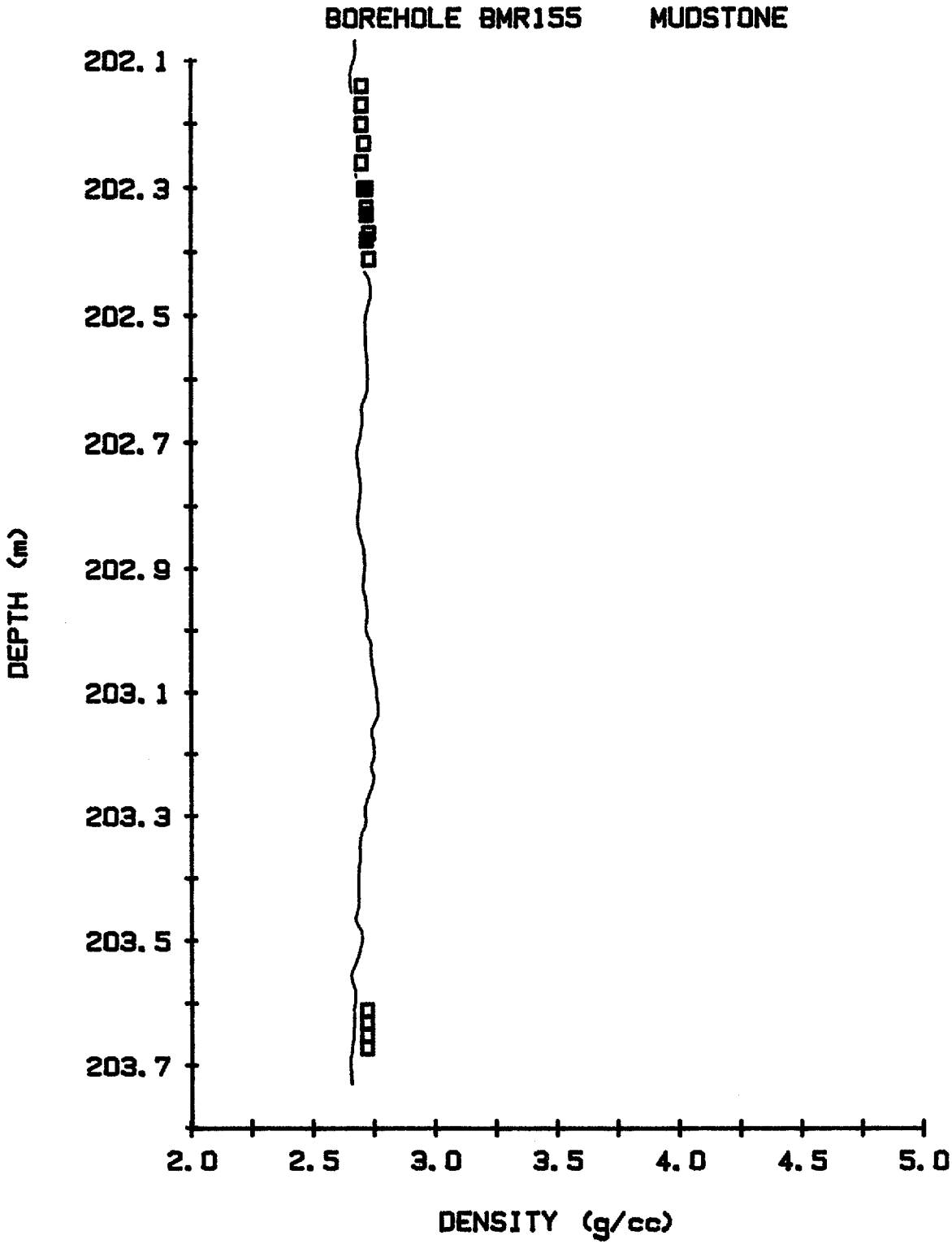
BOREHOLE BMR155 MUDSTONE
202.1
202.3
202.5
202.7
202.9
203.1
203.3
203.5
203.7
DEPTH (m)
2.0
2.5
3.0
3.5
4.0
4.5
5.0
DENSITY (g/cc)

Figure 11j

Figures 12a - 12s

Comparisons of the two sets of laboratory rock density data made on core samples from borehole W with the density estimates computed from the well-logging tool's short spaced density detector.

Symbols:

solid boxes - Archimedes principle density estimates
open boxes - CORAN density estimates
line - short spaced detector density estimates

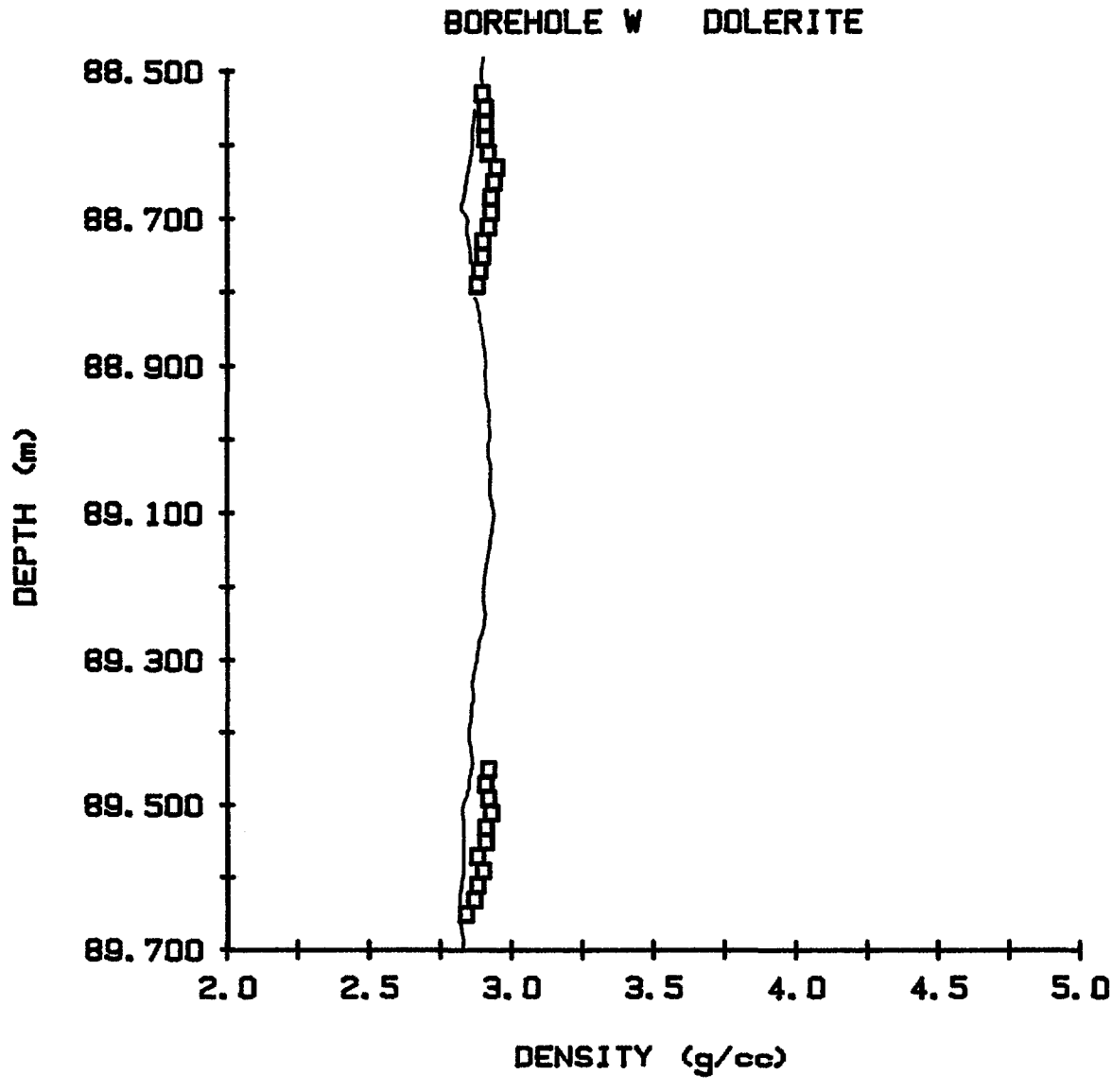
BOREHOLE W DOLERITE
88.500
88.700
88.900
89.100
89.300
89.500
89.700
DEPTH (m)
2.0
2.5
3.0
3.5
4.0
4.5
5.0
DENSITY (g/cc)

Figure 12a

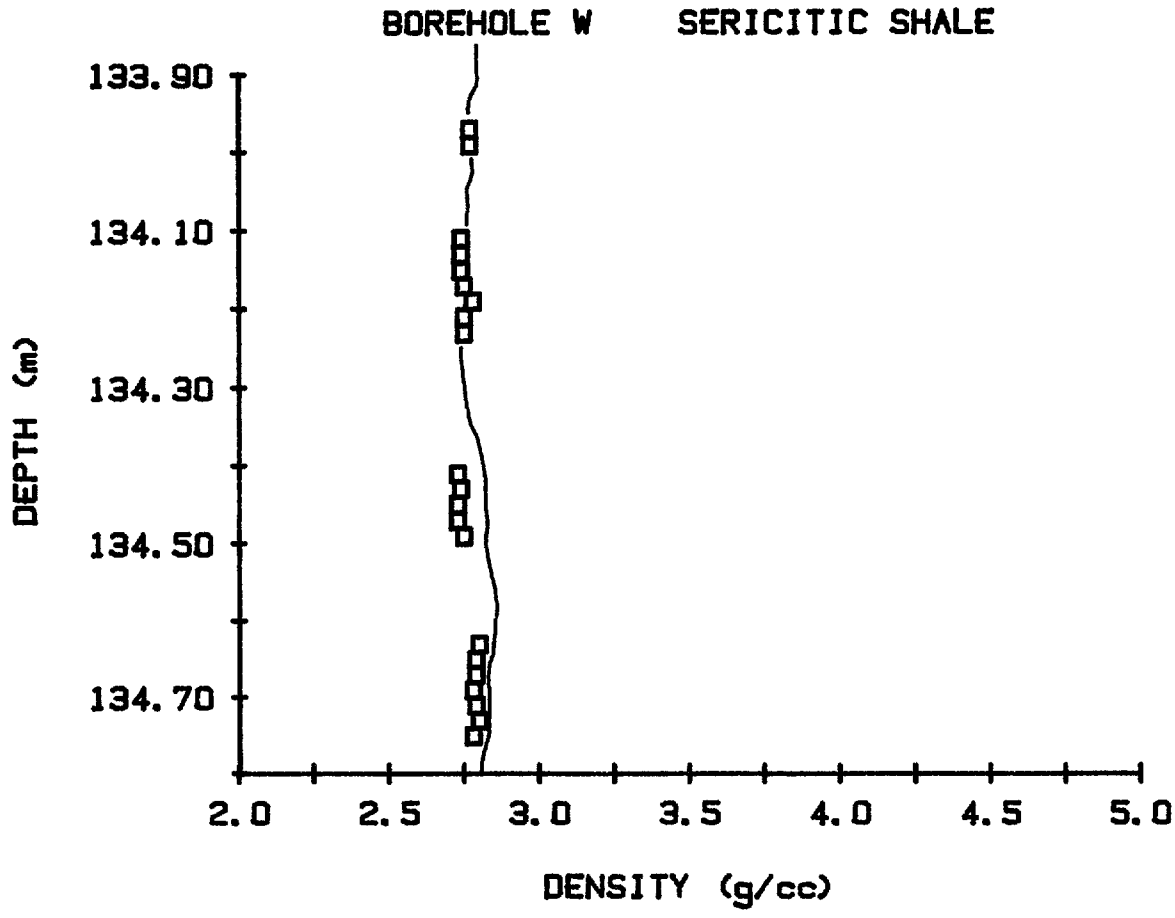
BOREHOLE W
SERICITIC SHALE
133.90
134.10
134.30
134.50
134.70
DEPTH (m)
2.0
2.5
3.0
3.5
4.0
4.5
5.0
DENSITY (g/cc)

Figure 12b

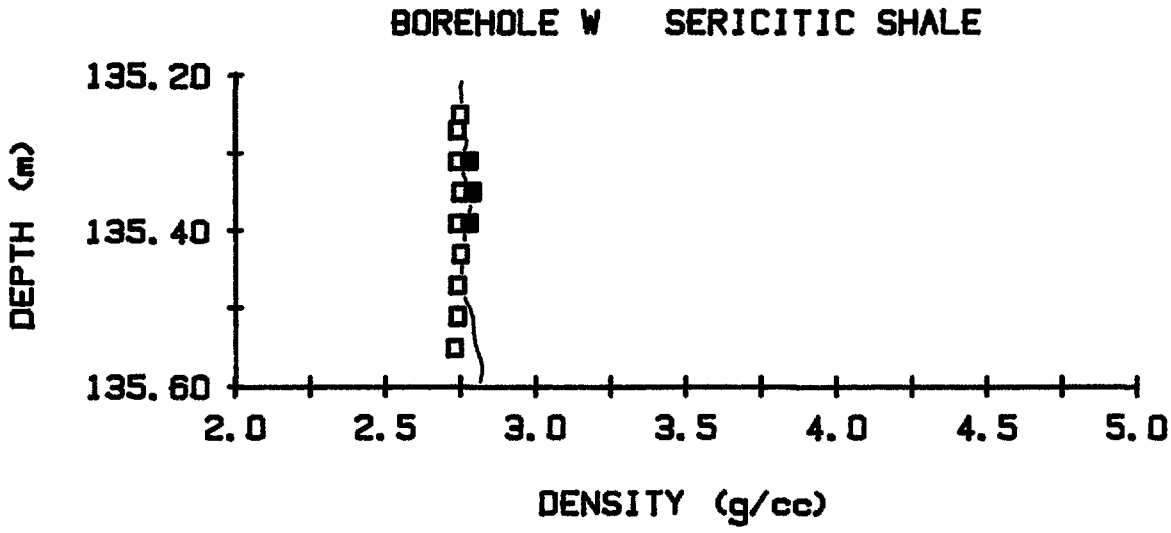

Figure 12c

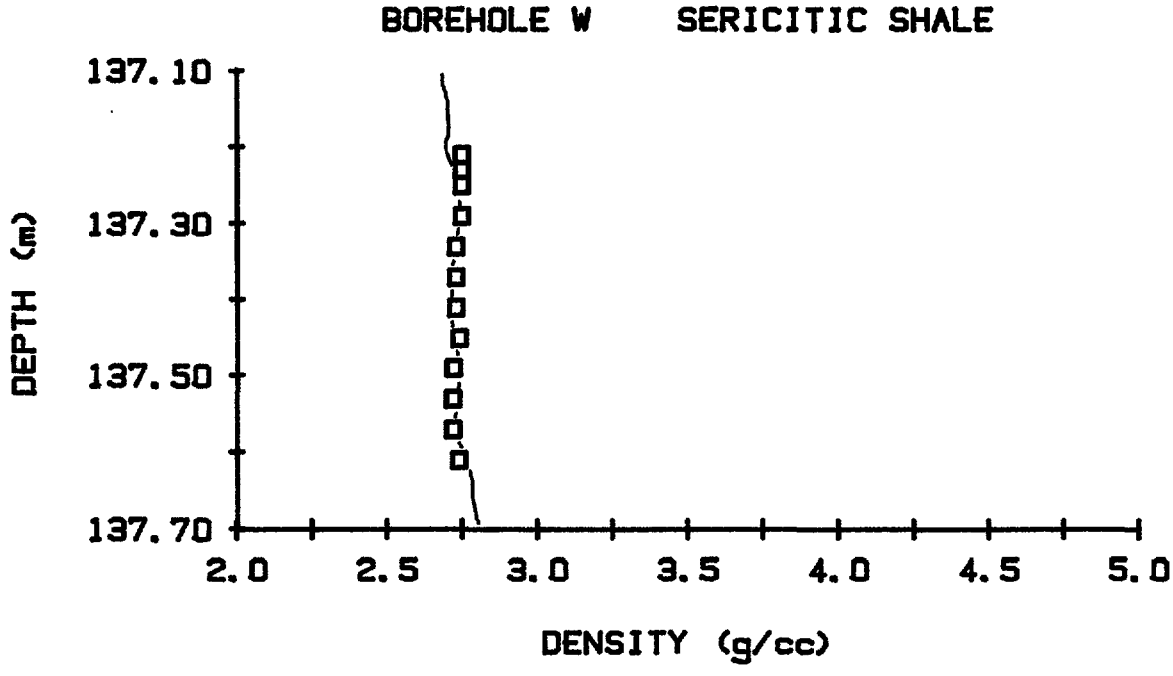

Figure 12d

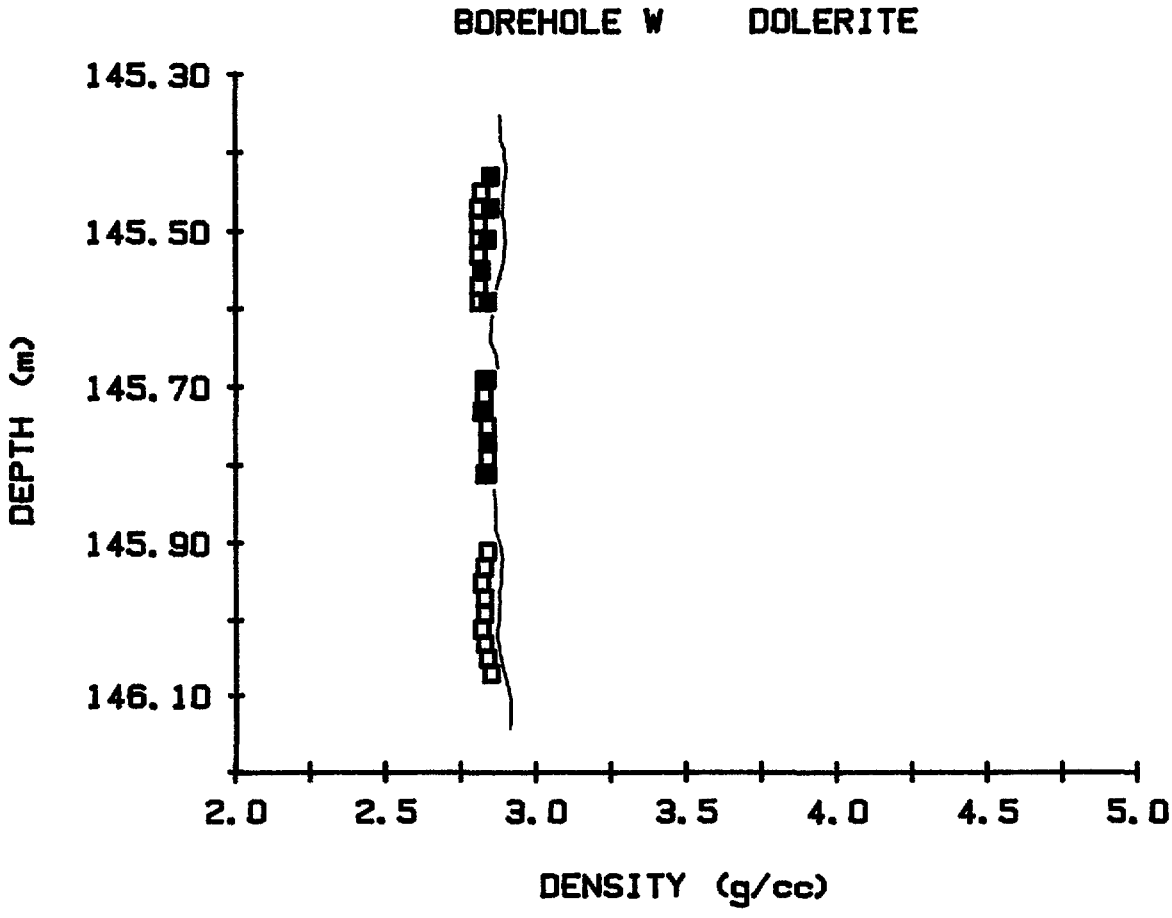

Figure 12e

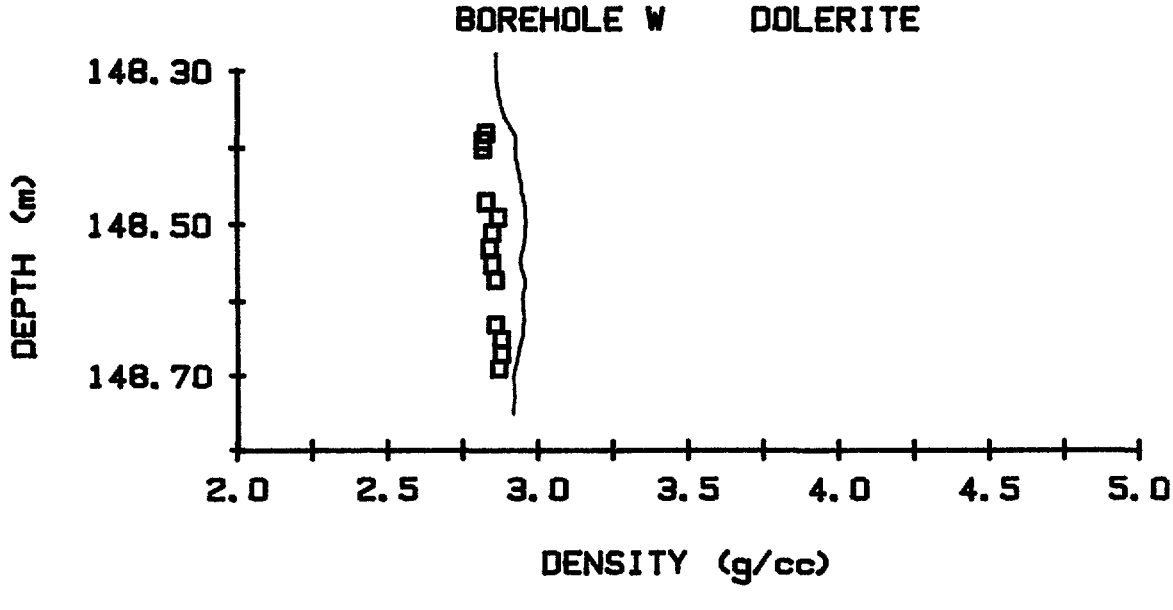

Figure 12f

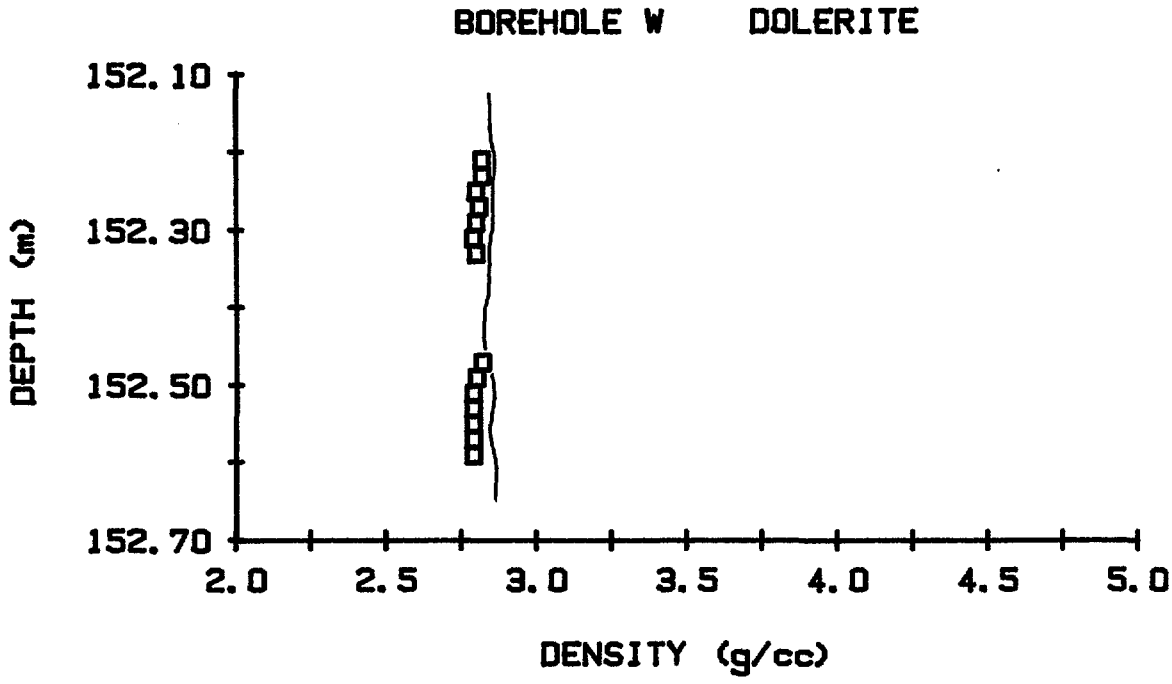
BOREHOLE W DOLERITE
152.10
152.30
152.50
152.70
DEPTH (m)
2.0
2.5
3.0
3.5
4.0
4.5
5.0
DENSITY (g/cc)

Figure 12g

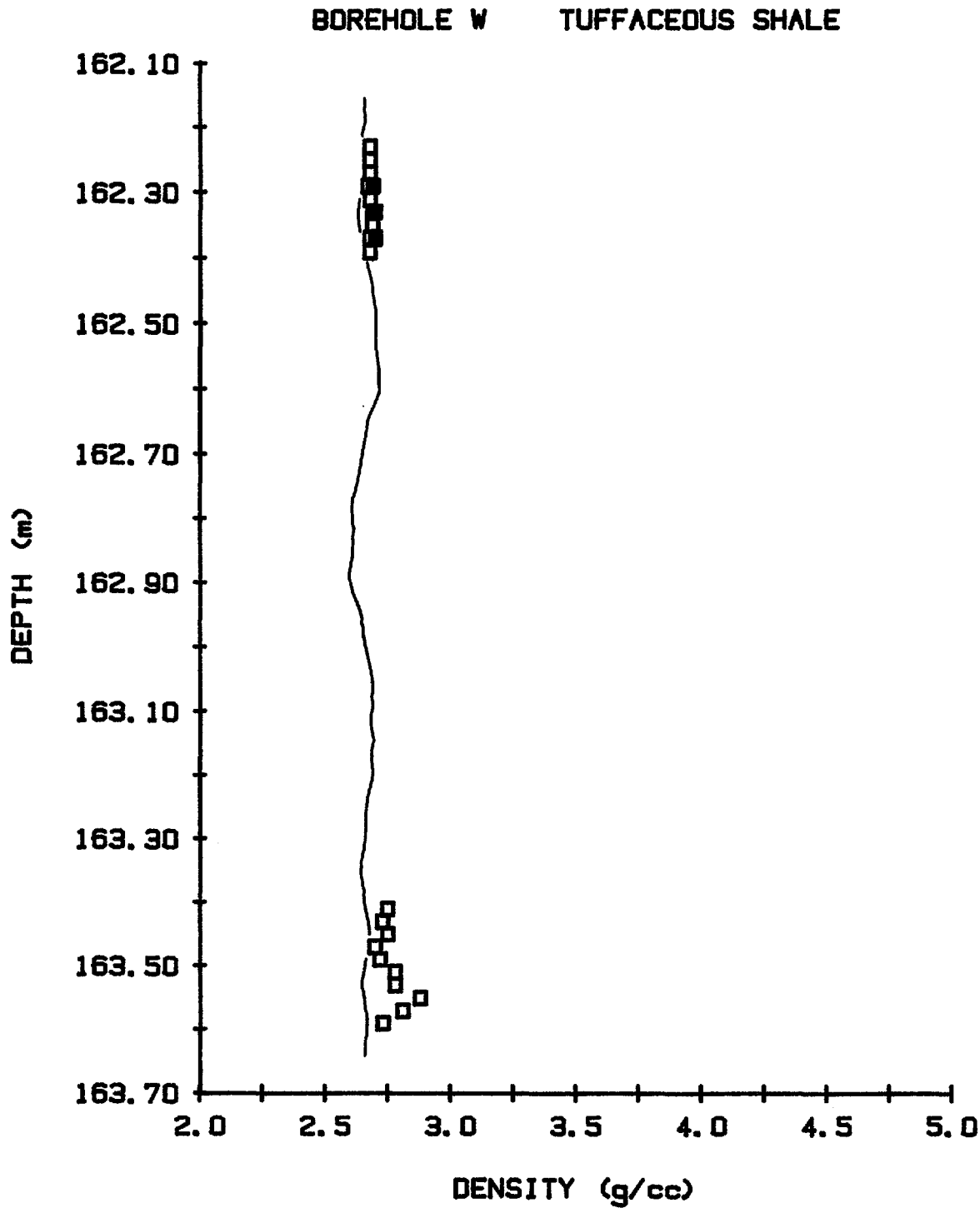
BOREHOLE W TUFFACEOUS SHALE
162.10
162.30
162.50
162.70
162.90
163.10
163.30
163.50
163.70
DEPTH (m)
2.0
2.5
3.0
3.5
4.0
4.5
5.0
DENSITY (g/cc)

Figure 12h

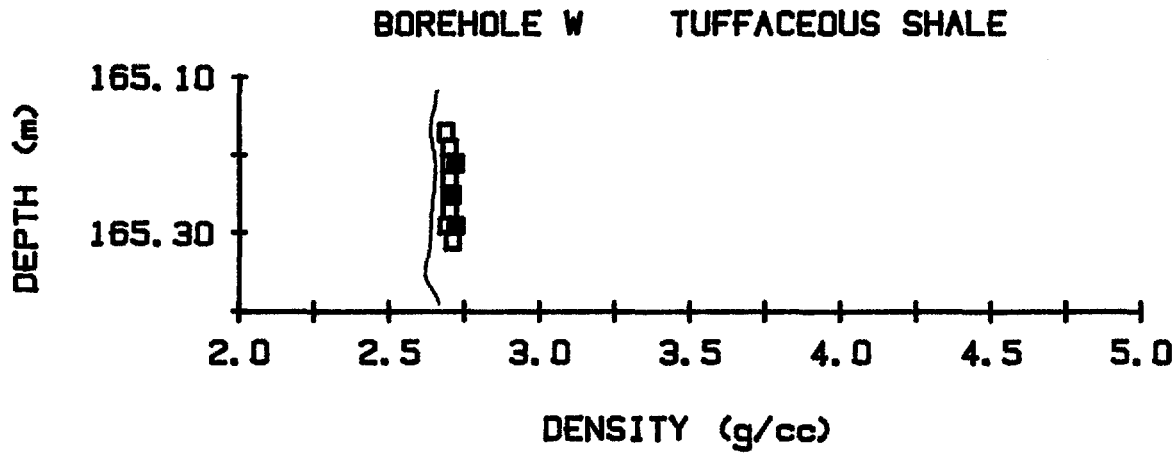

Figure 12i

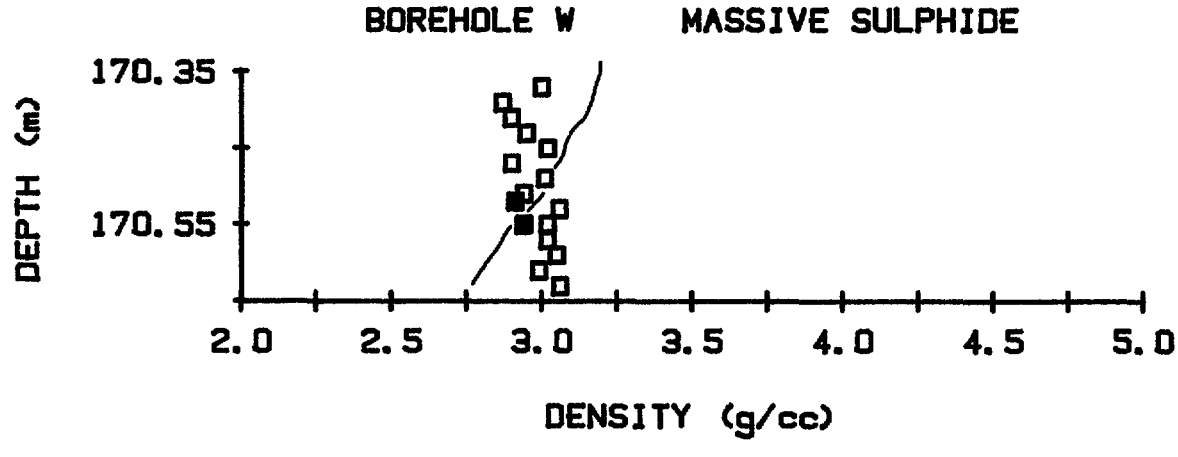

Figure 12j : The 25 cm thickness of the massive sulphide layer is too small to permit an accurate estimate of its density.

Figure 12k

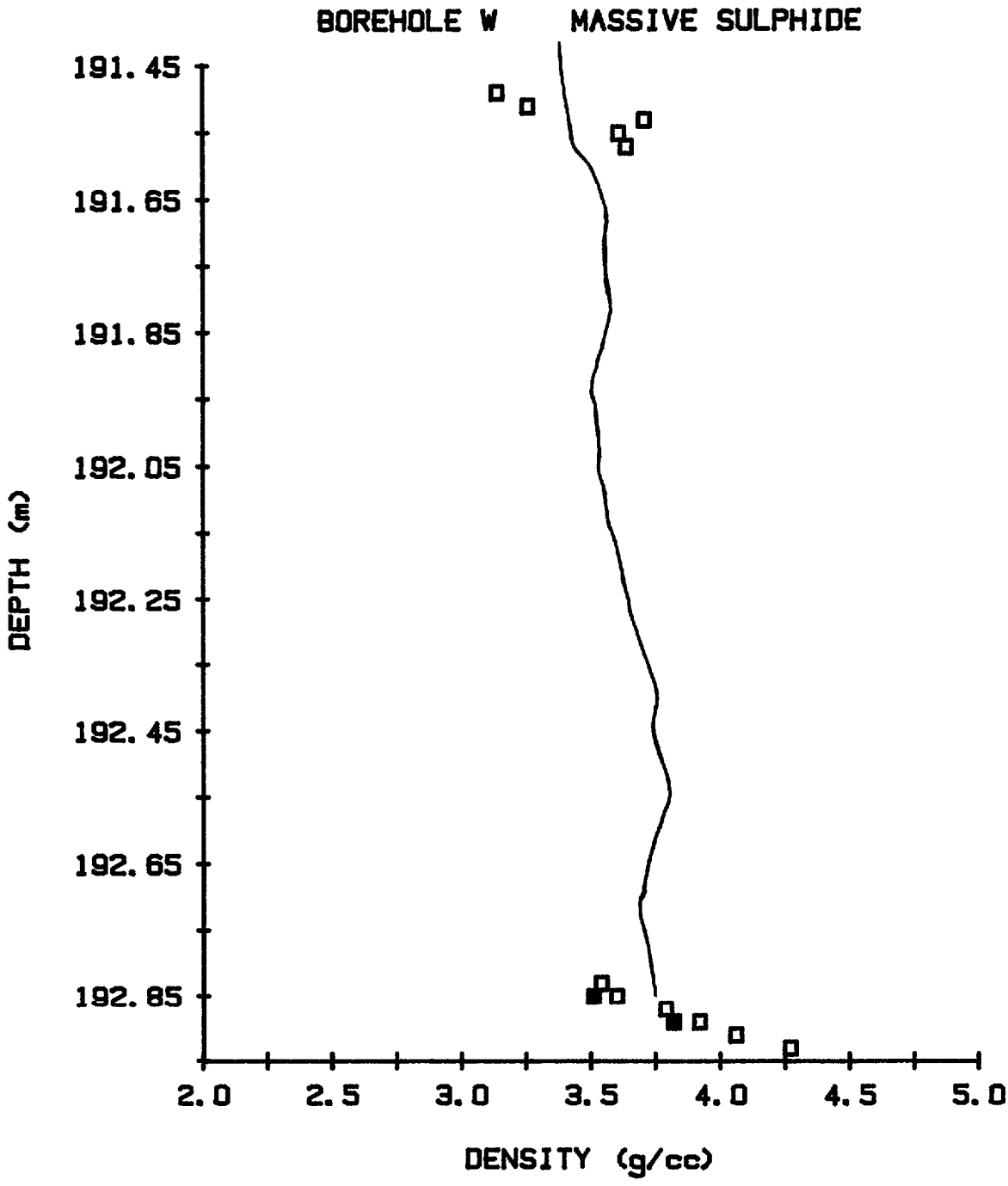

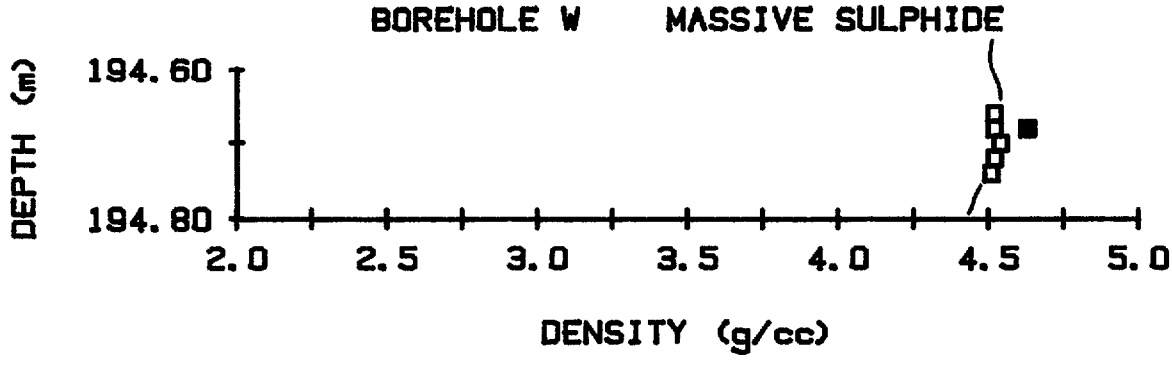

Figure 12L

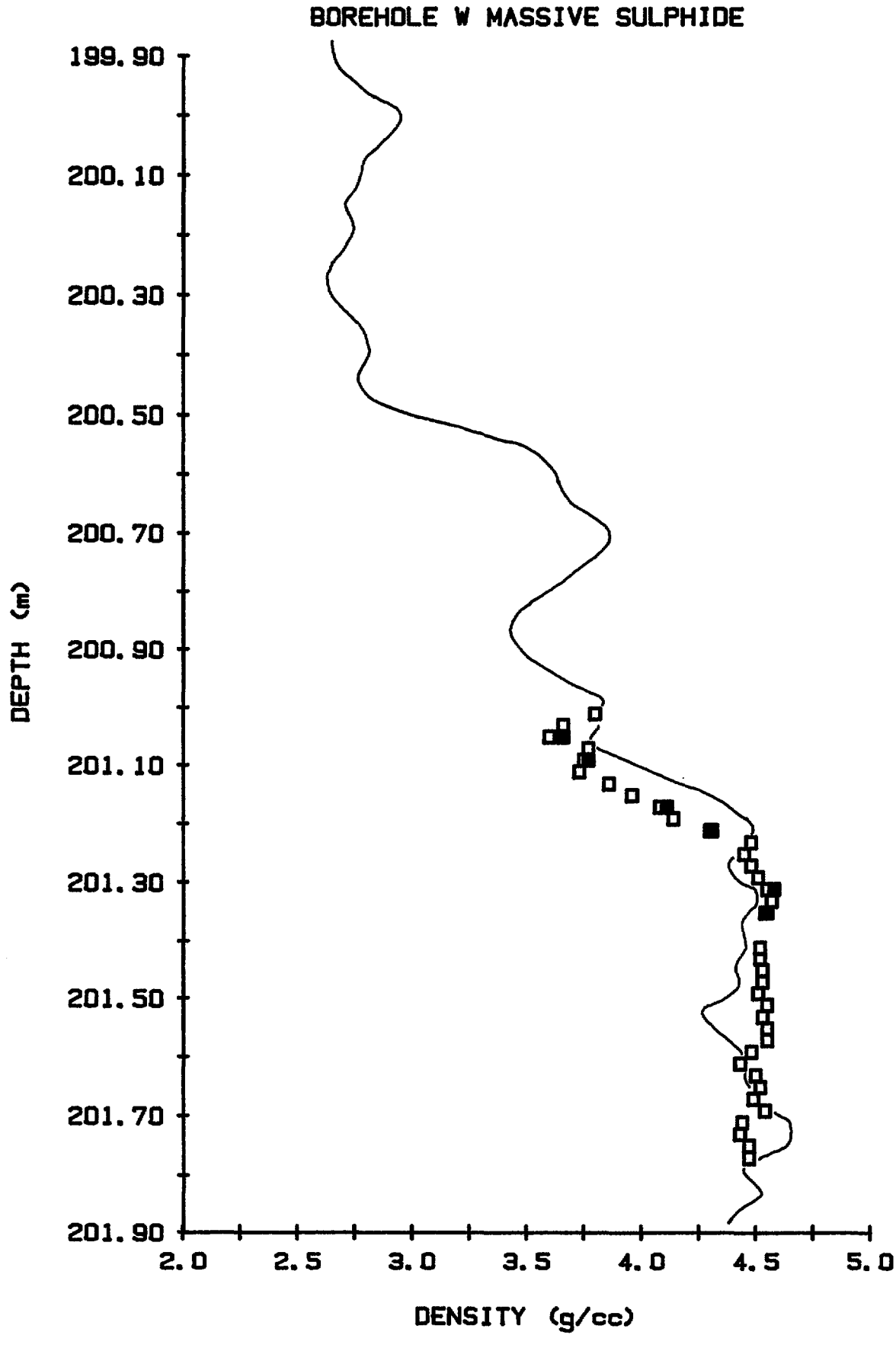
BOREHOLE W MASSIVE SULPHIDE
199.90
200.10
200.30
200.50
200.70
200.90
201.10
201.30
201.50
201.70
201.90
DEPTH (m)
2.0
2.5
3.0
3.5
4.0
4.5
5.0
DENSITY (g/cc)

Figure 12m

Figure 12n

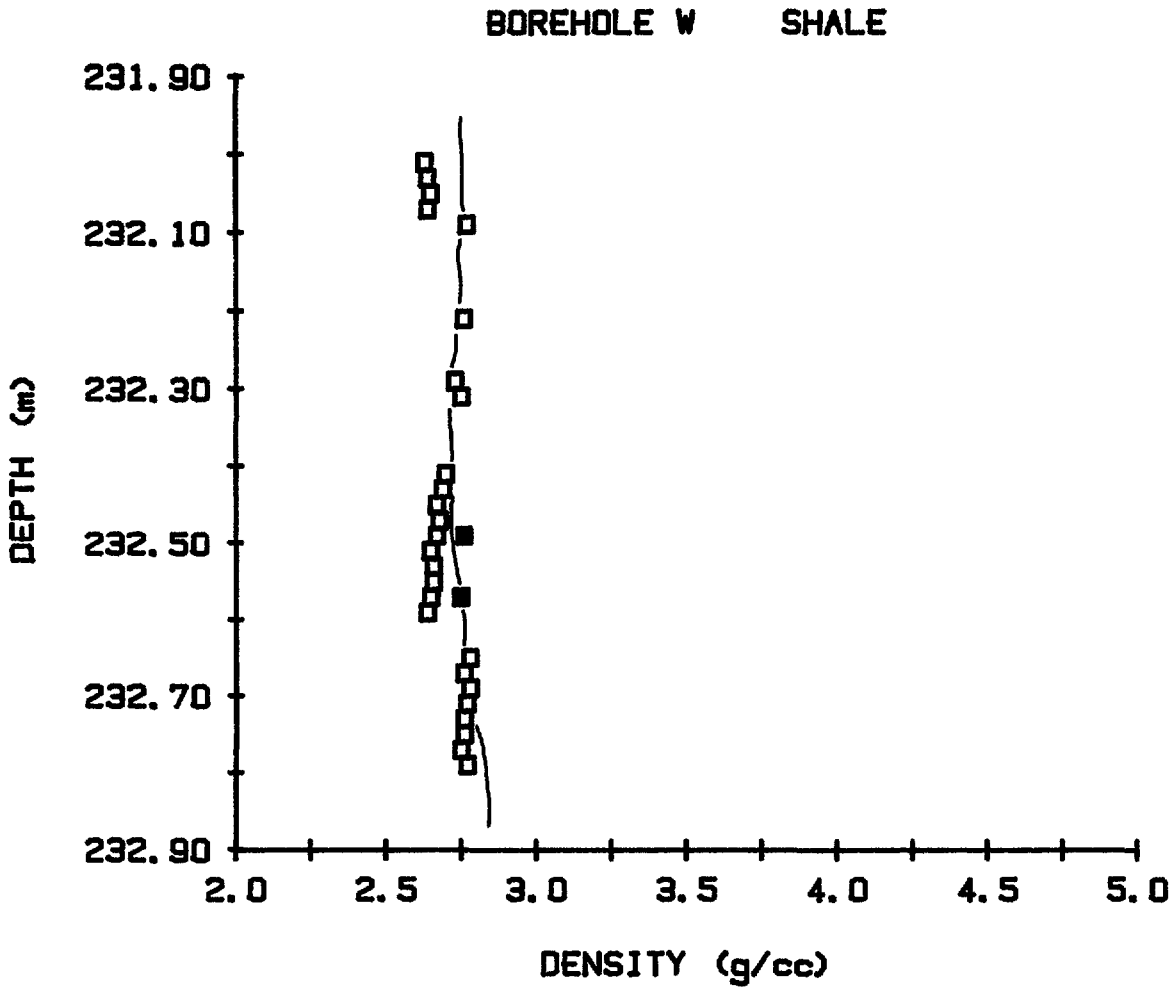

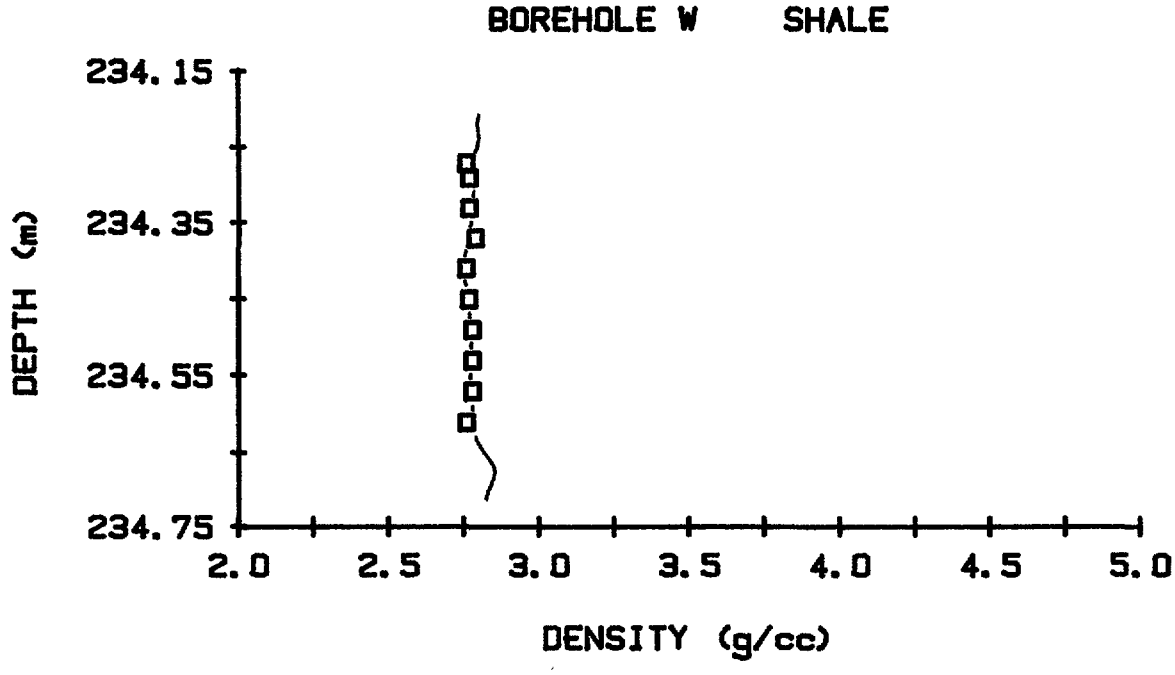

Figure 12o

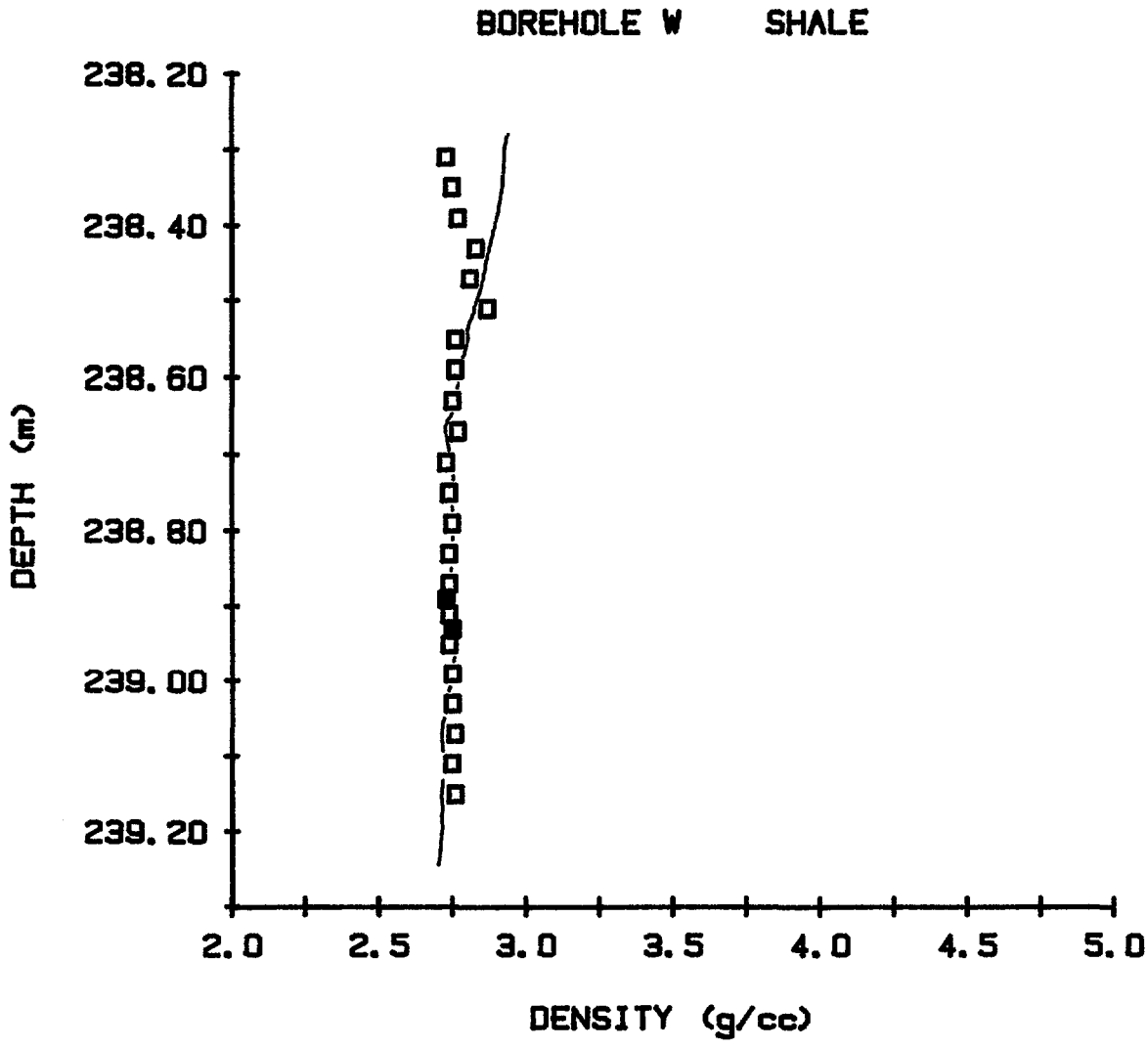
BOREHOLE W SHALE
238.20
238.40
238.60
238.80
239.00
239.20
DEPTH (m)
2.0
2.5
3.0
3.5
4.0
4.5
5.0
DENSITY (g/cc)

Figure 12p

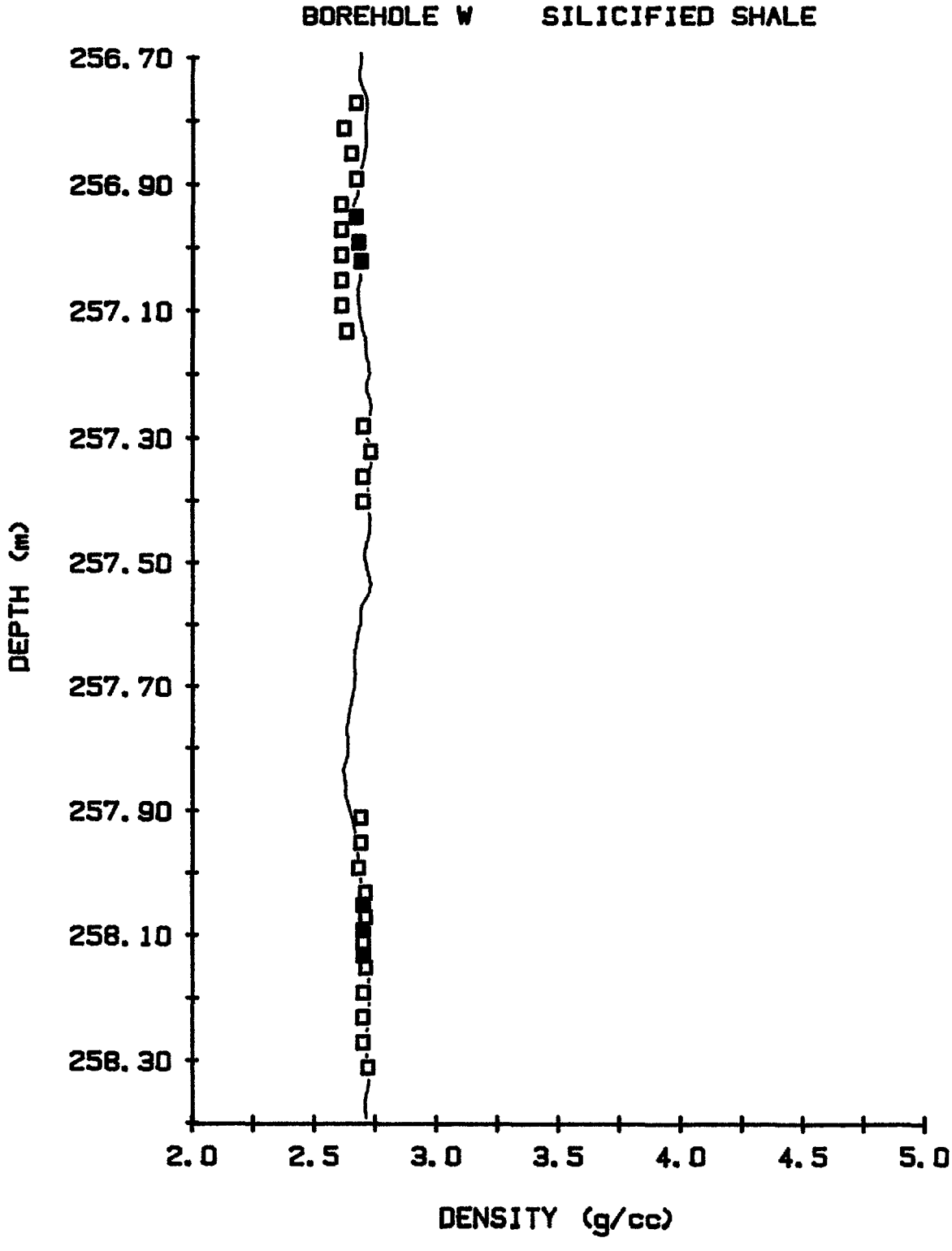
BOREHOLE W SILICIFIED SHALE
256.70
256.90
257.10
257.30
257.50
257.70
257.90
258.10
258.30
DEPTH (m)
2.0
2.5
3.0
3.5
4.0
4.5
5.0
DENSITY (g/cc)

Figure 12q

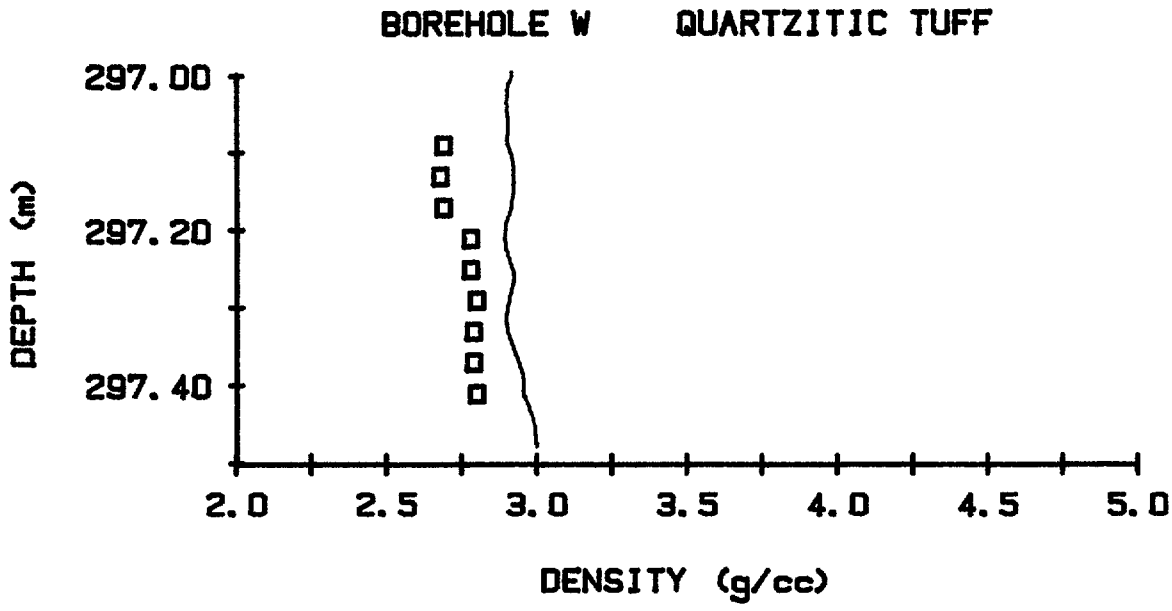

Figure 12r

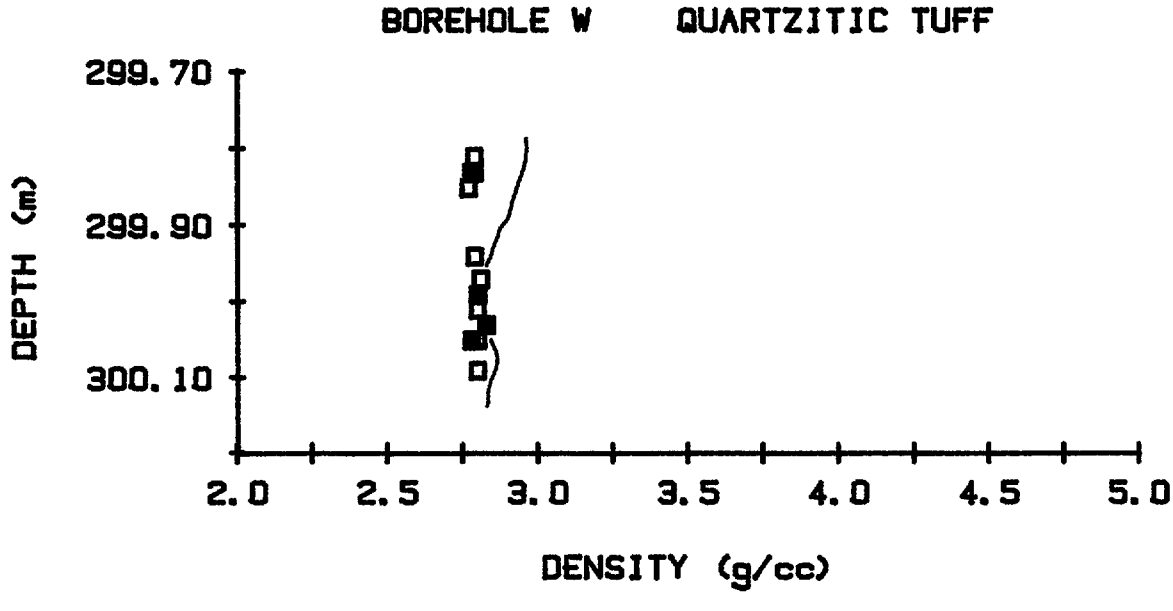

Figure 12s

Figures 13a - 13e

Comparisons of the laboratory rock density estimates made on core samples from borehole Newcastle 1 with the density estimates computed from the well-logging tool's short spaced density detector.

Symbols:

solid boxes - Archimedes principle density estimates

line - short spaced detector density estimates

Figure 13a

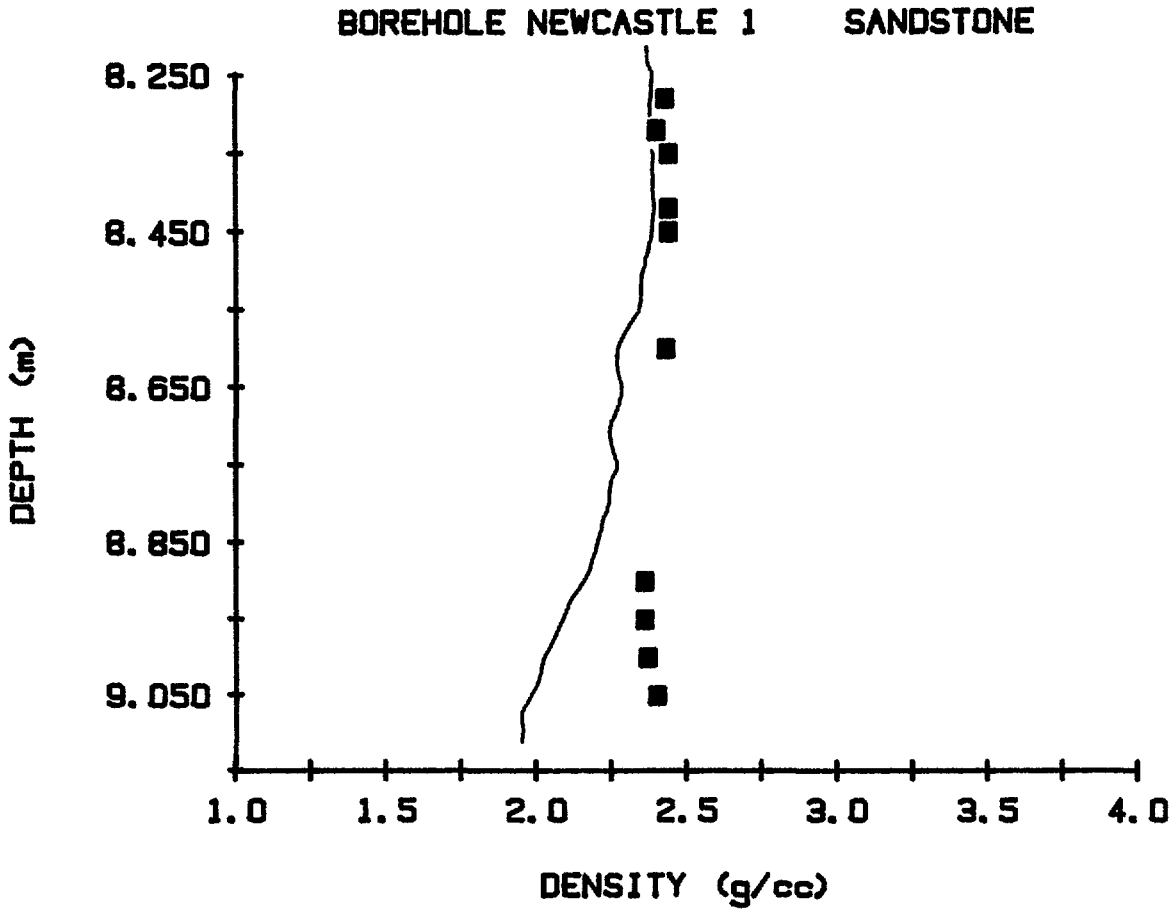

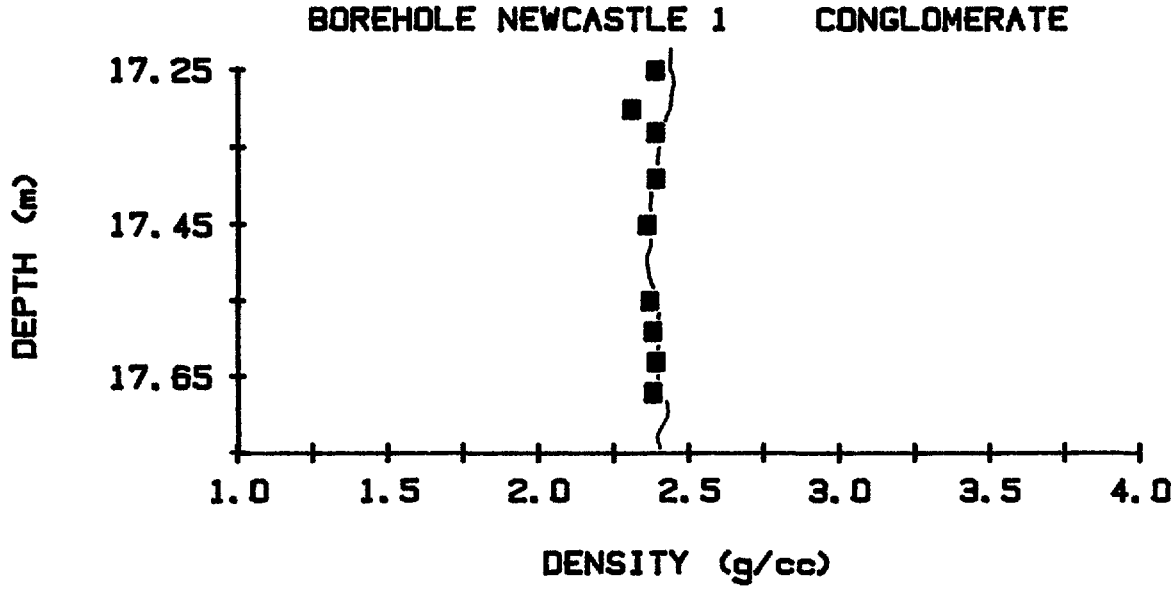

Figure 13b

Figure 13c

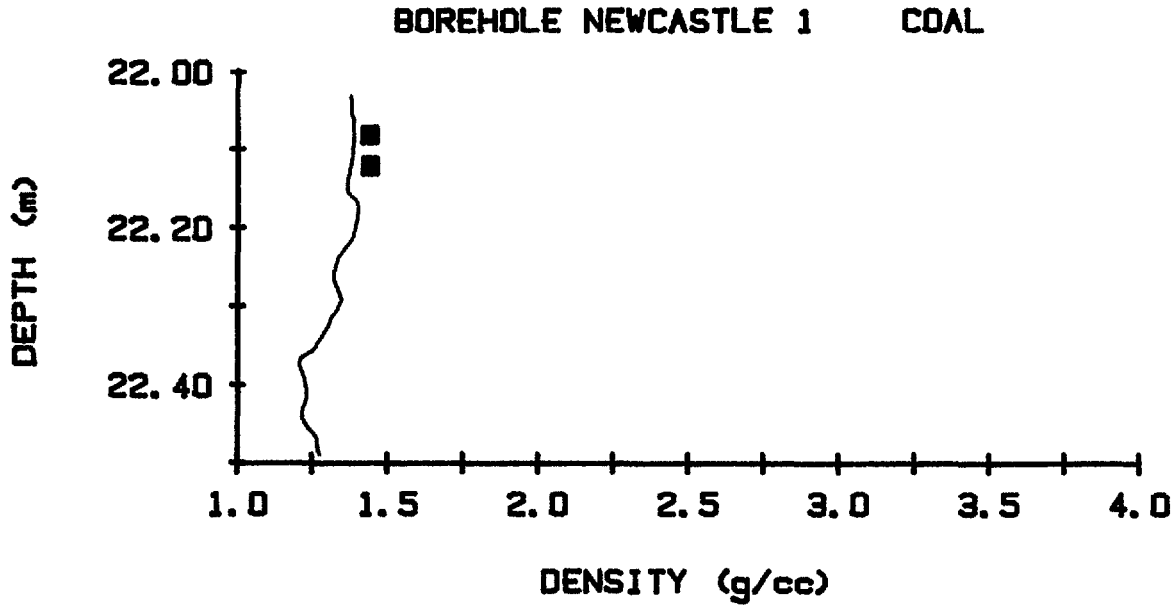

Figure 13d

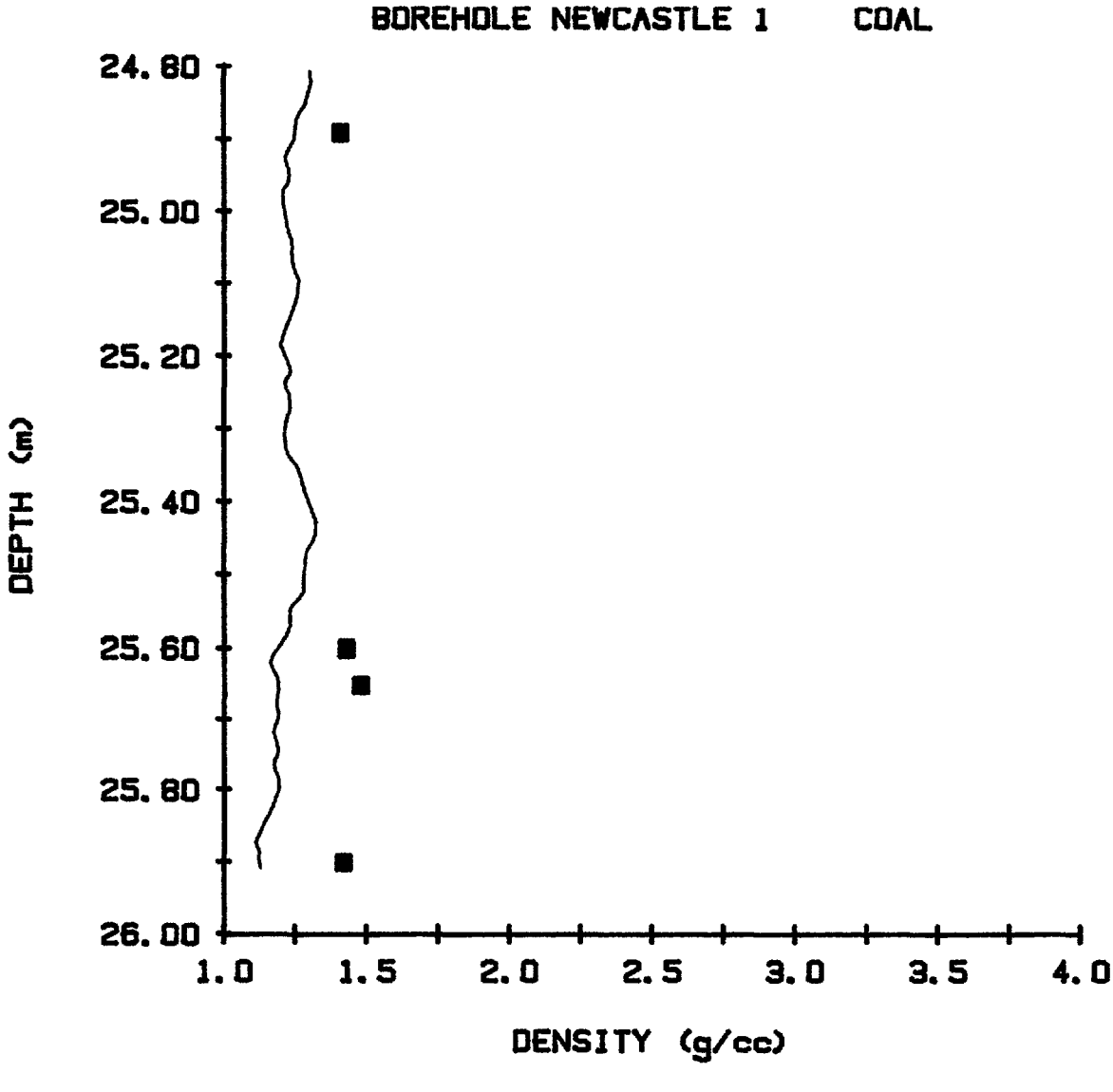

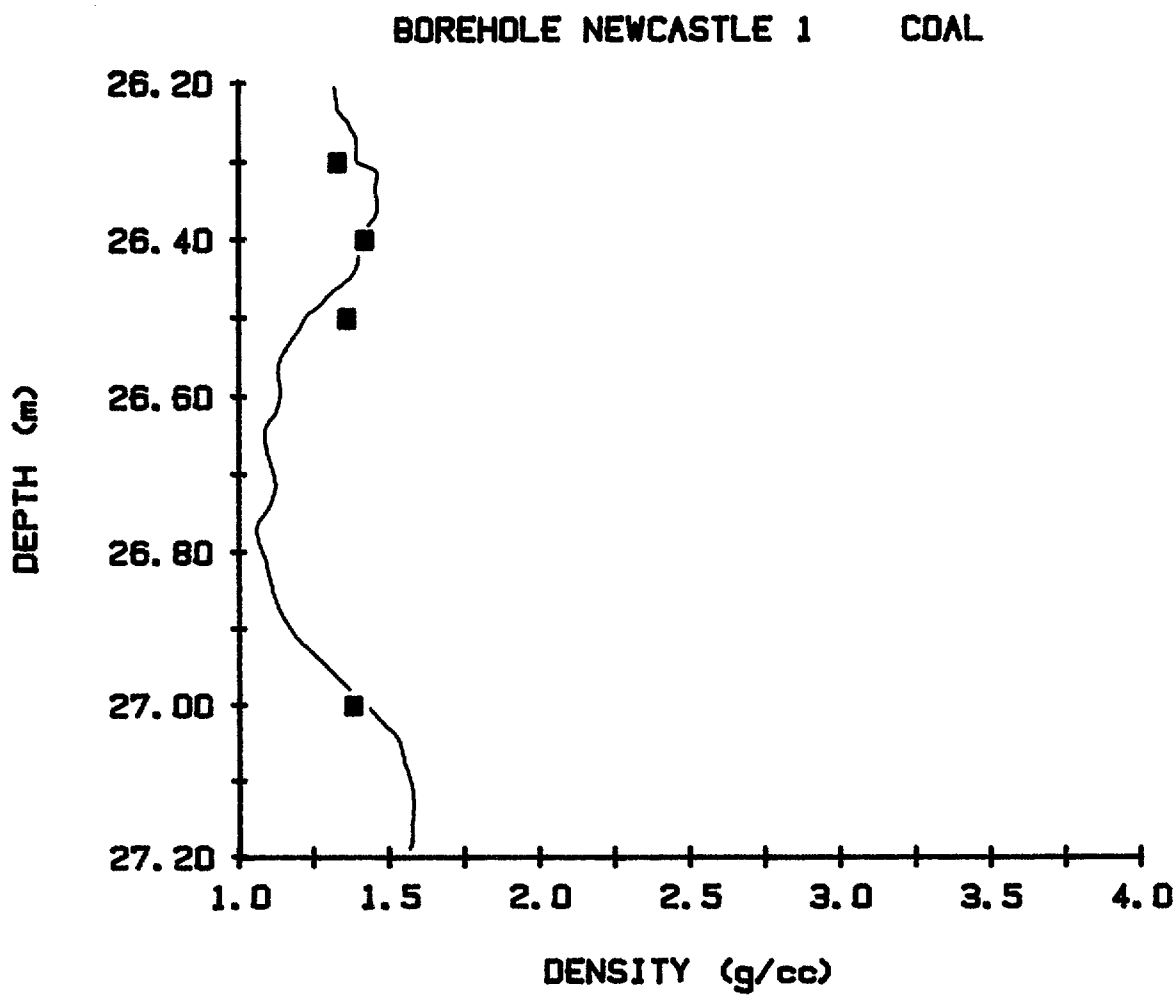
BOREHOLE NEWCASTLE 1 COAL
26.20
26.40
26.60
26.80
27.00
27.20
DEPTH (m)
1.0
1.5
2.0
2.5
3.0
3.5
4.0
DENSITY (g/cc)

Figure 13e